FINITE ELEMENT MODEL UPDATING OF PLATE STRUCTURE USING LAGRANGE MULTIPLIER METHOD

A thesis paper by

SOUVIK ROY
ROLL NO: 001710402017
REGISTRATION NO.: 140644 OF 2017 – 2018
EXAMINATION ROLL NO.: M4CIV19021

Under the guidance of

PROF. PARTHA BHATTACHARYA

Submitted in partial fulfillment of the requirements for the degree of

MASTER OF ENGINEERING IN CIVIL ENGINEERING (STRUCTURAL ENGINEERING)

DEPARTMENT OF CIVIL ENGINEERING
FACULTY OF ENGINEERING AND TECHNOLOGY
JADAVPUR UNIVERSITY
KOLKATA- 700032

MAY - 2019

DEPARTMENT OF CIVIL ENGINEERING

FACULTY OF ENGINEERING AND

TECHNOLOGY JADAVPUR UNIVERSITY

KOLKATA- 700032

CERTIFICATE OF RECOMMENDATION

This is to certify that SOUVIK ROY (Class Roll No.: 001710402017, Examination Roll No. M4CIV19021, Registration No.:140644of 2017 - 2018) has carried out the thesis work titled, **"FINITE ELEMENT MODEL UPDATING OF PLATE STRUCTURE USING LAGRANGE MULTIPLIER METHOD",** under my direct supervision and guidance. He has carried out this work independently. I hereby recommend that the thesis be accepted in partial fulfillment of the requirements for awarding the degree of **"MASTER OF ENGINEERING IN CIVIL ENGINEERING (STRUCTURAL ENGINEERING)".**

Countersigned by

……

Prof. Partha Bhattacharya
Professor
Department of Civil Engineering
Jadavpur University
Kolkata- 700032

……. …….

Prof. Dipankar Chakravorty
Head of the Department
Department of Civil Engineering
Jadavpur University
Kolkata- 700032

……. ……..

Dr. Chiranjib Bhattacharjee
Dean, FET
Jadavpur University
Kolkata-700032

DEPARTMENT OF CIVIL ENGINEERING
FACULTY OF ENGINEERING AND TECHNOLOGY
JADAVPUR UNIVERSITY
KOLKATA- 700032

CERTIFICATE OF APPROVAL

This thesis paper is hereby approved as a credible study of an engineering subject carried out and presented in a manner satisfactorily to warrant its acceptance as a pre-requisite for the degree for which it has been submitted. It is understood that, by this approval the undersigned do not necessarily endorse or approve any statement made, opinion expressed or conclusion drawn therein, but approves the thesis paper only for the purpose for which it is submitted.

Committee of Thesis Paper Examiners

_____
Signature of Examiner

DECLARATION

I, Souvik Roy, Master of Engineering in Civil Engineering (Structural Engineering), Jadavpur University, Faculty of Engineering and Technology , hereby declare that the work being presented in the thesis work titled, **"FINITE ELEMENT MODEL UPDATING OF PLATE STRUCTURE USING LAGRANGE MULTIPLIER METHOD",** is an authentic record of work that has been carried out in the Department of Civil Engineering, Jadavpur University, Kolkata under **Dr. PARTHA BHATTACHARYA**, Professor, Department of Civil Engineering, Jadavpur University. The work contained in this thesis has not yet been submitted in parts or full to any other university or institute or professional body for award of any degree or diploma or any fellowship.

Place: Kolkata

Date:

SOUVIK ROY

Roll No.: 001710402017

Registration no.: 140644 of 2017-2018

Examinations roll no. M4CIV19021:

ACKNOWLEDGEMENT

I would like to express my deepest gratitude to **Prof. Partha Bhattacharya,** Department of Civil Engineering, Jadavpur University, Kolkata-700032 for providing valuable advices, constant guidance and close supervision in all respect throughout. It is due to his regular encouragement and enlightening discussions for which this thesis has been brought to the current shape.

I would also like to convey reverences to my parents. Without their constant inspiration it would have been impossible.

I am also very much thankful to my classmates and senior research scholars for their constant encouragement and co-operation during the preparation of this report.

Date:

…….....

SOUVIK ROY

Roll No: 001710402017

M.E in Civil Engineering

Jadavpur University

Kolkata- 700032

Abstract

Finite Element (FE) model updating has been focused as an important topic of research in the field of structural dynamics for the last few decades. Various updation algorithms have been developed globally by many researchers and accuracy of these algorithms also have been verified through real-life application. Damage localization is also possible by proper updation of the model. So, FE model updating of a 2D cantilever plate and lumped mass localization in the plate is carried out in present thesis work using experimental modal analysis.

At first, a finite element model of the plate is developed in MATLAB environment using plate dimensions, material property and proper boundary condition. The plate is discretized using 4 noded iso-parametric elements. Numerical mass and stiffness matrices are generated from the developed model and using free vibration analysis, modal parameters (natural frequencies and mode shapes) are calculated. The calculated mode shapes are not mass normalized. Mass normalization of the mode shapes are done using proper mathematical formulation. After that, two numerical masses (100gms each) are lumped in the model at 2 nodes and corresponding mass matrix, stiffness matrix and modal parameters are estimated. Calculated mode shapes are mass normalized.

Then, experimental modal analysis is performed in the laboratory to extract the modal parameters of original plate and plate with lumped mass at different locations using Impact hammer test. Mode shapes obtained from hammer test are not mass normalized. For mass normalization of the mode shapes, shaker test is performed.

To verify the accuracy of Lagrange Multiplier method, mass and stiffness matrices of baseline FE model are updated using numerically calculated modal parameters (when two 100gms masses are lumped at 2 nodes) using two different approaches. It is observed that location and amount of lumped masses are correctly located from updated mass matrix when all the modes are considered for model updating. But accuracy is low when less number of modes (3 modes, 5 modes etc.) are considered.

Modal parameters obtained from experimental modal analysis are also used to update the baseline FE model. Location of lumped mass can be identified from updated mass matrix (not for all cases) but the accuracy of percentage mass recovery is low as only 3 modes are considered in model updating. 2^{nd} approach of model updating does not produce significant results when experimental mode shapes are used.

Keywords: FE model updating, Damage localization, Lagrange Multiplier method, Impact hammer test, Shaker test, Lumped mass

TABLE OF CONTENTS

LIST OF SYMBOLS

T = Kinetic energy

U = Potential energy

L= Lagrangian function

I = functional

q = Coordinates

$\dot{q}$ = Coordinate derivative

F = Load on system

ε = Strain

σ = Stress

[C] = Compliance matrix

ε_{xx} = Normal strain

γ_{xy} = Shear strain

σ_{xx} = Normal stress

τ_{xy} = Shear stress

ν = Poisson's ratio

E = Modulus of Elasticity

Ψ_x = Rotation in Y-Z plane

Ψ_y = Rotation in X-Z plane

α = Shear correction factor

[D] = Constitutive relationship matrix

ξ, η = Natural Coordinates

d = Nodal displacement

N = Shape function

[B] = Strain-displacement relationship matrix

[J] = Jacobian matrix

[K] = Stiffness matrix

[M] = Mass matrix

$\{\emptyset_i\}$ = Mode shape of i^{th} mode

$M_{gen,i}$ = Generalized mass of i^{th} mode

ω_i = Angular velocity of i^{th} mode

K_U = Updated stiffness matrix

M_U = Updated mass matrix

LIST OF FIGURES

LIST OF TABLES

CHAPTER-1

INTRODUCTION

1.1 Introduction

Finite Element (FE) analysis plays an important role in structural analysis in various field of civil engineering. An accurate and effective FE model is very important for parameter identification, damage detection and assessing the condition of the structure. FE modelling of any structure based on initial parameters does not always satisfy the present dynamic behaviour of the structure due to various reasons like occurrence of damage, change in boundary condition, material specification and change in geometry during construction etc. Damage identification is very important to avoid capacity reduction of the structure and thereby catastrophic failure. Visual inspection is the general process of assessment of a structure, but it is not sufficient for structural health monitoring in most of the cases. Due to advancement of technology, various measuring instruments are available nowadays to record the dynamic behaviour of real life structure which are considered noise free. Such recorded Modal parameters (Mode Shape and Natural Frequency) are used to update the existing FE model or particularly to update the Numerical Stiffness and Mass matrix to comply with the orthogonality condition. Location of major change in Mass or Stiffness matrix will indicate the addition of some local mass or occurrence of some local damage in the structure. However, it is not very easy to identify the damage from field measurements. Because, sometimes there are little variation in Modal Parameters even if the critical members are severely damaged.

In Finite Element Model Updating, three major steps are followed:

i) Setting up of an objective function
ii) Setting of updating parameters
iii) Use of an optimization algorithm

In Model updating process, not only satisfactory correlation is required between analytical and experimental results but also the updated parameters should preserve the physical significance.

Three common form of errors which are responsible for inaccurate model prediction are as follows:

a) Model structure errors: These errors occur when the model does not represent the physical behaviour of the prototype. Examples of such type of error are the assumptions on the linearity of the system and the boundary conditions.

b) Model order errors: A sufficient number of degrees of freedom (DOF) must be used in the analysis so that the actual behaviour can be modelled. The model must be fully converged with respect to the natural frequency.

c) **Model parameter errors:** These type of errors are encountered when the model is perfect but the numerical value of the physical parameters are incorrect. This type of errors are targeted for Model updating.

FE Model Updating methods can be broadly classified into 2 methods – Direct methods and Iterative methods. Direct methods are non-iterative in nature and essentially one step method. Updated FE models produced by such methods may not be symmetric. Hence, such methods are not much useful for industrial application. Industry only rely upon iterative methods. One of the most commonly used iterative method is Response Surface Methodology (RSM). There are many other FE model updating techniques available in which various researches have been performed. Among those techniques, Lagrangian Multiplier method, Derringer Desirability Function, Neural Networking are much familiar.

In recent years, system identification is developed for accurate assessment of damage in a structure based on input and output signal. Though it is very popular among researchers in the field of civil engineering, but its application to real life structure is limited so far. Some experiments have been carried out in the laboratory to examine the effectiveness of the system identification algorithm without paying much attention to developed noise in the measurement. Further researches are necessary on real-size models to resolve the complications associated with the application of such algorithm on real life structures.

Extensive researches have been performed in the area of parameter identification and divided into two major categories-

i. Static Technique
ii. Dynamic Technique

Both the techniques are based on Finite Element model utilizing the experimental Modal parameters. In Static parameter identification, optimization is done by differentiating the numerical and correct stiffness matrix subjected to equilibrium constraints. The method requires displacement measurement at all DOFs used to define the FEM of the structure which is not practical. A limited number of displacement measurement at all DOFs used to artificially create the remaining. This introduces a major error in the calculation of stiffness matrix.

Dynamic approach is chosen as an alternative to reduce the error. Vibration testing is the most common method of parameter identification in structural system. But there are still some limitations of this approach. Since dynamic parameter identification uses stiffness, mass and damping property of the structure, it is much more complicated than static method. In structural dynamics, experimental modal analysis from vibration test can be considered as a special case of system identification.

As experimental data are the basis for updating the mathematical model, it is important that equivalent quantities be compared. This might represent a problem because the Discrete Mathematical Model (DMM) contains many DOF, some of which are not accessible or measurable by current techniques. Examples consist of internal

variables or rotational DOF. This means that the model identified by the experiment has fewer DOF than DMM. Most of the techniques developed for Model updating are based on the identified modal parameters like natural frequencies and mode shapes. There are two ways of circumventing the problem of incompleteness. The first way is to expand the measured modes by filling the unknown entries of the measured mode shapes with data from analytical model. As the model is not correct, it is necessary to iterate until convergence occurs. The second way is to condense the DMM to a model with fewer DOF by eliminating the rotational and unimportant DOF. The problem with this approach is that the model loses the physical meaning. For this study, condensation of the DMM has been done to fit it with the experimental results.

When comparing experimental and analytical result, it is very important that Eigen vectors are paired correctly. Modal Assurance Criterion (MAC) is a popular technique to estimate the degree of correlation between the analytical and measured mode shapes. The MAC value is calculated by-

$$M_{i,j} = \frac{[u_i^T v_j]^2}{[(u_i^T u_i)(v_j^T v_j)]} \tag{1a}$$

where, u_i is analytical mode shape and v_j is experimental mode shape. The value of $M_{i,j}$ is a number between 0 and 1. Closer the value to 1 signifies the vectors are more similar. Ideally, the matrix M should be an identity matrix. In practice, it should obtain the values close to 1 in the diagonal and small values in the off-diagonal entries.

The MAC can be modified to be mass normalized. This results in small off-diagonal terms. The modified MAC is calculated by-

$$M_{i,j} = \frac{[u_i^T M_a v_j]^2}{[(u_i^T M_a u_i)(v_j^T M_a v_j)]} \tag{1b}$$

where, M_a is the mass matrix. After all, measurements should be conducted carefully. Attention should be paid to the process of attaching transducers to the structure, since it can affect its behaviour. Special care must be taken in acquiring the data to avoid leakage and noise. It is very important to conduct accurate tests and derive the mathematical models to represent the structure being tested. Model Updating is not intended to be parameter identification scheme but rather a 'fine tuning' procedure.

Here, it is intended to update the FE model based on both numerical and experimental results and verify the accuracy of updation algorithm.

1.2 Organization of Dissertation

In *chapter-1*, the reasons behind variation of numerical and experimental result and preliminary concept about finite element model updating are described. Procedure of MAC value calculation is also discussed here.

In *chapter-2*, available literatures on FE model updating are mentioned and objectives of the present thesis have been discussed.

Mathematical basis to form the finite element model of the structure and to update the FE model are presented in *chapter-3*. Euler-Lagrangian equation of motion is discussed. Then, stress-strain relationship and strain displacement relationship formulation of a plate based on Reissner and Mindlin first order shear deformation theory is described. Thereafter, Finite element formulations of stiffness and mass matrix and procedure of condensation of those matrices are presented. Normalization procedures of analytical and experimental mode shapes are then mentioned. Finally, FE model updating procedures based on Lagrange multiplier method as discussed by Baruch is presented.

In *chapter*-4, complete experimental setup and procedure is described. Modal parameters calculation by Experimental modal analysis and impedance value calculation by shaker test are shown.

In *chapter-5*, numerical results obtained from finite element model and experimental results are presented. Results obtained after FE model updating are also shown. Discussions are also made based on results.

In *chapter-6* (final chapter of the dissertation), conclusions of the present study are drawn and future scopes of work are mentioned.

CHAPTER-2

LITERATURE REVIEW

2.1. Literature review:

Modal parameters like mode shapes, natural frequencies of a structure can be estimated from analytical model. But most of the cases these parameters do not match with the real life structure as discussed earlier. So, researchers have turned their attention to identify a system which can accurately detect the actual dynamic behaviour of real life structure. Many researches already have been done on model updating and many are going on. Some of the intensive research works have been discussed here.

Zadeh [1] defined system identification as "The determination on the basis of input and output of a system within a specific class of system, to which the system under test is equivalent". Elements with specific class of system are same structures with different parameters. **Ross [2]** synthesized the stiffness and mass matrix based on experimental result. An algorithm was developed assuming the physical significance of individual mass and stiffness matrix are preserved. Mass and stiffness matrix are derived for a cantilever beam and compared with the earlier techniques. **Gersch et al. [3]** estimated the modal parameters of linear multi-degree of freedom structures. AR-MA (Auto Regressive Moving Average) was used to estimate the parameters. **Berman [4]** used the same approach of Baruch but updated the mass matrix. He minimized the Euclidian norm which was calculated from the discrepancy of the updated and analytical mass matrix. The orthogonality conditions were satisfied as it was used as constraint equation. **Baruch [5]** developed an approach based on Lagrange multiplier. He discussed about two approaches to update the mass and stiffness matrix. First approach is to update the mass matrix first and then update the stiffness matrix based on updated mass matrix. Second approach is to update the stiffness matrix first and then update the mass matrix based on updated stiffness matrix. **Berman and Nagy [6]** used the measured natural frequencies and corresponding mode shapes to update the mass and stiffness matrix. **Sheena, Unger and Zalmanovich [7]** calculated the difference between the actual stiffness matrix and analytical stiffness matrix. Then they worked on the minimization of the change by adjusting the elements. Displacements were measured at some specific points and the displacement value at other points were estimated by Spline function. **Sanayei and Nelson [8]** estimated the structural stiffness matrix in the same way as Sheena, but least square minimization technique was used to minimize the calculated change in stiffness. The data were collected on the basis that displacement degrees of freedom and force degrees of freedom must be same which are practically not feasible. **Cheng S. Lin [9]** located the positions of modelling error in stiffness matrix. A unity method was developed based on modal test data and cross unity method was performed between experimental flexibility matrix and analytical stiffness matrix. **Sanayei and Onipede [10]** evaluated the structural parameter data using incomplete data. Static condensation technique was used for calculation. In calculation of stiffness change, a function was estimated based on force matrix. It was

applied on frame and truss structure. An accurate estimation of parameter was not achieved. **Hjelmstad, Wood and Clark [11]** estimated the structural parameter data using an error measure on complex linear structure. Monte-Carlo simulation was used to check the influence of noisy data on the estimated parameter. Finite Element model updating is the approach to update the analytical model by minimizing the difference between experimental data and the analytical data. It was discussed by **Mottershead and Friswell [12]. Banan and Hjelmstad [13]** worked on system identification based on measured response. They studied on a real life tall building at Oakland and compared the parameters estimated from the structure with simulated parameters obtained from dynamic transient response. **Sanayei and Saletnik [14]** used subsets of static applied force and strain measurement to have least sensitivity to noise and determined the input output relationship using Monte-Carlo simulation. **Hjelmstad and Shin [15]** developed an adaptive parameter grouping scheme assuming the baseline parameters are known and localize damage in a structural system. **Bakhtiari-Nejad [16]** utilized the applied static forces at a subset of DOFs and measurement of displacement at another DOFs for linear elastic structure. They introduced an optimization technique that minimizes the difference of the load vectors of damaged and undamaged structure. Load cases are selected by a method based on stored strain energy and measurement locations are selected using Fisher information matrix.

For the last few decades, dynamic identification techniques have been developed more maturely compared with the static approach and corresponding literatures are quite extensive. The basic premise of the vibration-based damage detection is that changes in physical properties of the structure change the dynamic behaviour of the structure or modal parameters. This change provide a feature to calculate the structural state. **Sanayei et al. [17]** introduced a modal stiffness based error function to estimate the stiffness and mass matrix. Natural frequencies and mode shapes data were also measured at element level. Finally, model updating was performed keeping the updated parameters within the stipulated value and thus reducing the error occurred in the estimation**. Sanayei and Slavsky [18]** worked on damage localization and Finite Element model updating using multi-response NDT data. A new protocol for combining multiple parameter estimation algorithms for model updating is presented. This approach allows for the simultaneous use of both static and modal NDT data to perform model updating at element level. A new damage index based on multi-response NDT data is presented for damage localization of the structure. This index is based on static and modal strain energy change in a structure due to damage. **F. Khoshnoudian & A. Esfandiari [19]** used incomplete measured mode shapes and natural frequencies in model updating for damage detection. Unmeasured mode shapes were expressed as the function of measured mode shapes, mass matrix and natural frequencies of the structure. **Idehara et al. [20]** developed a modal analysis procedure based on adaptive filter RLS/QRD and used a model of ASCE benchmark structure to simulate a numerical case. A harmonic noise was used to diminish the effect of external noise. Then a state space equation was used to model the dynamic behaviour and modal parameters in filter processing. **Minli Yu et al. [21]** experimented the modal testing on

a simple experimental rig comprised of a clamped horizontal bar with lumped masses. Apart from damping, the proposed method was used for modal parameter identification. A signal generator (shaker) was used for a steady sinusoidal signal generation, an accelerometer was used for acceleration measurement from the masses, data acquisition board and in house data processing software was used to analyze. The process is practically feasible if the problem due to excessive noise and round off error in calculation can be avoided. Many analytical methods have been developed by many researchers for the system identification based on model updating. All the analytical models are based on the fundamental of structural dynamics. The modal parameters are calculated based on Eigen-value problem or the orthogonality conditions mainly.

Arora [22] discussed that model updating techniques can be executed in two approaches- Direct method and Iterative method. **Kabe [23]** updated the stiffness matrix by adjusting the coefficient of the stiffness matrix. The percentage change in the coefficient was minimized preserving the physical configuration of the model. **Caesar [24]** used the same approach of Berman and also used the same constraints. But, preservation of total mass of the system and interface forces were done simultaneously. **Wei [25]** updated the mass and stiffness matrix using different Lagrange multiplier and element correction methods. **Yang and Chen [26]** updated the stiffness matrix and mass matrix by direct updating method. Orthogonality conditions were preserved in the updating. The proposed method can be utilized with few modes available from experiment. The advantage of the proposed method is due to its simplicity and accuracy in computation. **Lee and Eun [27]** simultaneously updated the mass and stiffness matrix without using any multiplier. The proposed equations were developed by Moore-Penrose inverse matrix. **Carvalho et al. [28]** proposed a new method for model updating of any undamped structure without using modal expansion or reduction techniques. Incomplete measured modal data was used for updating preserving the unaffected Eigenvalues and eigenvectors. **Mukhopadhyay et al. [29]** investigated the problem associated with mass normalization of the measured mode shapes and parameter identification from the measured modal data. No prior mass or stiffness data is required for identification. **Chen and Maung [30]** presented an approach for model updating based on perturbation theory using regularized algorithm. Incomplete modal data was used for model updating without using any optimization techniques. **Fu, Lu and Liu [31]** presented a response sensitivity based approach for damage localization in an isotropic plate using the measured dynamic response of the plate. The local damage is simulated by reduction in the elemental Young's modulus of the plate. In the forward analysis, the forced vibration response of the plate under external loads is obtained from Newmark direct integration. In the inverse analysis, a response sensitivity based finite element model updating approach is used to identify the local damages of the plate in time domain.

With recent advancement of Artificial Intelligence or Machine Learning, it has been used for model updating by many researchers. Neural Network is one of such technique which has been used frequently for the last two decades. **Zhou, Wang, Chen and Ou [32]** updated the FE model based on Response Surface Method (RSM) and

Radial Basis Function (RBF). They studied on a laboratory scale bridge model and actual bridge. On the basis of numerical simulation, experimental study and real life application, it is seen that the method works well. **Atalla et al. [33]** studied on Model updating using neural network. The neural network estimate the parameters being updated very quickly and accurately without measuring all degrees of freedom of the system. This also avoids the use of mode shape expansion or reduction. **Miller et al. [34]** updated the finite element model using Artificial Neural network. Beams and frames were investigated in the laboratory scale. Their models were updated by ANN with dynamic characteristics of the structure as the input vector. The ANN (Multi-layer feed forward or Bayesian network) are trained with numerical data disturbed by artificial noise. This process is also used for identification of damage or addition of local mass in the system. **Santamaria, Arras and Coppotelli [35]** worked on application of neural network on FE model updating of any structure in operating condition. Dynamic properties of the structure were identified from response data obtained during operating condition. Feed-forward neural network was used in the study with modal parameters (natural frequencies, mode shapes) as input and physical property of the structure as output to train the network. Trained neural network is when simulated data is used but have some limitations when experimental data is used. That's why an algorithm based on non-trained neural network is developed. **Marwala, Mdlazil and Sibisi [36]** studied on FE model updating using Bayesian approach. Maximum likelihood method and Bayesian method for model updating was compared. Maximum likelihood method was implemented using genetic algorithm where Bayesian approach was implemented using Markov chain Monte Carlo algorithm.

2.2 Objective of the present work:

From literature review it is seen that different methods have been used globally for Finite Element model updating of any structure based on experimental modal parameters. As experimental mode shapes and natural frequencies are the basis of model updating, mass normalization of the mode shapes is very important. So, based on literature review, objectives of the present study have been selected as follows-

- Selection of a mathematical model for estimation of the numerical results (mass matrix, stiffness matrix, mode shapes and natural frequencies) properly.
- Application of dynamic condensation technique on mathematical model to comply with the experimentally available degrees of freedom.
- Performance of experimental modal analysis to extract the modal parameters using B&K analyzer.
- Calculation of impedance value and generalized modal mass for mass normalization of experimental mode shapes.
- Comparison of numerical and experimental modal parameters.
- Updation of baseline FE model using experimental results through proper techniques.
- Localization of added mass from comparison between mass matrix after and before updation of baseline FE model.

CHAPTER-3

MATHEMATICAL BASIS

The dynamic characteristics of any structure are predicted at first by finite element model simulating the real structure with similar physical properties and boundary conditions. Then, the actual dynamic characteristics of the structure are estimated by some dynamic testing system. Numerical results obtained from FE model are not similar with the experimental results for most of the time due to uncertainty in boundary condition, damping value, damage initiation etc. So, FE model updating becomes inevitable to predict the existing behaviour of the structure. In such cases. System identification becomes an effective tool. System identification using experimental modal analysis is a two stage process. In the first stage, experimental modal analysis is performed on the structure. In the next stage, FE model is updated based on experimental modal parameters.

3.1 Finite Element Modelling of the Plate

In finite element modelling, a numerical model of the real structure is formed. Natural frequencies and corresponding mode shapes are calculated numerically by Eigen value analysis. So, formation of mass matrix and stiffness matrix is required.

For obtaining the stiffness matrix and mass matrix by FE modelling, the principal of virtual work done is used. The principle of virtual work done or Hamilton's principle describes the motion of a system under the action of conservative force. If T is the kinetic energy and U is the potential energy of a system from time t_1 to t_2 due to action of forces, then as per Hamilton's principle

$$I = \int_{t_1}^{t_2} (T - U)dt = \int_{t_1}^{t_2} L\, dt$$

(2)

where, L is the Lagrangian function, L = (T – U) and I is the functional.

Kinetic energy, $T = T(q_1, q_2, q_3 \ldots . q_n, \dot{q}_1, \dot{q}_2, \dot{q}_3 \ldots \ldots \dot{q}_n)$

Potential energy, $U = U(q_1, q_2, q_3 \ldots \ldots q_n)$

where q and $\dot{q}$ are coordinates and coordinate derivative respectively.

Using variational principle, functional I can be written as

$$\delta I = \int_{t_1}^{t_2} (\delta T - \delta U + \delta W_{non}) \qquad (3)$$

This is known as extended Hamiltonian principle. Here, δW_{non} is non-conservative energy. Expressing T and U in differential form-

$$\delta T = \sum_{k=1}^{n}\left(\frac{\partial T}{\partial q_k}\delta q_k + \frac{\partial T}{\partial \dot{q}_k}\,\delta \dot{q}_k\right) \tag{4}$$

$$\delta U = \sum_{k=1}^{n}\left(\frac{\partial U}{\partial q_k}\,\delta q_k\right) \tag{5}$$

So, L depends on the coordinates and coordinative derivatives of the system. It can be represented as

$$L = L\,(q_1, q_2, q_3 \ldots . q_n, \dot{q}_1, \dot{q}_2, \dot{q}_3 \ldots . \dot{q}_n)$$

Now, for a conservative system, the non-conservative energy must be zero. Putting the value of T and U from equation (4) and (5) into equation (3)

Now, one term of equation (6) can be rewritten as

$$\int_{t_1}^{t_2} \frac{\partial T}{\partial \dot{q}_k}\delta \dot{q}_k\, dt = -\int_{t_1}^{t_2} \frac{\partial}{\partial t}\left(\frac{\partial T}{\partial \dot{q}_k}\right)\delta q_k dt \tag{6}$$

Equation (6) now becomes

$$\delta I = \int_{t_1}^{t_2}\left[\sum_{k=1}^{n}\left[\frac{\partial T}{\partial q_k} - \frac{\partial}{\partial t}\left(\frac{\partial T}{\partial \dot{q}_k}\right) - \left(\frac{\partial U}{\partial q_k}\right)\right]\right]\delta q_k dt \tag{7}$$

Now, δq_k is arbitrary and q_k's are independent coordinates. Let us assume $\delta q_1 = 1$ and all other $\delta q_k = 0$.So,

$$\frac{\partial T}{\partial q_1} - \frac{\partial}{\partial t}\left(\frac{\partial T}{\partial \dot{q}_1}\right) - \left(\frac{\partial U}{\partial q_1}\right) = 0 \tag{8}$$

In generalized form, the equation (8) can be expressed as

$$\frac{\partial T}{\partial q_k} - \frac{\partial}{\partial t}\left(\frac{\partial T}{\partial \dot{q}_k}\right) - \left(\frac{\partial U}{\partial q_k}\right) = 0$$

where, k= 1, 2, 3……n. U is independent of $\dot{q}_k$. So, the above equation can be reduces to

$$\frac{\partial L}{\partial q_k} - \frac{\partial}{\partial t}\left(\frac{\partial L}{\partial \dot{q}_k}\right) = 0 \tag{9}$$

This is known as Euler – Lagrange equation of motion.

The work done, W_{non} due to loading F over a system can be written as

$$W_{non} = \int_A \{U\}^T \{F\} dA \tag{10}$$

The strain energy or potential energy, U over the volume of the system can be written as

$$U = \frac{1}{2} \int_V \{\varepsilon\}^T \{\sigma\} dV \tag{11}$$

The kinetic energy, T can be written as

$$T = \frac{1}{2} \int_V \{\dot{u}\}^T \{\rho\} \{\dot{u}\} dV \tag{12}$$

Putting the value of T, U and W_{non} in the equation (3), functional I can be expressed as

$$\delta I = \delta \left[\int_{t_1}^{t_2} \left[\frac{1}{2} \int_V \{\dot{u}\}^T \{\rho\} \{\dot{u}\} dV - \frac{1}{2} \int_V \{\varepsilon\}^T \{\sigma\} dV \right] dt \right] + \int_{t_1}^{t_2} \left[\int_A \{U\}^T \{F\} dA \right] dt \tag{13}$$

An isotropic material requires only two independent parameters E (Young's modulus of elasticity) and ν (poisson's ratio) to express the constitutive relationship matrix and compliance matrix.

The stress-strain relationship for any material can be expressed as

$$\{\sigma\} = [S]\{\epsilon\} \tag{14}$$

or in the other form

$$\{\epsilon\} = [C]\{\sigma\} \tag{15}$$

where, σ is the stress component, ε is the strain component, S is the constitutive relationship matrix and C is the compliance matrix. For an isotropic plate, the stress strain compliance relationship can be written as

$$\begin{Bmatrix} \varepsilon_{xx} \\ \varepsilon_{yy} \\ \gamma_{xy} \\ \gamma_{yz} \\ \gamma_{zx} \end{Bmatrix} = \frac{1}{E} \begin{bmatrix} 1 & -\nu & 0 & 0 & 0 \\ -\nu & 1 & 0 & 0 & 0 \\ 0 & 0 & 2(1+\nu) & 0 & 0 \\ 0 & 0 & 0 & 2(1+\nu) & 0 \\ 0 & 0 & 0 & 0 & 2(1+\nu) \end{bmatrix} \begin{Bmatrix} \sigma_{xx} \\ \sigma_{yy} \\ \tau_{xy} \\ \tau_{yz} \\ \tau_{zx} \end{Bmatrix} \tag{16}$$

The inverse of equation (16) or stress-strain relationship can be written as

$$\begin{Bmatrix}\sigma_{xx}\\ \sigma_{yy}\\ \tau_{xy}\\ \tau_{yz}\\ \tau_{zx}\end{Bmatrix} = \frac{E}{(1+\nu)(1-2\nu)}\begin{bmatrix}(1-\nu) & \nu & 0 & 0 & 0\\ \nu & (1-\nu) & 0 & 0 & 0\\ 0 & 0 & (1-2\nu)/2 & 0 & 0\\ 0 & 0 & 0 & (1-2\nu)/2 & 0\\ 0 & 0 & 0 & 0 & (1-2\nu)\end{bmatrix}\begin{Bmatrix}\varepsilon_{xx}\\ \varepsilon_{yy}\\ \gamma_{xy}\\ \gamma_{yz}\\ \gamma_{zx}\end{Bmatrix} \quad (17)$$

The kinematics equations required for the development of stress-strain relationship, strain-displacement relationship of rectangular plate structure is derived considering the first order shear deformation theory by Reissner and Mindlin. The assumptions made in this theory are "The normal to the mid-plane of the plate which is straight before deformation remains straight but not necessarily perpendicular to the mid-plane after deformation" and "there is a linear variation of displacement across the plate thickness but that the plate thickness does not change during deformation". Apart from the above assumptions, an additional assumption is considered which is "the normal stress through the thickness is ignored".

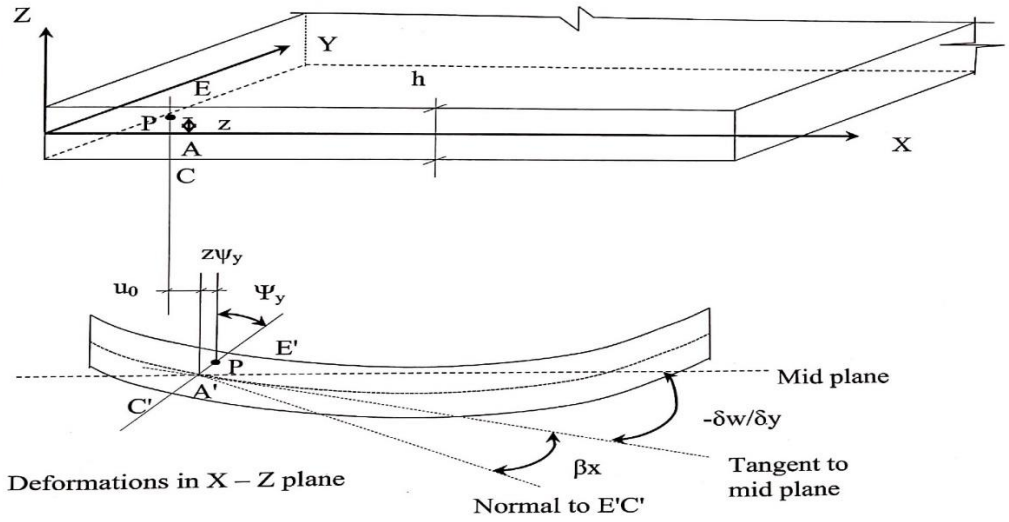

Fig 3.1a: Deformation and displacement of plate structure

In Fig 3.1a the deformation of plate in X-Z plane is shown. Now, it is assumed that u, v and w are the displacements along X, Y and Z directions respectively. Ψ_x, Ψ_y are the rotations in Y-Z and X-Z plane respectively. The displacements of the mid-plane are u_0, v_0 and w_0 in their respective axes. So, the displacement at any point can be written as

$$u = u_0 + z\psi_y$$
$$v = v_0 - z\psi_x$$
$$w = w_0 \quad (18)$$

The total rotations are given by

$$\psi_x = -\beta_y + \frac{\delta w}{\delta y}$$

$$\psi_y = \beta_x - \frac{\delta w}{\delta y} \tag{19}$$

where, β_x and $-\beta_y$ are transverse shear rotations respectively.

Normal strain and shear strain can be expressed as

$$\varepsilon_{xx} = \frac{\partial u}{\partial x} = \frac{\partial u_0}{\partial x} + z\frac{\partial \psi_y}{\partial x} = \varepsilon^0_{xx} + zk_{xx}$$

$$\varepsilon_{yy} = \frac{\partial v}{\partial y} = \frac{\partial v_0}{\partial y} - z\frac{\partial \psi_x}{\partial y} = \varepsilon^0_{yy} + zk_{yy}$$

$$\gamma_{xy} = \frac{\partial u}{\partial y} + \frac{\partial v}{\partial x} = \frac{\partial u_0}{\partial y} + \frac{\partial v_0}{\partial x} + z\left(\frac{\partial \psi_y}{\partial y} - \frac{\partial \psi_x}{\partial x}\right) = \gamma^0_{xy} + zk_{xy}$$

$$\gamma_{yz} = \frac{\partial v}{\partial z} + \frac{\partial w}{\partial y} = -\psi_x + \frac{\partial w_0}{\partial y} = \gamma^0_{yz}$$

$$\gamma_{zx} = \frac{\partial u}{\partial z} + \frac{\partial w}{\partial x} = \psi_y + \frac{\partial w_0}{\partial x} = \gamma^0_{zx} \tag{20}$$

where, $k_{xx} = \frac{\partial \psi_y}{\partial x}$, $k_{yy} = -\frac{\partial \psi_x}{\partial y}$ and $k_{xy} = \left(\frac{\partial \psi_y}{\partial y} - \frac{\partial \psi_x}{\partial x}\right)$ are the curvatures represented in terms of total rotations. Now, stress-strain relationship from equation (17) can be expressed in terms of mid-plane strains and curvatures as

$$\begin{Bmatrix} \sigma_{xx} \\ \sigma_{yy} \\ \tau_{xy} \\ \tau_{yz} \\ \tau_{zx} \end{Bmatrix} = \frac{E}{(1+\nu)(1-2\nu)} \begin{bmatrix} (1-\nu) & \nu & 0 & 0 & 0 \\ \nu & (1-\nu) & 0 & 0 & 0 \\ 0 & 0 & (1-2\nu)/2 & 0 & 0 \\ 0 & 0 & 0 & (1-2\nu)/2 & 0 \\ 0 & 0 & 0 & 0 & (1-2\nu) \end{bmatrix} \left\{ \begin{Bmatrix} \varepsilon^0_{xx} \\ \varepsilon^0_{yy} \\ \gamma^0_{xy} \\ \gamma^0_{yz} \\ \gamma^0_{zx} \end{Bmatrix} + z \begin{Bmatrix} k_{xx} \\ k_{yy} \\ k_{xy} \\ 0 \\ 0 \end{Bmatrix} \right\} \tag{21}$$

The forces and moments which acts on the plate can be expressed in terms of stresses or strains. The forces per unit width and the corresponding moments are shown in Fig 3.1b with their positive direction.

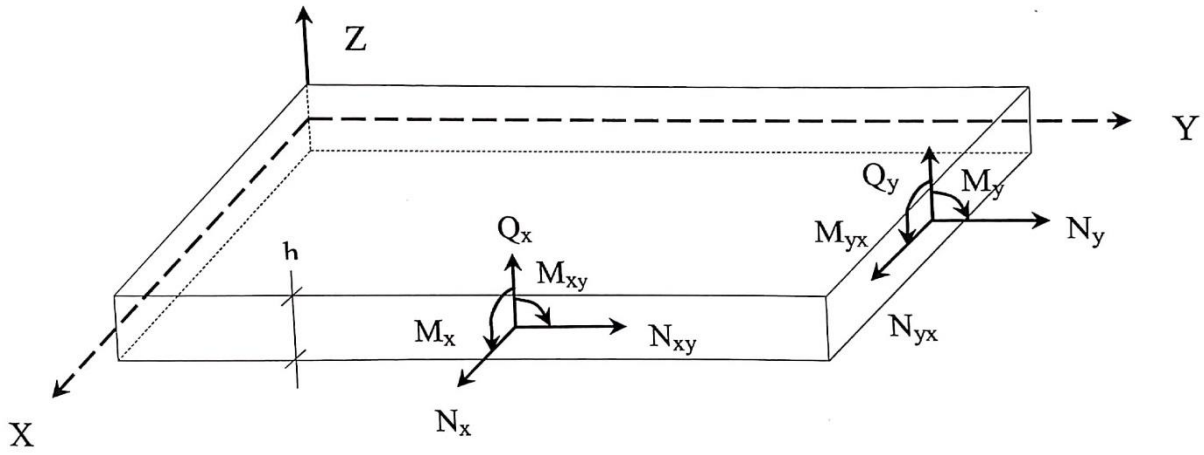

Fig3.1b: Resultant shear forces and bending moments in plate

The thickness of the plate is assumed as 'h'. All the forces are shown with respect to mid-plane of the plate. As force = stress × area, force per unit width = stress × thickness of the plate. Now, the forces per unit width and corresponding moments in terms of stresses or strains can be expressed as

$$\begin{Bmatrix} N_x \\ N_y \\ N_{xy} \end{Bmatrix} = \int_{-h/2}^{+h/2} \begin{Bmatrix} \sigma_{xx} \\ \sigma_{yy} \\ \tau_{xy} \end{Bmatrix} dz = \frac{Eh}{(1+\nu)(1-2\nu)} \begin{bmatrix} (1-\nu) & \nu & 0 \\ \nu & (1-\nu) & 0 \\ 0 & 0 & (1-2\nu)/2 \end{bmatrix} \begin{Bmatrix} \varepsilon_{xx}^0 \\ \varepsilon_{yy}^0 \\ \gamma_{xy}^0 \end{Bmatrix} \tag{22}$$

$$\begin{Bmatrix} M_x \\ M_y \\ M_{xy} \end{Bmatrix} = \int_{-h/2}^{+h/2} \begin{Bmatrix} \sigma_{xx} \\ \sigma_{yy} \\ \tau_{xy} \end{Bmatrix} z dz = \frac{Eh^3}{12(1+\nu)(1-2\nu)} \begin{bmatrix} (1-\nu) & \nu & 0 \\ \nu & (1-\nu) & 0 \\ 0 & 0 & (1-2\nu)/2 \end{bmatrix} \begin{Bmatrix} k_{xx} \\ k_{yy} \\ k_{xy} \end{Bmatrix} \tag{23}$$

The transverse shear forces can be expressed as

$$\begin{Bmatrix} Q_y \\ Q_x \end{Bmatrix} = \int_{-h/2}^{+h/2} \begin{Bmatrix} \tau_{yz} \\ \tau_{zx} \end{Bmatrix} dz = \frac{Eh\alpha}{(1+\nu)(1-2\nu)} \begin{bmatrix} \frac{(1-2\nu)}{2} & 0 \\ 0 & \frac{(1-2\nu)}{2} \end{bmatrix} \begin{Bmatrix} \gamma_{yz}^0 \\ \gamma_{zx}^0 \end{Bmatrix} \tag{24}$$

where, α = shear correction factor. $\alpha = 5/6$ for rectangular section. Equation (22), (23) & (24) can be rewritten in single matrix form as

$$\begin{Bmatrix} N_x \\ N_y \\ N_{xy} \\ M_x \\ M_y \\ M_{xy} \end{Bmatrix} = \frac{E}{(1+\nu)(1-2\nu)} \begin{bmatrix} (1-\nu)h & \nu h & 0 & 0 & 0 & 0 \\ \nu h & (1-\nu)h & 0 & 0 & 0 & 0 \\ 0 & 0 & \frac{(1-2\nu)h}{2} & 0 & 0 & 0 \\ 0 & 0 & 0 & \frac{(1-\nu)h^3}{12} & \frac{\nu h^3}{12} & 0 \\ 0 & 0 & 0 & \frac{\nu h^3}{12} & \frac{(1-\nu)h^3}{12} & 0 \\ 0 & 0 & 0 & 0 & 0 & \frac{(1-2\nu)h^3}{24} \end{bmatrix} \begin{Bmatrix} \varepsilon^0_{xx} \\ \varepsilon^0_{yy} \\ \gamma^0_{xy} \\ k_{xx} \\ k_{yy} \\ k_{xy} \end{Bmatrix} \tag{25}$$

Here, stress strain relationship can be written as

$$\{\sigma\} = [D]\{\varepsilon\} \tag{26}$$

where, $\{\sigma\}$ and $\{\varepsilon\}$ are stress vector at any point in the element and the corresponding strain vector respectively. [D] is the stress strain relationship matrix or constitutive relationship matrix. Again, [D] matrix can be represented as

$$[D] = \begin{bmatrix} D_{bending} \\ D_{shear} \end{bmatrix}$$

where,

$$D_{bending} = \frac{E}{(1+\nu)(1-2\nu)} \begin{bmatrix} (1-\nu)h & \nu h & 0 & 0 & 0 & 0 \\ \nu h & (1-\nu)h & 0 & 0 & 0 & 0 \\ 0 & 0 & \frac{(1-2\nu)h}{2} & 0 & 0 & 0 \\ 0 & 0 & 0 & \frac{(1-\nu)h^3}{12} & \frac{\nu h^3}{12} & 0 \\ 0 & 0 & 0 & \frac{\nu h^3}{12} & \frac{(1-\nu)h^3}{12} & 0 \\ 0 & 0 & 0 & 0 & 0 & \frac{(1-2\nu)h^3}{24} \end{bmatrix} \tag{27}$$

and

$$D_{shear} = \frac{Eh\alpha}{(1+\nu)(1-2\nu)} \begin{bmatrix} \frac{(1-2\nu)}{2} & 0 \\ 0 & \frac{(1-2\nu)}{2} \end{bmatrix}$$

In order to predict the exact analytical solution of a structure of complex geometry along with other factors such as boundary conditions, material non-homogeneity, it is not possible to use the thorough mathematical process by hand. In this situation, finite element analysis is the best numerical method to analyze any type of structure with any kind of boundary condition.

But in this method, the accuracy of the solution greatly depends on the number and arrangement of elemental mesh of the numerical model. If all the assumptions

during finite element modelling are taken perfectly, then the predicted results will surely match with the experimental results. A generalized governing equation is developed here for finite element modelling.

In order to predict the analytical frequencies and mode shape, it is required to derive the mass and stiffness matrix of the structure. At first, the mass and stiffness matrix of the 4 noded iso-parametric elements has been derived. One of such elements is shown in fig with node number and natural coordinates (ξ and η) of each node. At each node, 5 degrees of freedom (u, v, w, ψ_x, ψ_y) have been considered.

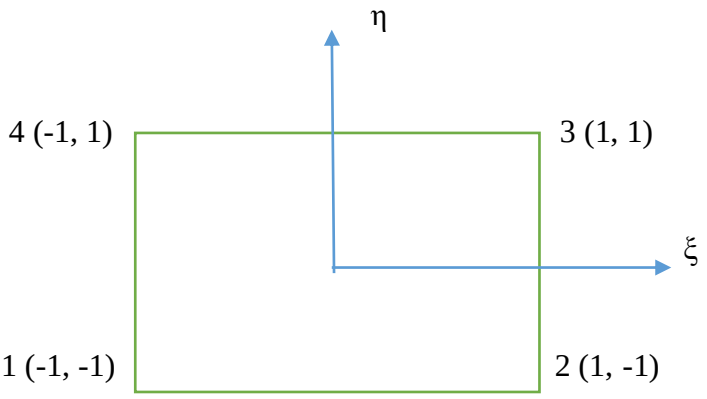

Fig 3.1c: Four noded element with natural coordinates

The shape functions (also called interpolation functions) at each node of the quadrilateral element can be found out as

$$N_1 = \frac{1}{4}(1-\xi)(1-\eta);$$
$$N_2 = \frac{1}{4}(1+\xi)(1-\eta)$$
$$N_3 = \frac{1}{4}(1+\xi)(1+\eta)$$
$$N_4 = \frac{1}{4}(1-\xi)(1+\eta) \quad (28)$$

The displacements and rotations at any point within the element can be expressed in terms of shape functions and displacements, rotations at the nodes.

$$u = \sum_{i=1}^{4} N_i u_i \; ; v = \sum_{i=1}^{4} N_i v_i \; ; w = \sum_{i=1}^{4} N_i w_i \; ; \psi_x = \sum_{i=1}^{4} N_i \psi_{xi} \; ; \psi_y = \sum_{i=1}^{4} N_i \psi_{yi}$$

where, N_i is the shape function and u_i, v_i, w_i, ψ_{xi}, ψ_{yi} are the nodal displacements and rotations of the i^{th} node.

In matrix form, it can be written as

$$\begin{Bmatrix} u \\ v \\ w \\ \psi_x \\ \psi_y \end{Bmatrix} = \sum_{i=1}^{4} \begin{bmatrix} N_i & 0 & 0 & 0 & 0 \\ 0 & N_i & 0 & 0 & 0 \\ 0 & 0 & N_i & 0 & 0 \\ 0 & 0 & 0 & N_i & 0 \\ 0 & 0 & 0 & 0 & N_i \end{bmatrix} \begin{Bmatrix} u_i \\ v_i \\ w_i \\ \psi_{xi} \\ \psi_{yi} \end{Bmatrix}$$

or, $$\{u\} = [N]\{d\} \tag{29}$$

Here, d is the nodal displacement vector and N is the shape function.

From equation (20), strains and curvatures are written in matrix form as

$$\begin{Bmatrix} \varepsilon_{xx}^0 \\ \varepsilon_{yy}^0 \\ \gamma_{xy}^0 \\ k_{xx} \\ k_{yy} \\ k_{xy} \\ \gamma_{yz}^0 \\ \gamma_{zx}^0 \end{Bmatrix} = \begin{bmatrix} \frac{\partial}{\partial x} & 0 & 0 & 0 & 0 \\ 0 & \frac{\partial}{\partial y} & 0 & 0 & 0 \\ \frac{\partial}{\partial y} & \frac{\partial}{\partial x} & 0 & 0 & 0 \\ 0 & 0 & 0 & 0 & \frac{\partial}{\partial x} \\ 0 & 0 & 0 & -\frac{\partial}{\partial y} & 0 \\ 0 & 0 & 0 & -\frac{\partial}{\partial x} & \frac{\partial}{\partial y} \\ 0 & 0 & \frac{\partial}{\partial y} & -1 & 0 \\ 0 & 0 & \frac{\partial}{\partial x} & 0 & 1 \end{bmatrix} \begin{Bmatrix} u_0 \\ v_0 \\ w_0 \\ \psi_x \\ \psi_y \end{Bmatrix} \tag{30}$$

Equation (30) can be expressed by putting the values of $u_0, v_0, w_0, \psi_x \; and \; \psi_y$ using equation (29) as

$$\begin{Bmatrix} \varepsilon_{xx}^0 \\ \varepsilon_{yy}^0 \\ \gamma_{xy}^0 \\ k_{xx} \\ k_{yy} \\ k_{xy} \\ \gamma_{yz}^0 \\ \gamma_{zx}^0 \end{Bmatrix} = \sum_{i=1}^{4} \begin{bmatrix} \frac{\partial N_i}{\partial x} & 0 & 0 & 0 & 0 \\ 0 & \frac{\partial N_i}{\partial y} & 0 & 0 & 0 \\ \frac{\partial N_i}{\partial y} & \frac{\partial N_i}{\partial x} & 0 & 0 & 0 \\ 0 & 0 & 0 & 0 & \frac{\partial N_i}{\partial x} \\ 0 & 0 & 0 & -\frac{\partial N_i}{\partial y} & 0 \\ 0 & 0 & 0 & -\frac{\partial N_i}{\partial x} & \frac{\partial N_i}{\partial y} \\ 0 & 0 & \frac{\partial N_i}{\partial y} & -N_i & 0 \\ 0 & 0 & \frac{\partial N_i}{\partial x} & 0 & N_i \end{bmatrix} \begin{Bmatrix} u_{0i} \\ v_{0i} \\ w_{0i} \\ \psi_{xi} \\ \psi_{yi} \end{Bmatrix}$$

or, $$\{\varepsilon\} = [B]\{d\} \tag{31}$$

where, $\{\varepsilon\}$ is the strain vector, $\{d\}$ is the nodal displacement vector and [B] is the strain displacement relationship matrix. Again, [B] matrix can be represented as

$$[B] = \begin{bmatrix} B_{bending} \\ B_{shear} \end{bmatrix}$$

where,

$$B_{bending} = \sum_{i=1}^{4} \begin{bmatrix} \frac{\partial N_i}{\partial x} & 0 & 0 & 0 & 0 \\ 0 & \frac{\partial N_i}{\partial y} & 0 & 0 & 0 \\ \frac{\partial N_i}{\partial y} & \frac{\partial N_i}{\partial x} & 0 & 0 & 0 \\ 0 & 0 & 0 & 0 & \frac{\partial N_i}{\partial x} \\ 0 & 0 & 0 & -\frac{\partial N_i}{\partial y} & 0 \\ 0 & 0 & 0 & -\frac{\partial N_i}{\partial x} & \frac{\partial N_i}{\partial y} \end{bmatrix}$$

and (32)

$$[B_{shear}] = \sum_{i=1}^{4} \begin{bmatrix} 0 & 0 & \frac{\partial N_i}{\partial y} & -N_i & 0 \\ 0 & 0 & \frac{\partial N_i}{\partial x} & 0 & -N_i \end{bmatrix}$$

3.2 Stiffness matrix formulation

Total strain energy (U) stored in an element can be written as per equation (11)

$$U = \frac{1}{2}\int_V \{\varepsilon\}^T\{\sigma\}dV \quad (33)$$

Putting the value of $\{\varepsilon\}$ from equation (31) in equation (26), the stress vector can be written as

$$\{\sigma\} = [D]\,[B]\,\{d\} \quad (34)$$

As the effect of thickness of the plate is employed in matrix [D], changing the integral from volume to area and substituting value of $\{\varepsilon\}$ from equation (31) and $\{\sigma\}$ from equation (34) in equation (33), it is obtained

$$U = \frac{1}{2}\int_0^a \int_0^b \{d\}^T\,[B]^T[D]\,[B]\,\{d\}dxdy \quad (35)$$

where, a and b are the length and width of the element respectively.

If {F} is the element load vector and {d} is the corresponding displacement vector, then from minimum potential energy principle-

$$[F] = [K]\,\{d\} \quad (36)$$

where, [K] is the element stiffness matrix.

The strain energy (U) stored in the stored in the element can be written as

$$U = \frac{1}{2}\{d\}^T[K]\,\{d\} \quad (37)$$

Comparing equation (35) and (37), stiffness matrix can be written as

$$[K] = \int_0^a \int_0^b [B]^T [D]\,[B]\,dx\,dy \tag{38}$$

The elemental area using natural coordinate can be written as

$$dx\,dy = |J| d\xi\,d\eta$$

Where, $|J|$ is the Jacobian matrix and it is expressed as

$$[J] = \begin{bmatrix} \frac{\partial x}{\partial \xi} & \frac{\partial y}{\partial \xi} \\ \frac{\partial x}{\partial \eta} & \frac{\partial x}{\partial \eta} \end{bmatrix}$$

Now, stiffness matrix from (38) can be written as

$$[K] = \int_{-1}^{+1} \int_{-1}^{+1} [B]^T [D]\,[B]\,|J| d\xi\,d\eta \tag{39}$$

In numerical analysis, numerical integration for stiffness matrix evaluation is performed using Gauss Quadrature method at predefined Gauss point. 2×2 sampling points are considered in numerical analysis.

3.3 Mass matrix formulation

As per the force equations of equilibrium, the stress resultants along X, Y and Z directions are calculated as

$$\begin{aligned} \frac{\partial \sigma_{xx}}{\partial x} + \frac{\partial \tau_{xy}}{\partial y} + \frac{\partial \tau_{zx}}{\partial z} &= \rho_m \frac{\partial^2 u}{\partial t^2} \\ \frac{\partial \tau_{xy}}{\partial x} + \frac{\partial \sigma_{yy}}{\partial y} + \frac{\partial \tau_{zy}}{\partial z} &= \rho_m \frac{\partial^2 v}{\partial t^2} \\ \frac{\partial \tau_{xz}}{\partial x} + \frac{\partial \tau_{yz}}{\partial y} + \frac{\partial \sigma_{zz}}{\partial z} &= \rho_m \frac{\partial^2 v}{\partial t^2} \end{aligned} \tag{40}$$

Substituting the value of u, v and w from equation (18) and integrated the resulted equation with limit –h/2 to +h/2, it is obtained

$$\begin{aligned} \frac{\partial N_x}{\partial x} + \frac{\partial N_{yx}}{\partial y} &= I\ddot{u}_0 + P\ddot{\psi}_y \\ \frac{\partial N_{xy}}{\partial x} + \frac{\partial N_y}{\partial y} &= I\ddot{v}_0 - P\ddot{\psi}_x \\ \frac{\partial Q_x}{\partial x} + \frac{\partial Q_y}{\partial y} + q &= I\ddot{w}_0 \end{aligned} \tag{41}$$

Establishing the moment relationship equations and integrating the resulted equation with limit –h/2 to +h/2, it is obtained

$$\frac{\partial M_x}{\partial x}+\frac{\partial M_{yx}}{\partial y}-Q_x=P\ddot{u}_0+Q\ddot{\psi}_y$$
$$\frac{\partial M_{xy}}{\partial x}+\frac{\partial M_y}{\partial y}-Q_y=P\ddot{v}_0+Q\ddot{\psi}_x \quad (42)$$

Equation (41) and (42) is arranged in matrix form as

$$\begin{bmatrix} \frac{\partial N_x}{\partial x}+\frac{\partial N_{yx}}{\partial y} \\ \frac{\partial N_{xy}}{\partial x}+\frac{\partial N_y}{\partial y} \\ \frac{\partial Q_x}{\partial x}+\frac{\partial Q_y}{\partial y}+q \\ \frac{\partial M_x}{\partial x}+\frac{\partial M_{yx}}{\partial y}-Q_x \\ \frac{\partial M_{xy}}{\partial x}+\frac{\partial M_y}{\partial y}-Q_y \end{bmatrix}=\begin{bmatrix} I & 0 & 0 & 0 & P \\ 0 & I & 0 & -P & 0 \\ 0 & 0 & I & 0 & 0 \\ P & 0 & 0 & 0 & Q \\ 0 & P & 0 & -Q & 0 \end{bmatrix}\begin{Bmatrix} \ddot{u}_0 \\ \ddot{v}_0 \\ \ddot{w}_0 \\ \ddot{\psi}_x \\ \ddot{\psi}_y \end{Bmatrix} \quad (43)$$

So, the inertia matrix is computed as

$$[\rho]=\begin{bmatrix} I & 0 & 0 & 0 & P \\ 0 & I & 0 & -P & 0 \\ 0 & 0 & I & 0 & 0 \\ P & 0 & 0 & 0 & Q \\ 0 & P & 0 & -Q & 0 \end{bmatrix}$$

where,

$$I=\int_{-h/2}^{+h/2}\rho_m\,dz$$
$$P=\int_{-h/2}^{+h/2}\rho_m\,z\,dz$$
$$Q=\int_{-h/2}^{+h/2}\rho_m\,z^2\,dz$$

Now, putting the value of {u} from equation (29) into equation (12), the kinetic energy can be rewritten as

$$T=\frac{1}{2}\int_A\{\dot{d}\}^T[N]^T[\rho][N]\{\dot{d}\}dxdy \quad (44)$$

Kinetic energy, T can be expressed as

$$T = \frac{1}{2}\{\dot{d}\}^T[M]\{\dot{d}\} \tag{45}$$

From equation (44) and (45), mass matrix for each element can be written as

$$[M] = \int_0^a \int_0^b [N]^T[\rho]\,[N]\; dx\, dy$$

$$[M] = \int_{-1}^{+1} \int_{-1}^{1} [N]^T[\rho]\,[N]\;|J| d\xi\, d\eta \tag{46}$$

3.4 Condensation of Mass and Stiffness matrix

The basic equation related to the dynamic behaviour of a system with n degree of freedom is as follows-

$$[M]\{\ddot{x}(t)\} + [C]\{\dot{x}(t)\} + [K]\{x(t)\} = \{f(t)\} \tag{47}$$

where, x(t), $\dot{x}(t)$, $\ddot{x}(t)$ denote the displacement, velocity and acceleration responses in time domain respectively. [M] is the system mass matrix, [C] is the system damping matrix, [K] is the system stiffness matrix. f(t) denotes the time dependent external force acting on the system. Assuming free vibration and undamped system, equation (47) becomes

$$[M]\{\ddot{x}(t)\} + [K]\{x(t)\} = 0 \tag{48}$$

The solution of the above eigenvalue problem can be solved in following way

$$([K] - \omega_i^2[M])\emptyset_i = 0, \text{ where i= 1, 2, 3…….n} \tag{49}$$

Equation (49) gives the i[th] frequency ω_i and corresponding i[th] mode shape $\emptyset_i$. It is not possible to measure all the degrees of freedom of the system experimentally due to lack of costly instruments. Master dof (measured) and slave dof (unmeasured) are chosen depending on the ratio of diagonal terms of [K] and corresponding diagonal terms of the [M] matrix. Slave dof are those which give large K/M ratio of the corresponding diagonal terms. But practically choosing of the slave dof are done depending on the availability of measuring instruments. The generalized dynamic equation (47) is partitioned and can be written as in the following form

$$\begin{bmatrix} M_{aa} & M_{ab} \\ M_{ba} & M_{bb} \end{bmatrix}\begin{Bmatrix} \ddot{x}_a \\ \ddot{x}_b \end{Bmatrix} + \begin{bmatrix} C_{aa} & C_{ab} \\ C_{ba} & C_{bb} \end{bmatrix}\begin{Bmatrix} \dot{x}_a \\ \dot{x}_b \end{Bmatrix} + \begin{bmatrix} K_{aa} & K_{ab} \\ K_{ba} & K_{bb} \end{bmatrix}\begin{Bmatrix} x_a \\ x_b \end{Bmatrix} = \begin{Bmatrix} f_a \\ f_b \end{Bmatrix} \tag{50}$$

where, x_a, $\dot{x}_a$, $\ddot{x}_a$ denote the displacement, velocity and acceleration responses to be preserved and x_b, $\dot{x}_b$, $\ddot{x}_b$ denote the displacement, velocity and acceleration responses to be eliminated.

Breaking down the equation (50) in the following form

$$[M_{aa}]\{\ddot{x}_a\} + [M_{ab}]\{\ddot{x}_b\} + [C_{aa}]\{\dot{x}_a\} + [C_{ab}]\{\dot{x}_b\} + [K_{aa}]\{x_a\} + [K_{ab}]\{x_b\} = \{f_a\} \tag{51}$$

$$[M_{ba}]\{\ddot{x}_a\} + [M_{bb}]\{\ddot{x}_b\} + [C_{ba}]\{\dot{x}_a\} + [C_{bb}]\{\dot{x}_b\} + [K_{ba}]\{x_a\} + [K_{bb}]\{x_b\} = \{f_b\} \tag{52}$$

In order to remove the degrees of freedom identified for elimination, a condensation procedure is carried out and described below.

Static condensation

Ignoring the mass and damping matrix, equation (52) becomes

$$\{x_b\} = [K_{bb}]^{-1}[\{f_b\} - [K_{ba}]\{x_a\}] \tag{53}$$

Equation (53) can be rewritten as

$$\{x_b\} = [G_0]\{x_a\} + \{x_b^0\} \tag{54}$$

where, $[G_0] = -[K_{bb}]^{-1}[K_{ba}]$ and $\{x_b^0\} = [K_{bb}]^{-1}\{f_b\}$

Dynamic condensation

In this case, the mass effect of the system is considered but the damping effect is ignored. The acceleration of the eliminated points can be written using equation (54) as

$$\{\ddot{x}_b\} \cong [G_0]\{\ddot{x}_a\} \tag{55}$$

Putting the value of $\{\ddot{x}_b\}$ from equation (55) in equation (52), it is obtained

$$\{x_b\} = [K_{bb}]^{-1}[(\{f_b\} - [K_{ba}]\{x_a\}) - ([M_{ba}] + [M_{bb}][G_0])\{\ddot{x}_a\}] \tag{56}$$

Rearranging the equation (56) and using the value of $[G_0]$, it is obtaineed

$$\{x_b\} = [K_{bb}]^{-1}[\{f_b\} - ([M_{ba}] - [M_{bb}][G_0])\{\ddot{x}_a\}] + [G_0]\{x_a\} \tag{57}$$

Putting the values of $\{\ddot{x}_b\}$ and $\{x_b\}$ from equation (55) and (57) respectively in equation (51) and keeping the damping matrix zero, it is obtained

$$[M_{aa}]\{\ddot{x}_a\} + [M_{ab}][G_0]\{\ddot{x}_a\} + [K_{aa}]\{x_a\} + [K_{ab}]([K_{bb}]^{-1}[\{f_b\} - ([M_{ba}] + [M_{bb}][G_0])\{\ddot{x}_a\}] + [G_0]\{x_a\}) = \{f_a\} \tag{58}$$

Rearranging equation (58), it is obtained

$$\left[[M_{aa}] + [M_{ab}][G_0] + [K_{ab}][K_{bb}]^{-1}([M_{ba}] + [M_{bb}][G_0])\right]\{\ddot{x}_a\} + ([K_{aa}] + [K_{ab}][G_0])\{x_a\} = \{f_a\} - G_0^T\{f_b\} \tag{59}$$

Taking $\{f_b\} = 0$, equation (59) can be rewritten as

$$[M_{aa}]_{dense}\{\ddot{x}_a\} + [K_{aa}]_{dense}\{x_a\} = \{f_a\} \tag{60}$$

where, $[M_{aa}]_{dense} = \left[[M_{aa}] + [M_{ab}][G_0] + [K_{ab}][K_{bb}]^{-1}([M_{ba}] + [M_{bb}][G_0])\right]$ and

$[K_{aa}]_{dense} = ([K_{aa}] + [K_{ab}][G_0])$

$[M_{aa}]_{dense}$ and $[K_{aa}]_{dense}$ are the reduced/condensed mass and stiffness matrix respectively and those matrices are used for finite element analysis.

3.5 Mass normalization of analytical mode shape

After calculating the ith frequency (ω_i) and corresponding ith mode shape ($\emptyset_i$) from eigenvalue problem using reduced mass and stiffness matrix, the generalized mass for different modes are calculated as

$$M_{gen,i} = \{\emptyset_i^T\}[M]\{\emptyset_i\} \tag{61}$$

where, $M_{gen,i}$ is the generalized mass of the ith mode and [M] is the reduced/condensed mass matrix.

Now, mass normalized mode shape $\{\emptyset_i\}_{norm}$ is calculated as

$$\{\emptyset_i\}_{norm} = \frac{\{\emptyset_i\}}{\sqrt{M_{gen,i}}} \tag{62}$$

3.6 Mass normalization of experimental mode shape

The equation (47) can be written for harmonic excitation as

$m_i\ddot{x}_i + c_i\dot{x}_i + k_i x_i = f_i(t,\omega)$ where, i= mode no = 1, 2, 3…….n.

m_i = generalized mass = $\{\emptyset_i^T\}[M]\{\emptyset_i\}$

k_i = generalized stiffness = $\{\emptyset_i^T\}[K]\{\emptyset_i\} = m_i\omega_i^2$

c_i = modal damping = $2\xi_i m_i \omega_i$

f_i = generalized force = $\{\emptyset_i^T\}\{f\}\sin\omega t$

$\emptyset_i$ = mode shape vector for ithmode

Now, modal impedance value can be calculated as

$$|Z_i(\omega_i)| = k_i\sqrt{\left[1 - \left(\frac{\omega^2}{\omega_i{}^2}\right)\right]^2 + \left[2\xi_i\frac{\omega}{\omega_i}\right]^2} \tag{63}$$

If the driving frequency ω = i^{th} natural frequency of the structure (ω_i), then the generalized stiffness and mass for the i^{th} mode can be written as

$$k_i = \frac{|Z_i(\omega = \omega_i)|}{2\xi_i} \tag{64}$$

$$m_i = \frac{k_i}{{\omega_i}^2} \tag{65}$$

Using generalized mass, the mass normalized experimental mode shape can be calculated as

$$\{\emptyset_i\}_{norm} = \frac{\{\emptyset_i\}}{\sqrt{m_i}} \tag{66}$$

3.8 Model updating techniques

System identification is done by model updating. Various model updating techniques are available globally based on experimental results. As modal parameters are estimated using experimental modal analysis, updation algorithm should be based on experimental modal parameters. Lagrange Multiplier method is one of such techniques which is discussed by **Baruch [5]**. Detailed description of the method is given below-

3.8.1 Lagrange Multiplier method

3.8.1.1 First variation: Mass matrix updation followed by stiffness matrix updation

At first, the mode shapes are mass normalized using analytical mass matrix by following equation

$$\{\emptyset_{EM}\} = \{\emptyset_E\}[\{\emptyset_E\}^T[M]\{\emptyset_E\}]^{-1/2} \tag{67}$$

where, $\{\emptyset_{EM}\}$ is mass normalized experimentally measured mode shape, $\{\emptyset_E\}$ is experimentally measured mode shape, [M] is analytical mass matrix which is assumed to be symmetric.

The basic equation of vibration

$$M\ddot{x} + Kx = 0 \tag{68}$$

where, M is the mass matrix, K is the stiffness matrix and x is the displacement.

If, M_U is the updated mass matrix, K_U is the updated stiffness matrix, $\emptyset_{EM}$ is the experimental measured mode shape and ω is the experimentally measured angular velocity, then following two orthogonality conditions are to be fulfilled.

$$\emptyset_{EM}{}^T M_U \emptyset_{EM} = I\,;\ \emptyset_{EM}{}^T K_U \emptyset_{EM} = \omega^2 \tag{69}$$

A new vector p is introduced which is defined as

$$p = K_U^{1/2} \emptyset_{EM}$$

Now, equation (68) can be written as

$$K_U^{-1/2} M K_U^{1/2} \ddot{p} + p = 0 \tag{70}$$

The norm is expressed as

$$\text{Norm (d)} = \frac{1}{2} \left\| K_U^{-\frac{1}{2}} (M_U - M) K_U^{\frac{1}{2}} \right\| \tag{71}$$

Where, M is the analytical mass matrix.

Minimization of the Norm with the constraint of orthogonality $(\emptyset_{EM}{}^T M_U \emptyset_{EM}) = I$) yields

$$M_U = M - K_U \emptyset_{EM} (\emptyset_{EM}{}^T K_U \emptyset_{EM})^{-1} (\emptyset_{EM}{}^T M \emptyset_{EM} - I)(\emptyset_{EM}{}^T K_U \emptyset_{EM})^{-1} \emptyset_{EM}{}^T K_U \tag{72}$$

By using the equilibrium equation ($M_U X \omega^2 = K_U X$), the following equation is obtained-

$$M_U = M - M \emptyset_{EM} (\emptyset_{EM}{}^T M \emptyset_{EM})^{-1} (\emptyset_{EM}{}^T M \emptyset_{EM} - I)(\emptyset_{EM}{}^T M \emptyset_{EM})^{-1} \emptyset_{EM}{}^T M \tag{73}$$

where, I is the identity matrix.

Updated stiffness matrix as given by Baruch [5]-

$$K_U = K - (K \emptyset_{EM} \emptyset_{EM}{}^T M_U) - (M_U \emptyset_{EM} \emptyset_{EM}{}^T K) + (M_U \emptyset_{EM} \emptyset_{EM}{}^T K \emptyset_{EM} \emptyset_{EM}{}^T M_U) + (M_U \emptyset_{EM} \omega^2 \emptyset_{EM}{}^T M_U) \tag{74}$$

where, K is the analytical stiffness matrix.

3.8.1.2 Second variation: Stiffness matrix updation followed by mass matrix updation

In this process, the experimental mode shapes are normalized using analytical stiffness matrix using the following equation-

$$\emptyset_{ES} = \omega \, \emptyset_E (\emptyset_E^T \, K \, \emptyset_E)^{-1/2} \tag{75}$$

where, $\emptyset_{ES}$ is the stiffness normalized experimentally measured mode shape, $\emptyset_E$ is the experimentally measured mode shape, K is the analytical stiffness matrix and ω is the experimentally measured angular velocity.

The natural norm to be minimized to obtain the updated stiffness matrix is given by-

$$\text{Norm (f)} = \frac{1}{2} \left\| M_U^{-\frac{1}{2}} (K_U - K) M_U^{\frac{1}{2}} \right\| \tag{76}$$

where, M_U is the updated mass matrix and K_U is the updated mass matrix and K is the analytical mass matrix.

By using Lagrange multipliers, the constraint $(\emptyset_{ES}^{T} K_U \emptyset_{ES} = \omega^2)$ is incorporated into the norm f.

Minimization of the so-obtained Lagrange function with to respect K_U yields-

$$K_U = K - M_U \emptyset_{ES} (\emptyset_{ES}{}^{T} K \emptyset_{ES} - \omega^2) \emptyset_{ES}{}^{T} M_U \tag{77}$$

By using the equilibrium equation $(M_U X \omega^2 = K_U X)$, equation (77) can be written as-

$$K_U = K - K_U \emptyset_{ES} \omega^{-2} (\emptyset_{ES}{}^{T} K \emptyset_{ES} - \omega^2) \omega^{-2} \emptyset_{ES}{}^{T} K_U \tag{78}$$

Multiplication of equation (78) by $\emptyset_{ES}$ and second usage of the equilibrium equation finally yields-

$$K_U = K - K\emptyset_{ES} \left(\emptyset_{ES}{}^{T} K \emptyset_{ES}\right)^{-1} (\emptyset_{ES}{}^{T} K \emptyset_{ES} - \omega^2)(\emptyset_{ES}{}^{T} K \emptyset_{ES})^{-1} \emptyset_{ES}{}^{T} K \tag{79}$$

Updated mass matrix derived by Baruch [5] is given below-

$$M_U = M - \left(M \emptyset_{ES} \omega^{-2} \emptyset_{ES}{}^{T} K_U\right) - \left(K_U \emptyset_{ES} \omega^{-2} \emptyset_{ES}{}^{T} M\right) + \left(K_U \emptyset_{ES} \omega^{-4} \emptyset_{ES}{}^{T} K_U\right) + \left(K_U \emptyset_{ES} \omega^{-2} \emptyset_{ES}{}^{T} M \emptyset_{ES} \omega^{-2} \emptyset_{ES}{}^{T} K_U\right) \tag{80}$$

where, M is the analytical mass matrix.

CHAPTER-4

EXPERIMENTAL SETUP AND PROCEDURE

Modal parameters estimated by analytical model does not always represent the actual behaviour of the existing structure. For proper estimation of the dynamic behaviour of any structure, experimental measurements are necessary. In present thesis work, experimental modal analysis is performed in the laboratory to extract the modal parameter of plate vibration using Hammer Test. Mass normalization of the mode shapes is done using vibration parameters obtained through shaker test. Details of the experimental setup and test procedure is described below.

4.1 Details of Hammer test:

Experimental setup is established in the laboratory where an Aluminium plate is fixed along one edge and other three edges are kept free. So, ideally it behaves like a cantilever plate as shown in the Fig 4.1a. The plate is discretized into 16 numbers of 4 noded iso-parametric elements (shown in Fig 4.1b) which create 25 nodes (5 along length × 5 along width) in the plate. This experiment can be performed in two different ways- i) striking the hammer at all the nodes and measuring the response at a particular node ii) striking the hammer at a particular node and measuring the response at all the nodes. In present experiment, the hammer is roved at all the nodes and response is measured at a single node. It is also called Roving Hammer Test.

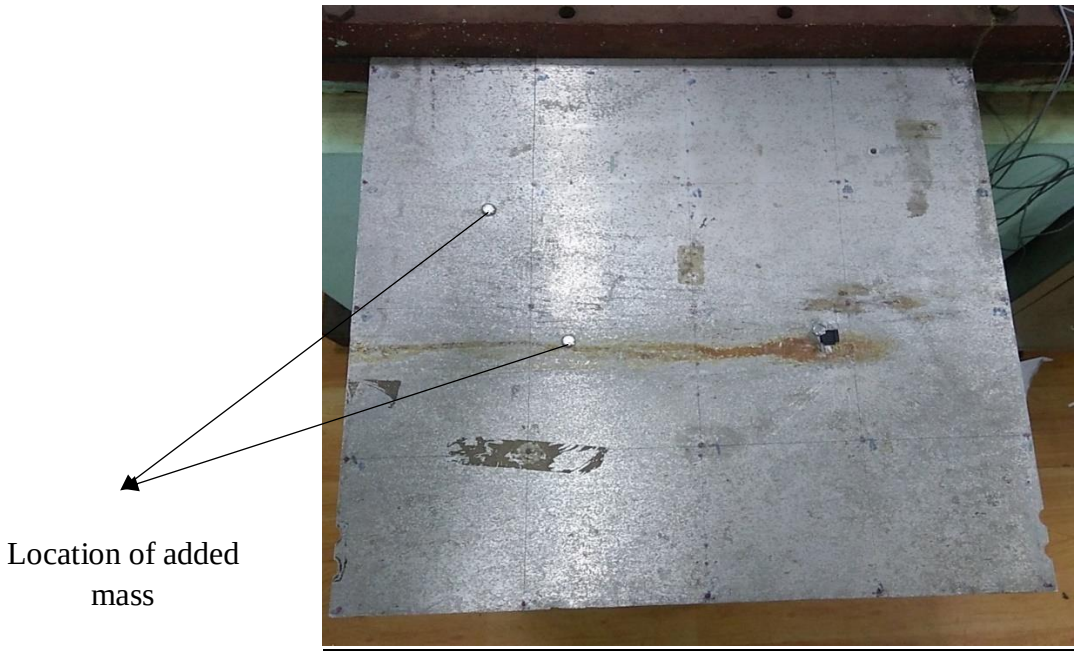

Fig 4.1a: Actual experimental plate

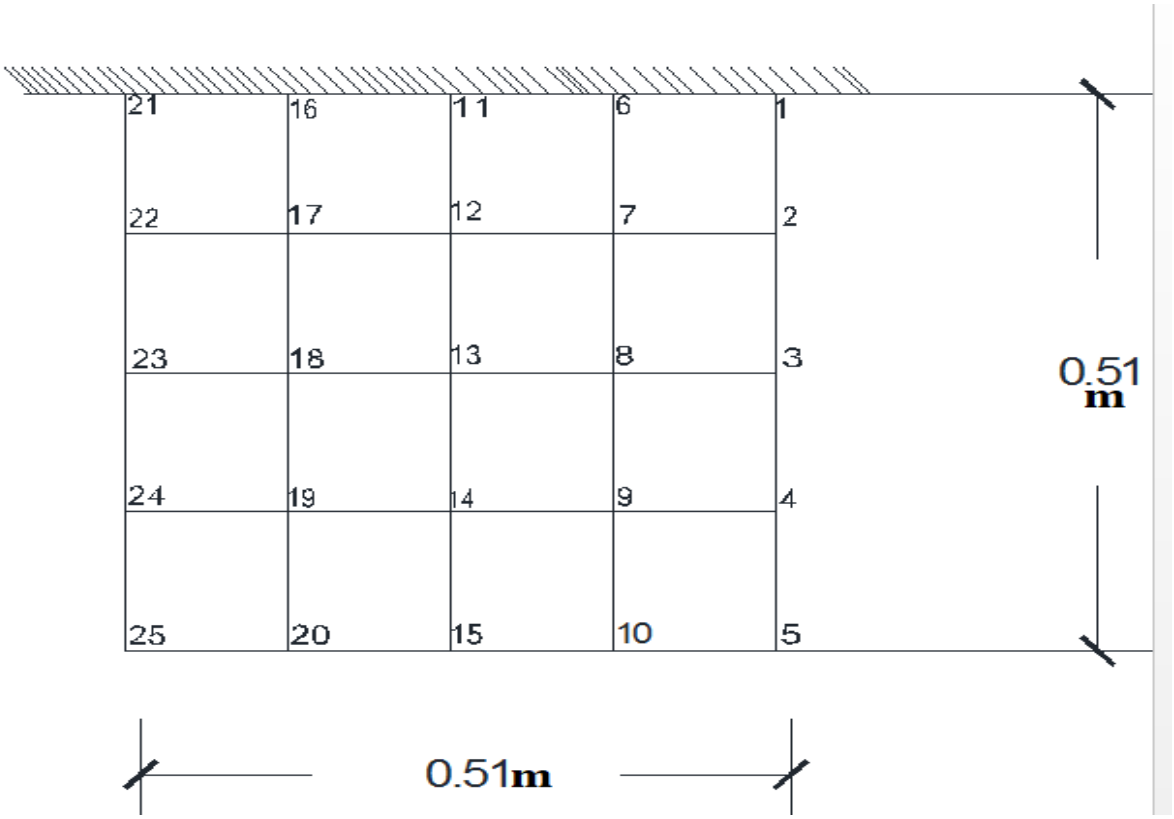

Fig 4.1b: Schematic representation of the plate

Hardware and Software used:

Hardware accessories used for hammer test-

i. Impact hammer attached with load cell to measure the excitation (B&K, Type-8206-003).
ii. Accelerometer to measure the acceleration as response (B&K, Type-4507).
iii. Data Acquisition system to collect the excitement and response data from hammer and accelerometer (B&K).
iv. BNC (Bayonet Neill-Cocelman) cable to connect the input and output devices with the Data Acquisition system.
v. Personal computer to process the signal received via Data Acquisition system.
vi. LAN interface to connect the Data Acquisition system to the computer.
vii. Dongle for specific software authentication.

Software used for data collection and extraction are as follows:

i. PULSE LabShop version 15.1.0 software for Fast Fourier Transformation (FFT) of the signal and measurement of Frequency Response Function (FRF).
ii. ME'scope VES v5.1 software for extraction of modal parameters from measured FRF data.

Excitation measurement:

Excitation or impulse load on the plate is given by an impact hammer. Impact hammer is specially designed to produce vibration of short duration when the target structure is

stroked and particularly used in laboratory scale. A load cell is mounted on it to convert the mechanical load into proportional signal. Different impact tips are used depending on required energy content of excitation. Soft rubber tip produces low frequency vibration as energy content is less and hard metal tip produces high frequency vibration as energy content is high. Impact hammer attached with load cell and metal tip is shown in Fig 4.1c

Fig 4.1c: B&K 8206-003 type impact hammer

Response measurement:

Dynamic response of any structure can be measured as acceleration, velocity or displacement. Here, an accelerometer is used to measure the acceleration at a particular point. This is uni-axial accelerometer which measures the acceleration in Z direction only. A typical accelerometer is shown in Fig 4.1d

Fig 4.1d: B&K 4507 type accelerometer

Data Acquisition system:

B&K Data Acquisition system is used to collect the excitation and response data from hammer and accelerometer. It is connected with the PC through a LAN cable. Data Acquisition system is shown in Fig 4.1e

Fig 4.1e: B&K Data Acquisition system

Procedure:

Hammer test is performed to extract the experimental modal parameters (natural frequency and mode shapes) of plate vibration. Impulse load is applied at every node by roving the impact hammer (shown in Fig 4.1c). An accelerometer (shown in Fig 4.1d) is mounted at node 7 of the plate to measure the acceleration during vibration when the plate is stroked by hammer. Hammer and accelerometer is connected by BNC cable to the Data Acquisition system (shown in Fig 4.1e). Data Acquisition system is connected to the PC through a LAN cable (shown in fig). PULSE LabShop software is installed in PC for Fast Fourier Transformation of the incoming signals. Transfer function or Frequency Response function (FRF) is calculated during every excitation. FRF is calculated based on average value of three excitations at each node and stored as Universal ASCII file for modal parameter extraction in ME'scope software. In ME'scope software these ASCII files are imported as data block to calculate the natural

frequency and mode shapes. Flow diagram of hammer test is shown below. Experimental setup is shown in Fig 4.1f.

FLOW DIAGRAM OF HAMMER TEST

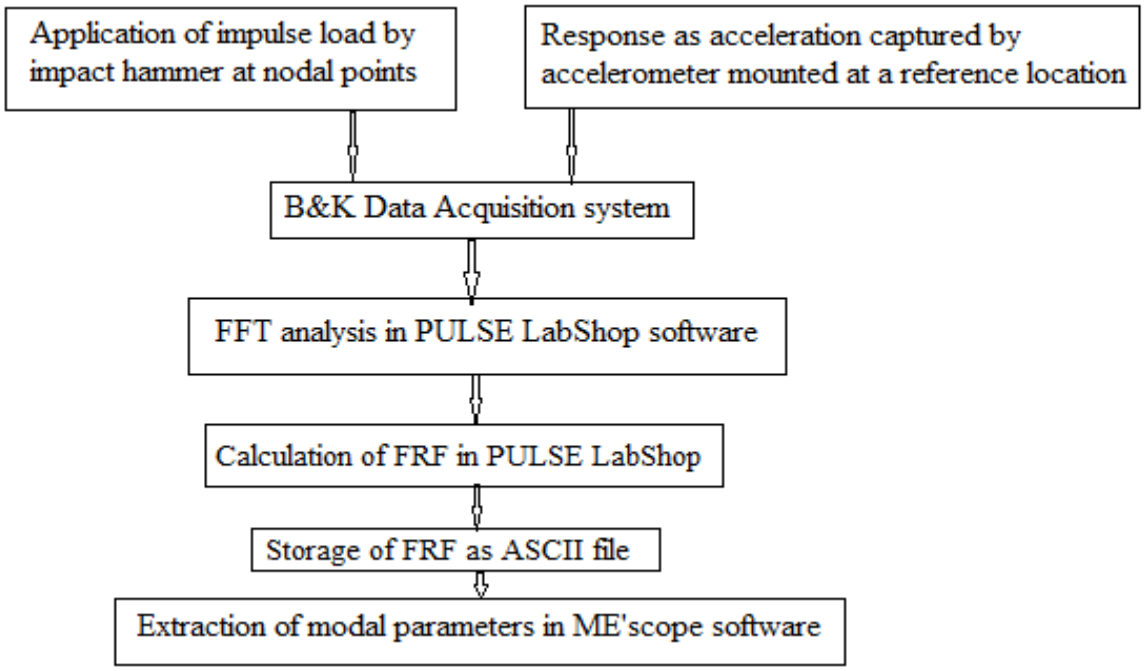

Fig 4.1f: Complete setup of Hammer Test

4.2 Shaker test details:

After Hammer test, Shaker test is performed to measure the impedance values at those frequencies obtained from hammer test. From measured impedance values, generalized modal masses are calculated to normalize the mode shape values.

Hardware and Software used

Different hardware and software are used to perform the shaker test in the laboratory. Hardware are as follows-

i. Shaker (B&K, Type-4825)
ii. Accelerometer to measure the response (B&K, Type-4507)
iii. Force transducer (B&K, Type-8230-001)
iv. Stringer
v. Power amplifier
vi. Data Acquisition system (B&K)

Software used-

i. PULSE LabShop version 15.1.0

Excitation measurement

In shaker test, harmonic oscillation is applied to the plate at a particular location through Data Acquisition system, Power Amplifier, Shaker and stringer. A Force Transducer is mounted at the top of the stringer to produce equivalent signal of applied load. Instruments required for excitation are shown in following Fig.

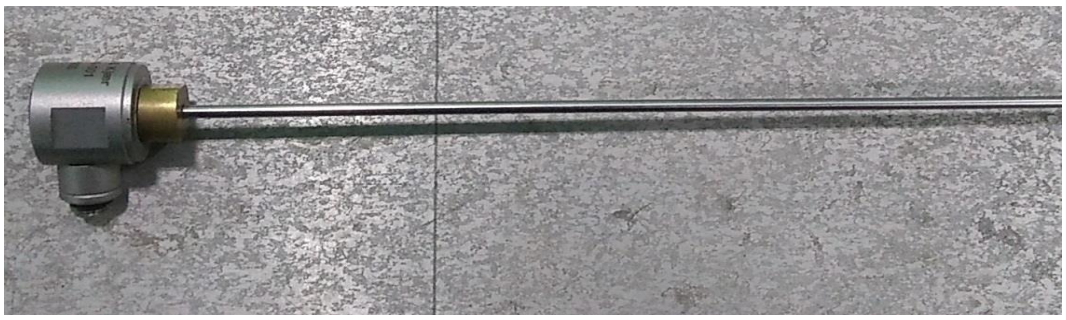

Fig 4.2a: Stringer attached with load cell at the top

Fig 4.2b: B&K Shaker (Type-4825)

Fig 4.2c: Power Amplifier

Response measurement

Response is measured as acceleration by an accelerometer (B&K, Type-4507). Same accelerometer which was used in hammer test is also used here but the location is shifted. Accelerometer is already shown in Fig 4.1d.

Procedure

For Shaker test, sinusoidal signals are generated from Data Acquisition system (B&K) by PULSE LabShop software at individual modal frequency as obtained from experimental modal analysis. The generated signals are then transmitted to the Power Amplifier from Data Acquisition system (B&K). From Power amplifier, the amplified signals are transmitted to the B&K Shaker and finally a harmonic load is applied at a particular location of the plate by a vertical stringer. Vertical stringer is connected to the plate by a Force Transducer which produces an equivalent signal of the applied load. An accelerometer (B&K) is attached on the upper side of the plate just above the stringer location. Signals produced by Force Transducer and Accelerometer are received by Data Acquisition system and then analyzed by PULSE LabShop software to calculate the impedance value of each mode. From modal impedance value, generalized modal masses are calculated using mathematical formation of equation. Flow diagram is shown below. Complete experimental setup is shown in Fig 4.2d.

FLOW DIAGRAM OF SHAKER TEST

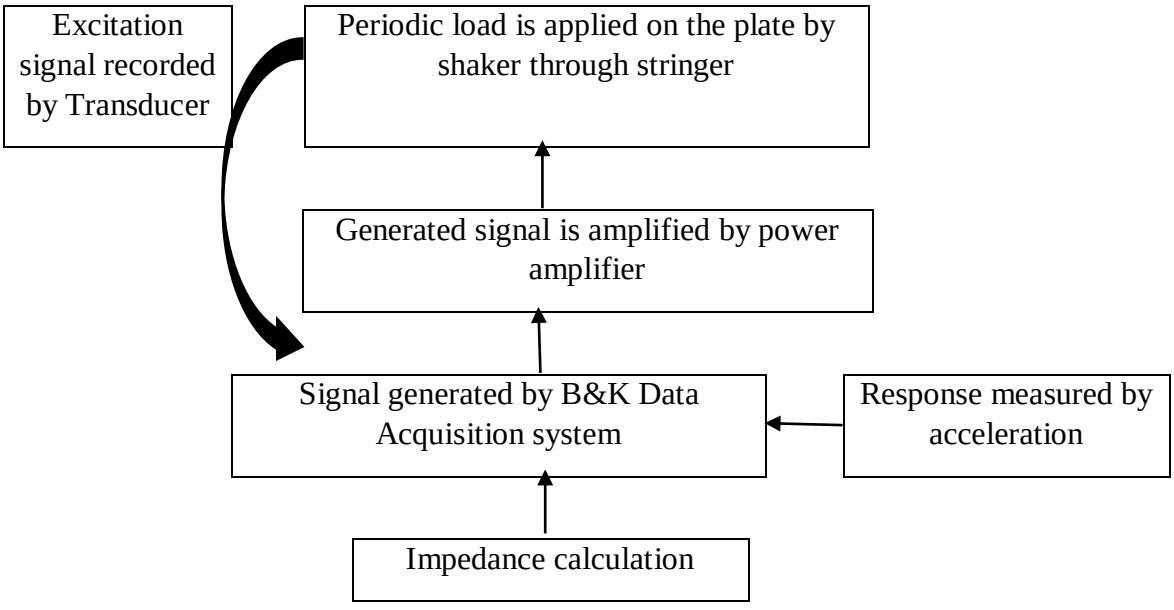

Fig 4.2d: Complete setup of shaker test

CHAPTER-5

RESULTS AND DISCUSSION

Finite Element model updating of a Two-dimensional (2D) cantilever plate and localization of added mass based on experimental modal parameters have been studied in the present thesis work. The procedure of measurement of experimental dynamic parameters using B&K analyzer and Shaker is already discussed in previous chapter. The numerical results are obtained from Finite Element model of the structure in MATLAB environment. Finite Element model is set up based on the mathematical formulation discussed in chapter 3.

5.1 Details of the structure:

5.1.1 Dimension:

Length = 0.51m Width = 0.51m Thickness = 0.00569m

5.1.2 Material Property:

- Material- Aluminium
- Modulus of elasticity = 69 GPa
- D ensity = 2700 Kg/m^3
- Poisson's ratio = 0.332

5.1.3 Boundary condition:

The plate is fixed along one edge and all the three edges are kept free. So, it behaves like a cantilever plate.

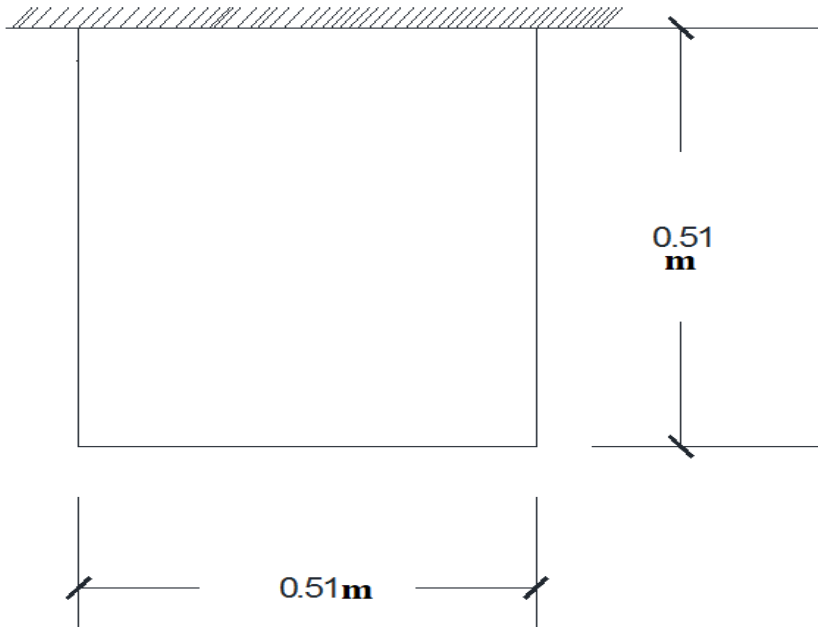

Fig 5.1a: Schematic diagram of the plate

5.2 Numerical results:

Finite Element model of the plate is set up in MATLAB environment. For analysis, an in-house FE code is developed. The plate is discretized into 4×4 meshes using 4 noded iso-parametric element. As at every node there are 5 degrees of freedom (3 translational, 2 rotational), total 125 (25×5) degrees of freedom are considered for the plate. So, the developed mass matrix and stiffness matrix are of size (125×125). But, measurement of all 5 degrees of freedom at a node is not practically feasible. Therefore, Dynamic Condensation is applied considering displacement along Z direction only to reduce the size of the mass and stiffness matrix to (25×25). As there is no movement of the fixed edge, displacement of that 5 nodes (along fixed edge) is completely locked which further reduces the size of the mass and stiffness matrix to (20×20). Free vibration analysis is carried out in MATLAB using the mass and stiffness matrix to calculate the modal parameters. Numerical study is carried out considering 2 different conditions-

Model-I: Plate without any lumped mass

Model-II: Plate with 100gms lumped mass at node 17 and 18

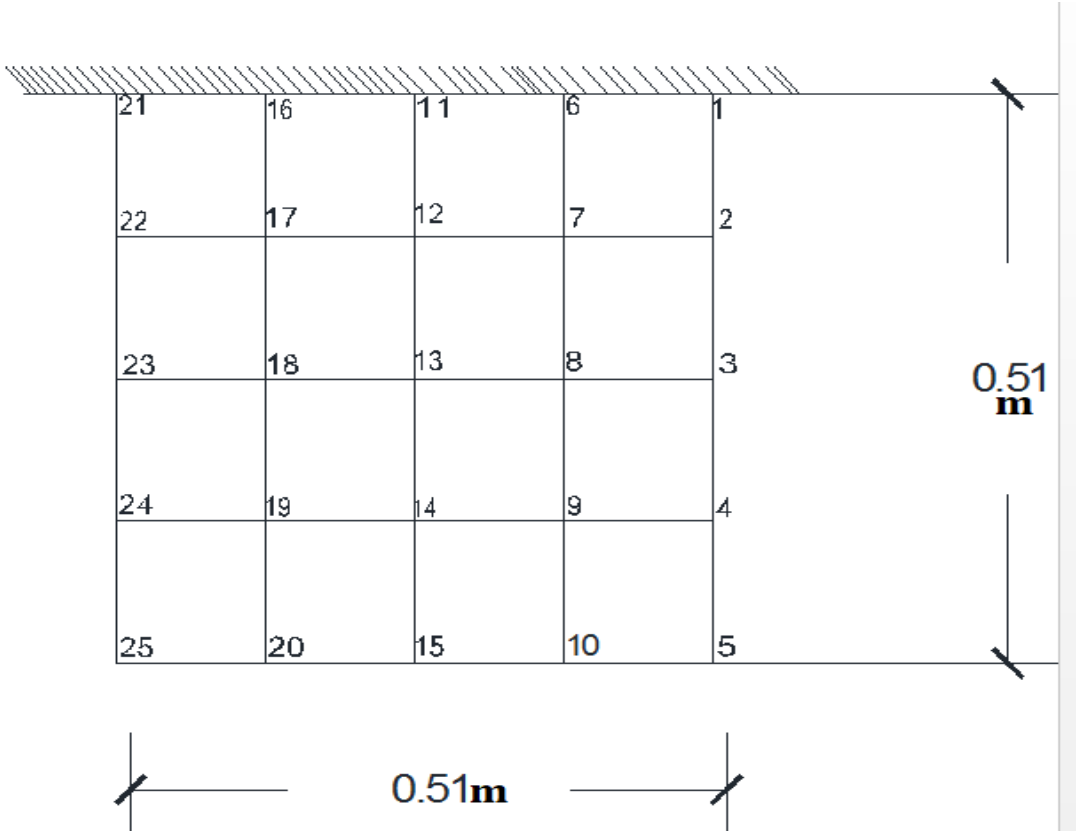

Fig 5.2a: Discretization of the plate into 4-noded iso-parametric element

5.2.1 Model-I: Plate without any lumped mass

Natural frequencies of the numerical model before and after condensation are listed below-

Table 5.2a: Numerical natural frequencies of the plate before and after condensation

Mode	Frequency before condensation (Hz)	Frequency after condensation (Hz)	Error
1st	19.22	19.22	0
2nd	46.64	46.64	0
3rd	131.14	131.14	0
4th	159.96	159.96	0
5th	189.34	189.34	0
6th	318.09	318.09	0
7th	456.69	456.69	0
8th	538.52	538.52	0
9th	572.25	572.25	0
10th	646.62	646.62	0
11th	701.77	701.77	0
12th	1038.19	1038.19	0
13th	1337.09	1337.09	0
14th	1381.23	1381.23	0
15th	1441.10	1441.10	0
16th	1486.31	1486.31	0
17th	2281.06	2281.06	0
18th	2297.03	2297.03	0
19th	2445.14	2445.14	0
20th	2511.95	2511.95	0

From Table 5.2a, it is seen that there is no error in frequency measurement before and after condensation. So, a perfect condensation is ensured. Mode shapes obtained from Eigenvalue analysis is not mass normalized. Therefore, mass normalization of the mode shapes is done through proper mathematical formation. Mass normalized mode shapes are listed in Table 5.2b. Corresponding mode shapes are plotted in Figs 5.2b, 5.2c and 5.2d to get a visual knowledge about the modes of vibration. Major diagonal elements of mass and stiffness matrices are shown in Table 5.2c and 5.2d respectively.

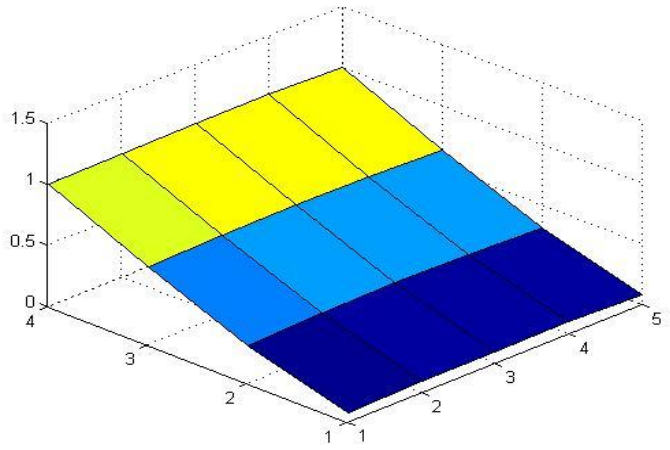

Fig 5.2b: Numerical mode shape (1st mode) of plate without lumped mass

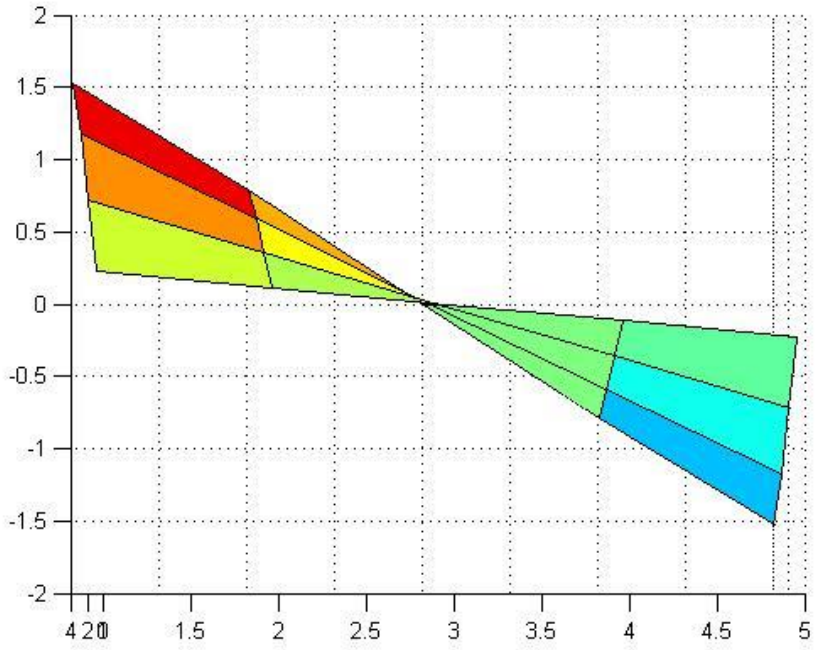

Fig 5.2c: Numerical mode shape (2nd mode) of plate without lumped mass

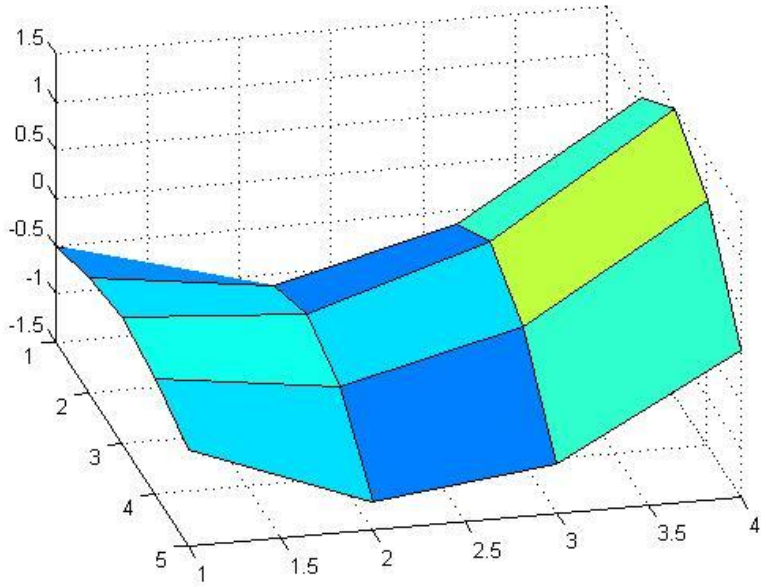

Fig 5.2d: Numerical mode shape (3rd mode) of plate without lumped mass

From the above mode shapes, it is observed that 1st and 3rd mode is pure bending mode and 2nd mode is torsional mode. Torsional mode is one of the predominant mode in the vibration of plate structure. Higher modes are not plotted here.

Table 5.2b: Mass normalized numerical mode shape values of plate without lumped mass

1st mode	2nd mode	3rd mode	4th mode	5th mode	6th mode	7th mode	8th mode	9th mode	10th mode	11th mode	12th mode	13th mode	14th mode	15th mode	16th mode	17th mode	18th mode	19th mode
0.078	0.228	-0.506	0.026	-0.716	-0.988	-0.054	0.811	-1.589	1.46	-1.43	0.85	0.40	-1.90	0.35	0.79	-1.58	-1.41	1.83
0.311	0.714	-1.209	0.313	-1.325	-1.555	0.622	0.212	-1.224	0.22	0.01	-0.17	1.25	1.52	-1.10	-0.82	1.65	1.49	-1.97
0.638	1.170	-0.994	1.062	-0.307	0.047	1.695	-1.085	1.037	-2.00	1.87	0.83	0.19	-0.30	1.68	0.63	-1.22	-1.15	1.47
0.999	1.528	0.020	2.023	1.749	2.094	1.296	1.329	-0.916	2.23	-2.50	1.59	-1.03	0.52	-1.59	-0.69	1.06	1.15	-1.11
0.096	0.115	-0.293	-0.277	-0.346	0.147	-0.431	0.698	-0.061	-0.40	1.05	-0.48	-0.86	1.89	-0.09	0.97	-0.86	-0.28	-1.49
0.336	0.358	-0.545	-0.556	-0.627	0.300	-0.799	0.200	0.640	-0.08	0.05	-0.23	-1.39	-1.27	1.17	-1.01	0.89	0.31	1.61
0.659	0.590	-0.084	-0.275	-0.060	0.066	-0.797	-0.844	0.967	0.58	-1.51	-0.92	-0.30	-0.25	-2.10	0.67	-0.60	-0.13	-1.19
1.015	0.793	1.059	0.302	1.142	-0.482	-1.586	1.039	-1.308	-0.43	1.96	-1.98	1.36	-0.08	2.06	-0.27	0.33	-0.26	0.90
0.094	-1.124	-0.185	-0.415	1.004	0.600	-2.95	0.744	2.595	-0.84	-9.93	0.47	1.09	-1.95	-0.22	1.01	3.11	1.78	1.31
0.343	-4.662	-0.314	-0.953	2.008	0.948	-2.801	0.260	1.527	-0.13	-6.89	0.39	1.66	1.12	-1.10	-1.05	-3.37	-1.88	-1.42
0.666	-7.318	0.262	-0.852	1.153	0.065	1.993	-0.980	-2.204	1.12	1.47	1.05	0.36	0.68	2.37	0.81	2.60	1.26	1.10
1.022	-4.773	1.481	-0.421	-3.365	-1.507	1.678	0.703	-8.510	-1.69	-2.03	2.41	-1.65	-0.22	-2.40	-0.84	-2.78	-0.51	-8.66
0.096	-0.115	-0.293	-0.277	0.346	0.147	0.431	0.698	0.061	-0.40	-1.05	-0.48	-0.86	1.89	-0.09	0.97	0.86	-0.28	1.49
0.336	-0.358	-0.545	-0.556	0.627	0.300	0.799	0.200	-0.640	-0.08	-0.05	-0.23	-1.39	-1.27	1.17	-1.01	-0.89	0.31	-1.61
0.659	-0.590	-0.084	-0.275	0.060	0.066	0.797	-0.844	-0.967	0.58	1.51	-0.92	-0.30	-0.25	-2.10	0.67	0.60	-0.13	1.19
1.015	-0.793	1.059	0.302	-1.142	-0.482	1.586	1.039	1.308	-0.43	-1.96	-1.98	1.36	-0.08	2.06	-0.27	-0.33	-0.26	-0.90
0.078	-0.228	-0.506	0.026	0.716	-0.988	0.054	0.811	1.589	1.46	1.43	0.85	0.40	-1.90	0.35	0.79	1.58	-1.41	-1.83
0.311	-0.714	-1.209	0.313	1.325	-1.555	-0.622	0.212	1.224	0.22	-0.01	-0.17	1.25	1.52	-1.10	-0.82	-1.65	1.49	1.97
0.638	-1.170	-0.994	1.062	0.307	0.047	-1.695	-1.085	-1.037	-2.00	-1.87	0.83	0.19	-0.30	1.68	0.63	1.22	-1.15	-1.47
0.999	-1.528	0.020	2.023	-1.749	2.094	-1.296	1.329	0.916	2.23	2.50	1.59	-1.03	0.52	-1.59	-0.69	-1.06	1.15	1.11

Table 5.2c: Major diagonal elements of mass matrix of the plate without lumped mass (in Kg)

Node	1st	2nd	3rd	4th	5th	6th	7th	8th	9th	10th	11th	12th	13th	14th	15th	16th	17th	18th	19th	20th	21st	22nd	23rd	24th	25th
1st	Locked																								
2nd		0.055																							
3rd			0.055																						
4th				0.055																					
5th					0.0275																				
6th						Locked																			
7th							0.11																		
8th								0.11																	
9th									0.11																
10th										0.055															
11th											Locked														
12th												0.11													
13th													0.11												
14th														0.11											
15th															0.055										
16th																Locked									
17th																	0.11								
18th																		0.11							
19th																			0.11						
20th																				0.055					
21st																					locked				
22nd																						0.055			
23rd																							0.055		
24th																								0.055	
25th																									0.0275

Table 5.2d: Major diagonal elements of the stiffness matrix of the plate without lumped mass (in N/m)

Node	1st	2nd	3rd	4th	5th	6th	7th	8th	9th	10th	11th	12th	13th	14th	15th	16th	17th	18th	19th	20th	21st	22nd	23rd	24th	25th
1st	Locked																								
2nd		4e6																							
3rd			2.6e6																						
4th				1.1e6																					
5th					2.8e5																				
6th						Locked																			
7th							8.7e6																		
8th								6e6																	
9th									3.3e6																
10th										7.9e5															
11th											Locked														
12th												9.6e6													
13th													6.9e6												
14th														4.1e6											
15th															1.2e6										
16th																Locked									
17th																	8.7e6								
18th																		6e6							
19th																			3.3e6						
20th																				7.9e5					
21st																					Locked				
22nd																						4e6			
23rd																							2.6e6		
24th																								1.1e6	
25th																									2.8e5

5.2.2 Model-II: Plate with 100gms lumped mass at node 17 and 18

In baseline FE model of the plate, two 100gms mass are lumped at node 17 and 18 numerically as shown in Fig 5.2e. But as the nodes along the fixed edge are locked, mass and stiffness matrices are condensed to a size of (20×20) which is already discussed. So, in condensed form of numerical mass matrix, the change of mass take place in node 13 and 14. Due to lumping of mass, mass matrix is changed but stiffness matrix remains unchanged. As a result, natural frequencies and mode shape values also changes. Natural frequencies and mode shape values of all modes are shown in Table 5.2e and 5.2f.

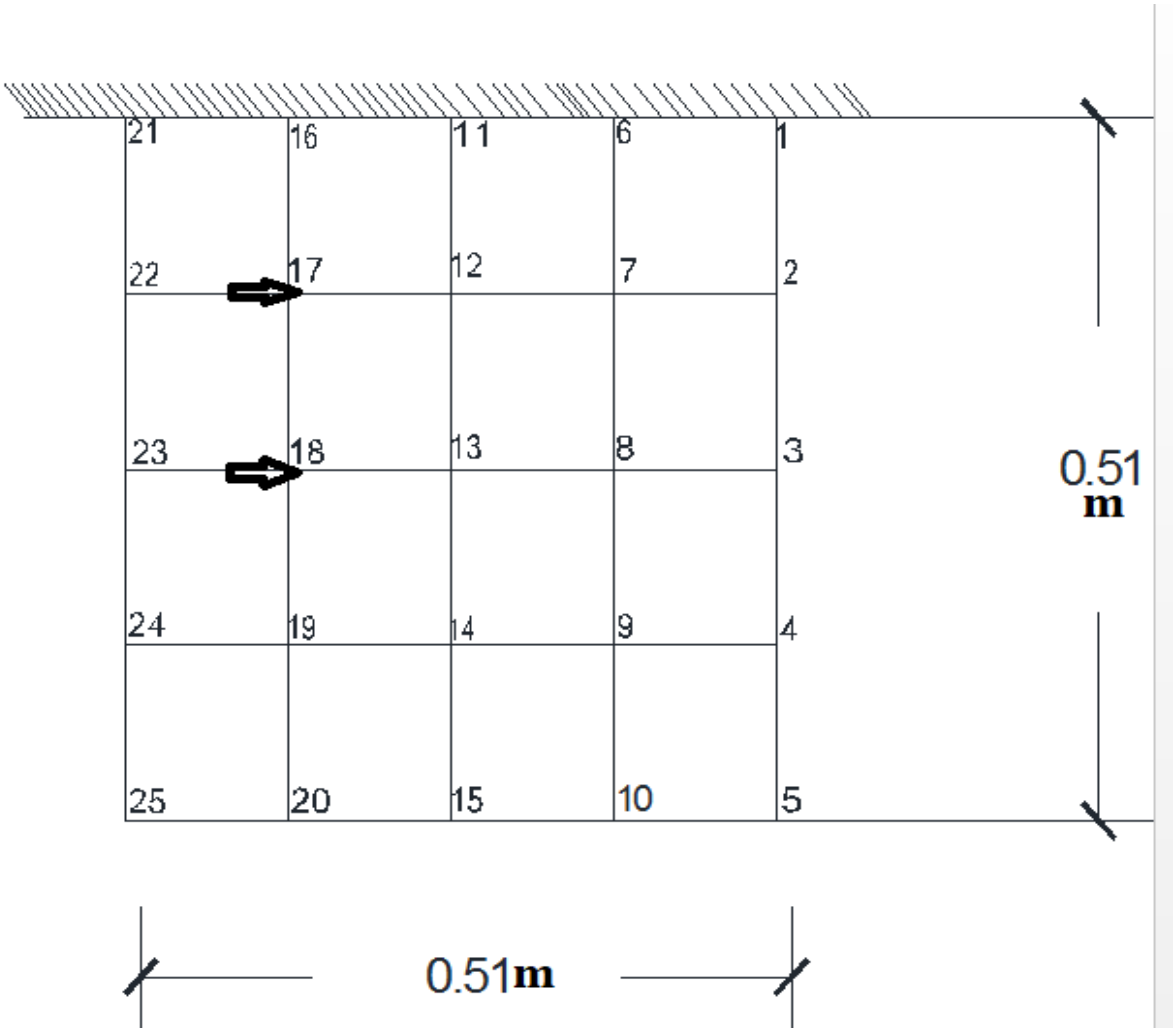

Fig 5.2e: Location of lumped mass (shown by arrow)

Table 5.2e: Numerical natural frequencies of the plate with 100gms mass lumped at node 17 &18

Mode	Natural frequency (Hz)
1st	19.10
2nd	46.32
3rd	128.41
4th	156.97
5th	185.41
6th	316.36
7th	436.73
8th	521.42
9th	560.24
10th	604.05
11th	697.89
12th	964.42
13th	1148.09
14th	1268.93
15th	1344.60
16th	1468.34
17th	2039.87
18th	2290.02
19th	2404.75
20th	2449.93

From the above frequencies, it is seen that the values are reduced slightly from the frequency values of the plate without any lumped mass. When mass of any system is increased, frequency of the system is reduced which is a natural phenomenon.

Mode shapes of the plate with 100gms lumped mass at node 17 and 18 are shown in Fig 5.2f, 5.2g and 5.2h. Major diagonal elements of mass and stiffness matrices are also shown in Table 5.2g and 5.2h respectively.

Table 5.2f: Mass normalized mode shape values of the plate with 100gms lumped mass at node 17 & 18

1st mode	2nd mode	3rd mode	4th mode	5th mode	6th mode	7th mode	8th mode	9th mode	10th mode	11th mode	12th mode	13th mode	14th mode	15th mode	16th mode	17th mode	18th mode	19th mode	20th mode
-0.077	0.227	0.466	-0.151	0.723	0.944	-0.252	0.810	-1.541	0.443	-1.47	0.82	-1.43	-1.46	-0.19	-0.14	1.42	1.59	-2.33	0.51
-0.307	0.712	1.112	-0.565	1.317	1.473	-0.946	0.364	-1.257	-0.530	-0.32	0.26	1.53	-0.82	0.45	-0.20	-1.56	-1.65	2.50	-0.52
-0.631	1.170	0.898	-1.155	0.191	-0.107	-1.507	-1.220	0.997	-0.835	1.85	-1.93	0.36	-0.04	-0.70	1.51	1.09	1.24	-1.85	0.43
-0.988	1.533	-0.071	-1.761	-2.020	-2.093	-0.946	0.388	-0.057	3.316	-1.77	2.66	-0.72	-0.33	-1.83	-1.50	-0.99	-1.18	1.49	-0.59
-0.095	0.115	0.289	0.195	0.402	-0.125	0.451	0.553	0.136	1.023	0.53	-0.34	1.13	1.68	-0.33	0.25	-1.16	1.37	1.16	0.87
-0.333	0.359	0.543	0.406	0.735	-0.259	0.882	0.128	0.645	0.631	0.18	-0.25	-1.45	1.21	-0.19	0.29	1.28	-1.42	-1.26	-0.94
-0.653	0.596	0.096	0.245	0.112	-0.031	0.835	-0.499	0.650	-1.136	-0.61	1.31	-0.51	-0.04	0.85	-2.10	-0.82	0.96	0.93	0.60
-1.007	0.806	-1.009	-0.060	-1.218	0.500	1.152	1.456	-1.555	-0.482	0.23	-1.83	0.83	0.43	2.23	2.14	0.80	-0.49	-0.80	-0.11
-0.094	-0.001	0.213	0.382	0.065	-0.583	0.016	0.622	0.092	0.267	0.74	-0.68	-0.77	-1.66	0.41	-0.47	1.09	0.67	0.91	-1.59
-0.341	0.002	0.373	0.881	0.157	-0.898	0.170	0.165	0.157	0.211	0.13	0.22	1.41	-1.38	0.17	-0.18	-1.16	-0.69	-0.94	1.69
-0.662	0.009	-0.208	0.841	0.118	-0.031	0.180	-0.973	-0.053	-0.148	-1.06	0.21	0.05	-0.13	-0.98	2.50	0.56	0.54	0.73	-1.11
-1.015	0.020	-1.436	0.562	-0.016	1.473	-0.235	0.777	0.005	-0.027	1.63	-0.25	-0.22	-0.30	-2.71	-2.60	-0.66	-0.56	-0.47	0.41
-0.096	-0.116	0.324	0.273	-0.290	-0.152	-0.540	0.837	0.084	-0.750	0.29	1.27	0.84	0.73	-0.17	0.07	0.66	-0.02	-0.19	-0.05
-0.336	-0.355	0.593	0.534	-0.502	-0.289	-0.790	0.132	-0.633	-0.443	-0.10	-0.59	-1.37	0.51	-0.05	0.19	-0.69	0.02	0.22	0.06
-0.656	-0.576	0.072	0.234	0.012	-0.046	-0.525	-1.131	-0.704	0.816	-0.44	-0.70	1.47	0.69	0.67	-2.11	1.13	-0.05	-0.37	-0.19
-1.010	-0.766	-1.143	-0.306	1.020	0.391	-1.569	0.570	1.638	0.901	0.52	1.37	-1.39	-0.25	2.38	2.15	-0.64	0.10	0.30	0.51
-0.079	-0.227	0.503	-0.039	-0.637	1.036	0.091	0.471	1.630	0.412	-1.56	-1.76	-0.60	-0.67	-0.33	-0.04	1.47	-0.62	1.54	2.12
-0.312	-0.708	1.161	-0.376	-1.183	1.672	0.891	0.036	1.395	0.736	-0.07	0.50	1.31	-0.45	0.38	-0.14	-1.50	0.65	-1.63	-2.24
-0.637	-1.152	0.841	-1.175	-0.320	0.026	1.681	-0.635	-1.215	-0.168	2.14	1.40	-1.39	-0.68	-0.57	1.50	0.71	-0.45	1.32	1.74
-0.996	-1.494	-0.303	-2.166	1.440	-2.166	0.825	1.881	0.334	-2.113	-2.70	-2.22	1.41	0.32	-1.96	-1.49	-0.77	0.30	-1.03	-1.6

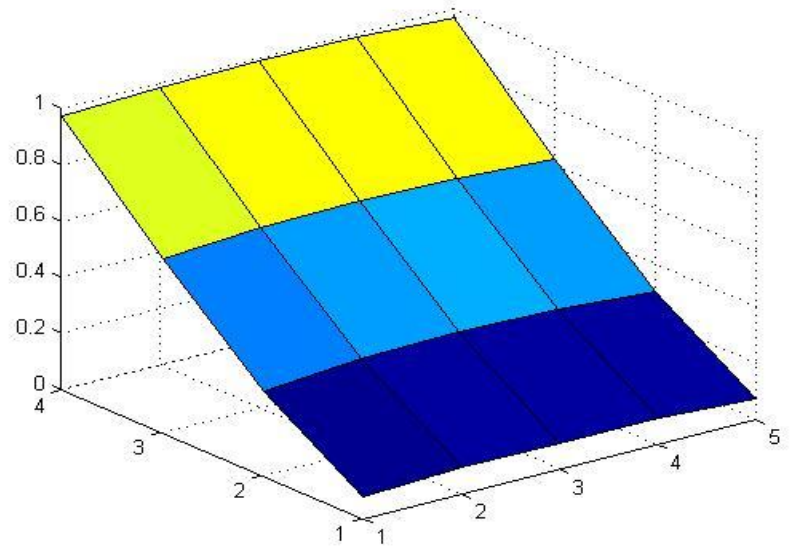

Fig 5.2f: Numerical mode shape (1st mode) of the plate with lumped mass at node 17 & 18

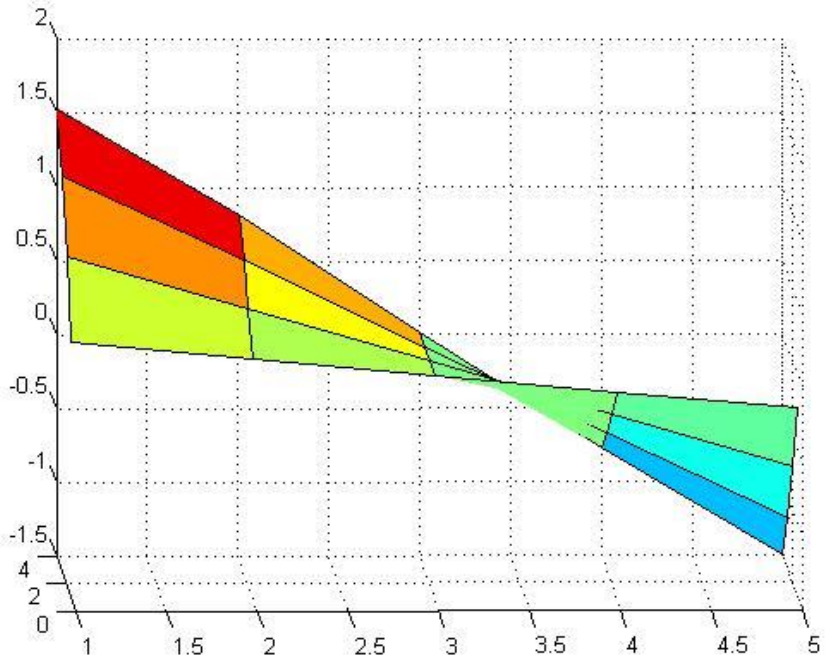

Fig 5.2g: Numerical mode shape (2nd mode) of the plate with lumped mass at node 17 & 18

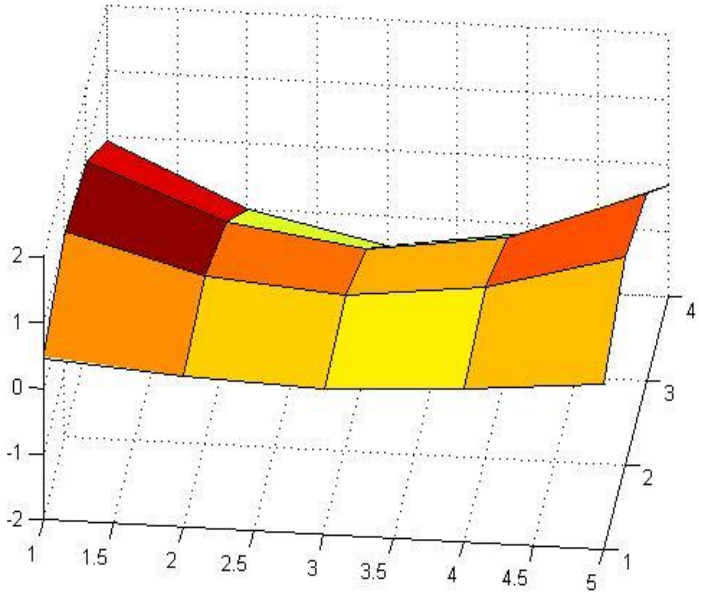

Fig 5.2h: Numerical mode shape (3rd mode) of the plate with lumped mass at node 17 & 18

Here also, 1st and 3rd modes are pure bending mode and 2nd mode is a torsional mode. Higher modes are not plotted but mode shape values of these modes are considered for model updating which is discussed in next section.

Table 5.2g: Major diagonal elements of mass matrix of the plate with 100gms lumped mass at node 17 & 18 (in Kg)

Node	1st	2nd	3rd	4th	5th	6th	7th	8th	9th	10th	11th	12th	13th	14th	15th	16th	17th	18th	19th	20th	21st	22nd	23rd	24th	25th
1st	Locked																								
2nd		0.055																							
3rd			0.055																						
4th				0.055																					
5th					0.0275																				
6th						Locked																			
7th							0.11																		
8th								0.11																	
9th									0.11																
10th										0.055															
11th											Locked														
12th												0.11													
13th													0.11												
14th														0.11											
15th															0.055										
16th																Locked									
17th																	**0.21**								
18th																		**0.21**							
19th																			0.11						
20th																				0.055					
21st																					Locked				
22nd																						0.055			
23rd																							0.055		
24th																								0.055	
25th																									0.0275

Table 5.2h: Major diagonal elements of the stiffness matrix of the plate with 100gms mass lumped at node 17 and 18 (in N/m)

Node	1st	2nd	3rd	4th	5th	6th	7th	8th	9th	10th	11th	12th	13th	14th	15th	16th	17th	18th	19th	20th	21st	22nd	23rd	24th	25th
1st	Locked																								
2nd		4e6																							
3rd			2.6e6																						
4th				1.1e6																					
5th					2.8e5																				
6th						Locked																			
7th							8.7e6																		
8th								6e6																	
9th									3.3e6																
10th										7.9e5															
11th											Locked														
12th												9.6e6													
13th													6.9e6												
14th														4.1e6											
15th															1.1e6										
16th																Locked									
17th																	8.7e6								
18th																		6e6							
19th																			3.3e6						
20th																				7.9e5					
21st																					Locked				
22nd																						4e6			
23rd																							2.6e6		
24th																								1.1e6	
25th																									2.8e5

5.3 Model updating using Lagrange multiplier method to localize the numerical added mass based on numerical modal parameters

Model updating using Lagrange multiplier method based on modal parameters is already discussed in chapter 3. Here, it is applied to update the baseline FE model (for **Model I**) using modal parameters (mode shape and natural frequency) of **Model II** (two 100gms mass are lumped at node 17 & 18). The purpose of finite element model updating or health monitoring is to identify the location of damage or certain change of mass and also the extent of damage or mass change. So, usefulness of the aforesaid model updating method in localization of lumping mass and amount of that added mass is mainly studied here.

5.3.1 Procedure-I: Mass matrix updation followed by Stiffness matrix updation

As discussed by Baruch [5] in 1st procedure of model updating using Lagrange multiplier method, the mass matrix is first updated using mass normalized modal parameters followed by the stiffness matrix updation. This study is performed considering different number of mode shapes and frequency values to get a clear idea about the significance of accounting higher number of modes in model updating and localizing the actual amount of lumped mass.

5.3.1.1 Approach-I: Three (3) modes accounted

Natural frequencies of updated model and Model II (described above) are shown in Table 5.3.1a and difference of major diagonal elements of mass matrix between updated model and model I is shown Fig 5.3.1a. Difference of diagonal entries will show the location and amount of added mass. Stiffness matrix remains same after updation as that of Model I which is shown in Fig 5.3.1b.

Table 5.3.1a: Natural frequencies of updated model and Model II accounting 3 modes

Mode	Frequency of updated model	Frequency of model II
1st	19.10	19.10
2nd	46.32	46.32
3rd	128.41	128.41
4th	159.80	156.97
5th	189.25	185.41
6th	318.09	316.36
7th	456.69	436.73
8th	538.52	521.42
9th	572.25	560.24

Mode	Frequency of updated model	Frequency of model II
10th	646.62	604.05
11th	701.77	697.89
12th	1038.19	964.42
13th	1337.09	1148.09
14th	1381.23	1268.93
15th	1441.10	1344.60
16th	1486.31	1468.34
17th	2281.06	2039.87
18th	2297.03	2290.02
19th	2445.14	2404.75
20th	2511.95	2449.93

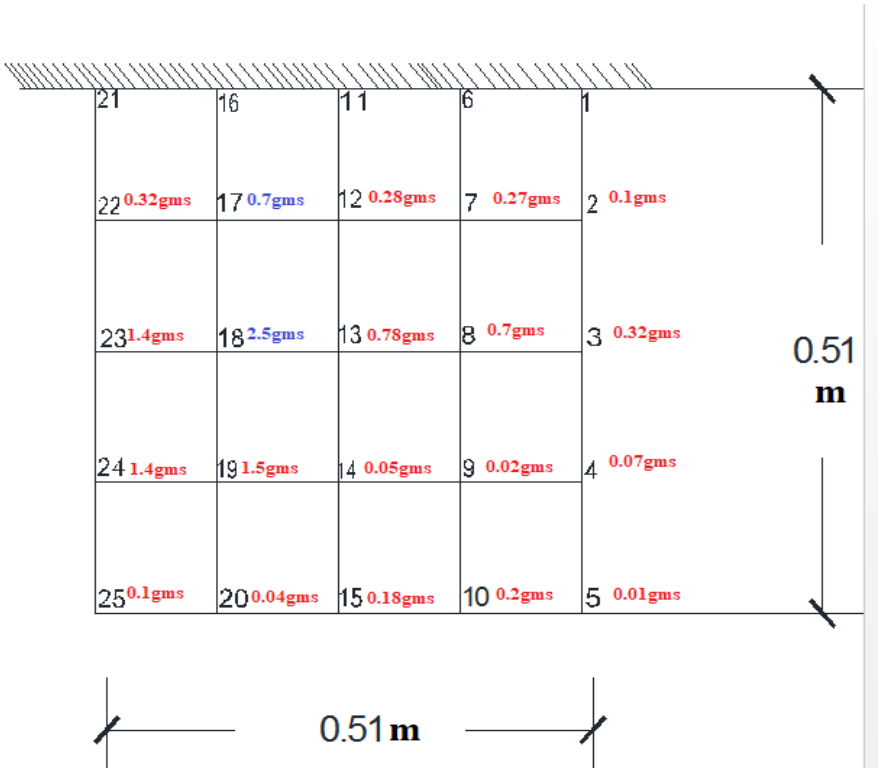

Fig 5.3.1a: Schematic representation of nodal mass Change after updation by procedure-I accounting 3 modes

Table 5.3.1b: Percentage recovery of actual mass after updation accounting 3 modes

Node	Numerical mass addition (Gms)	Mass recovered after updation (Gms)	% recovery
At 17	100	0.7	0.7
At 18	100	2.5	2.5

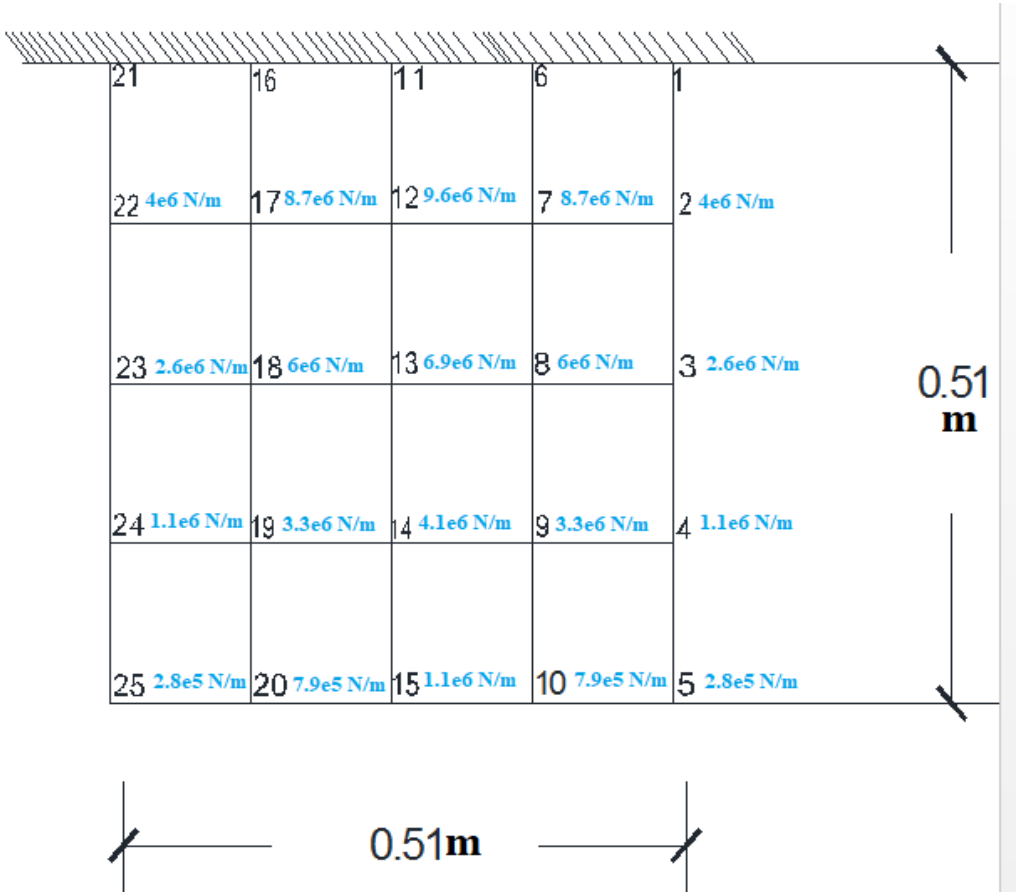

Fig 5.3.1b: Schematic representation of diagonal elements of stiffness matrix after updation accounting 3 modes

From diagonal elements of stiffness matrix after updation, it is seen that stiffness values are same as that of Model II and does not change from Model-I because lumped masses do not alter the stiffness of any structure.

5.3.1.2 Approach-II: Five (5) modes accounted

Here, difference of diagonal entries of mass matrix of updated model and Model I is shown in Fig 5.3.1c. Natural frequencies of updated model and Model-II are shown in Table 5.3.1c. Stiffness matrix remains same after updation as that of Model I like approach-I. So, it is not shown here.

Table 5.3.1c: Natural frequencies of updated model and model II accounting 5 modes

Mode	Frequency of updated model	Frequency of model II
1st	19.10	19.10
2nd	46.32	46.32
3rd	127.70	128.41
4th	154.21	156.97
5th	182.71	185.41
6th	318.07	316.36
7th	456.65	436.73
8th	538.52	521.42
9th	572.24	560.24
10th	646.59	604.05
11th	701.77	697.89
12th	1038.19	964.42
13th	1337.09	1148.09
14th	1381.22	1268.93
15th	1441.10	1344.60
16th	1486.30	1468.34
17th	2281.06	2039.87
18th	2297.03	2290.02
19th	2445.14	2404.75
20th	2511.95	2449.93

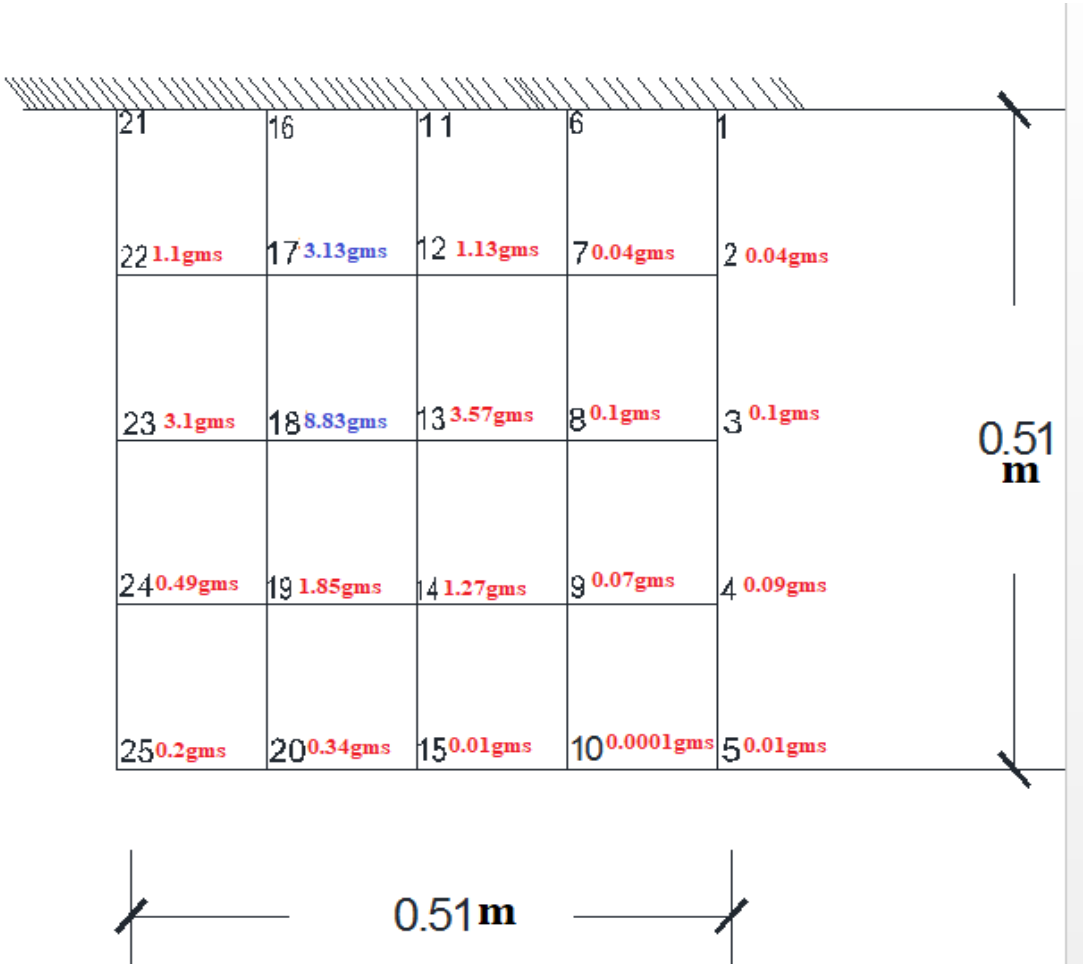

Fig 5.3.1c: Schematic representation of nodal mass Change after updation by procedure-I accounting 5 modes

Table 5.3.1d: Percentage recovery of actual mass after updation accounting 5 modes

Node	Numerical mass addition (Gms)	Mass recovered after updation (Gms)	% recovery
At 17	100	3.13	3.13
At 18	100	8.83	8.83

5.3.1.3 Approach-III: Eight (8) modes accounted

Here also, the difference of major diagonal elements of mass matrix between updated model and Model I is shown in Fig 5.3.1d and comparison of natural frequencies of updated model and Model II is shown in Table 5.3.1e. Stiffness matrix is not shown because it remains unchanged.

Table 5.3.1e: Natural frequencies of updated model and Model II accounting 8 modes

Mode	Frequency after updation of model I	Frequency of model II
1st	19.10	19.10
2nd	46.32	46.32
3rd	128.41	128.41
4th	156.97	156.97
5th	185.41	185.41
6th	316.36	316.36
7th	436.73	436.73
8th	521.42	521.42
9th	571.70	560.24
10th	640.05	604.05
11th	701.43	697.89
12th	1037.71	964.42
13th	1337.03	1148.09
14th	1380.83	1268.93
15th	1440.79	1344.60
16th	1486.25	1468.34
17th	2281.04	2039.87
18th	2297.01	2290.02
19th	2445.14	2404.75
20th	2511.92	2449.93

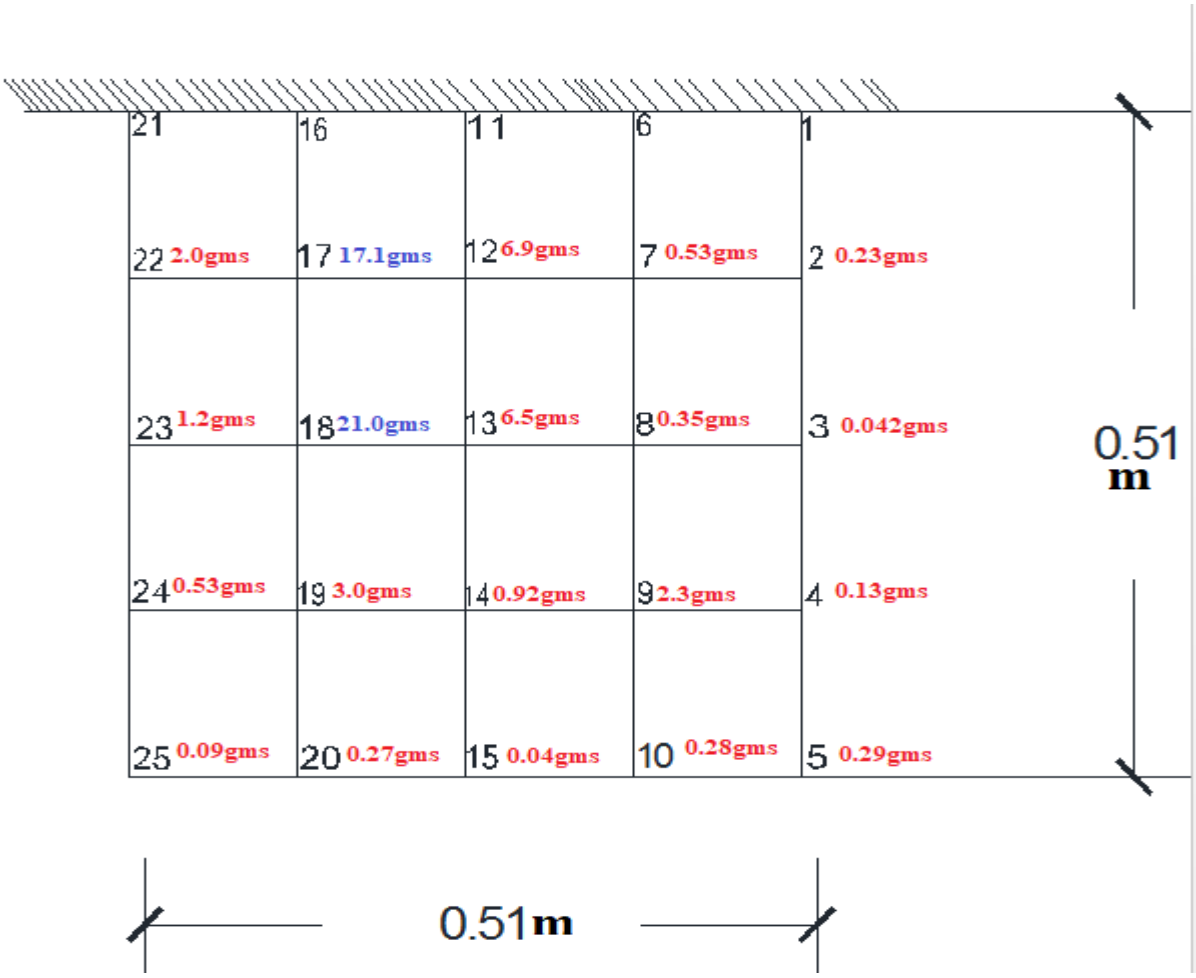

Fig 5.3.1d: Schematic representation of nodal mass Change after updation by procedure-I accounting 8 modes

Table 5.3.1f: Percentage recovery of actual mass after updation accounting 8 modes

Node	Numerical mass addition (Gms)	Mass recovered after updation (Gms)	% recovery
At 17	100	17.1	17.1
At 18	100	21.0	21.0

5.3.1.4 Approach-IV: Twelve (12) modes accounted

The difference of major diagonal elements of mass matrix between updated model and Model I is shown in Fig 5.3.1e and comparison of natural frequencies of updated model and Model II is shown in Table 5.3.1g. As stiffness matrix remains unchanged, it is not shown here.

Table 5.3.1g: Natural frequencies of updated model and model II accounting 12 modes

Mode	Frequency of updated model	Frequency of model II
1st	19.10	19.10
2nd	46.32	46.32
3rd	128.41	128.41
4th	156.97	156.97
5th	185.41	185.41
6th	316.36	316.36
7th	436.73	436.73
8th	521.42	521.42
9th	560.24	560.24
10th	604.05	604.05
11th	697.89	697.89
12th	964.42	964.42
13th	1335.38	1148.09
14th	1379.19	1268.93
15th	1408.92	1344.60
16th	1485.02	1468.34
17th	2278.85	2039.87
18th	2295.68	2290.02
19th	2444.99	2404.75
20th	2508.53	2449.93

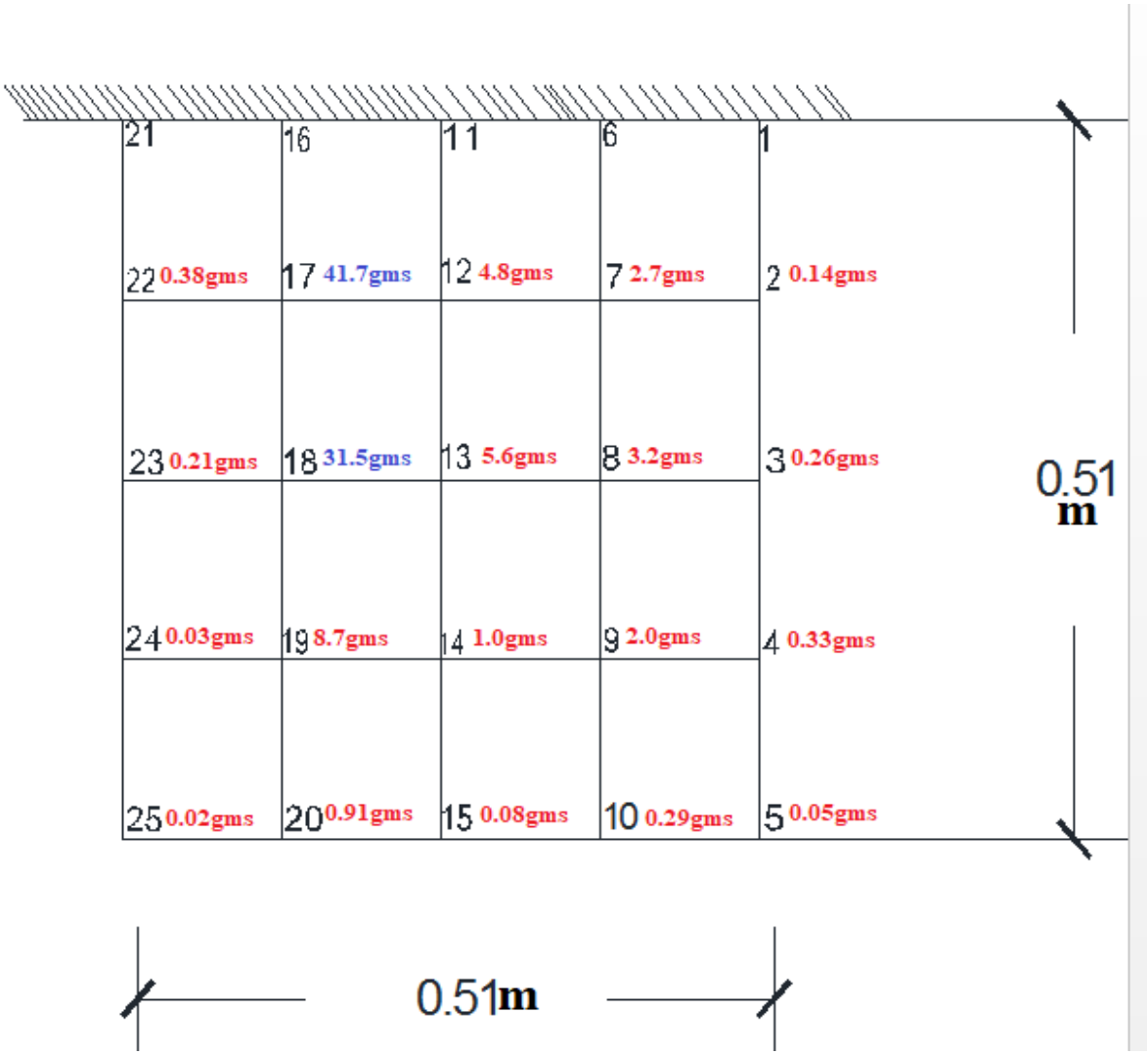

Fig 5.3.1e: Schematic representation nodal mass Change after updation by procedure-I accounting 12 modes

Table 5.3.1h: Percentage recovery of actual mass after updation accounting 12 modes

Node	Numerical mass addition (Gms)	Mass recovered after updation (Gms)	% recovery
At 17	100	41.7	41.7
At 18	100	31.5	31.5

5.3.1.5 Approach-V: Twenty (20) modes accounted

The difference of major diagonal elements of mass matrix between updated model and Model I is shown in Fig 5.3.1f and comparison of natural frequencies of updated model and Model II is shown in Table 5.3.1i. As stiffness matrix remains unchanged, it is not shown here.

Table 5.3.1i: Natural frequencies of updated model and Model II accounting 20 modes

Mode	Frequency of Updated model	Frequency of model II
1st	19.10	19.10
2nd	46.32	46.32
3rd	128.41	128.41
4th	156.97	156.97
35th	185.41	185.41
6th	316.36	316.36
7th	436.73	436.73
8th	521.42	521.42
9th	560.24	560.24
10th	604.05	604.05
11th	697.89	697.89
12th	964.42	964.42
13th	1148.09	1148.09
14th	1268.93	1268.93
15th	1344.60	1344.60
16th	1468.34	1468.34
17th	2039.87	2039.87
18th	2290.02	2290.02
19th	2404.75	2404.75
20th	2449.93	2449.93

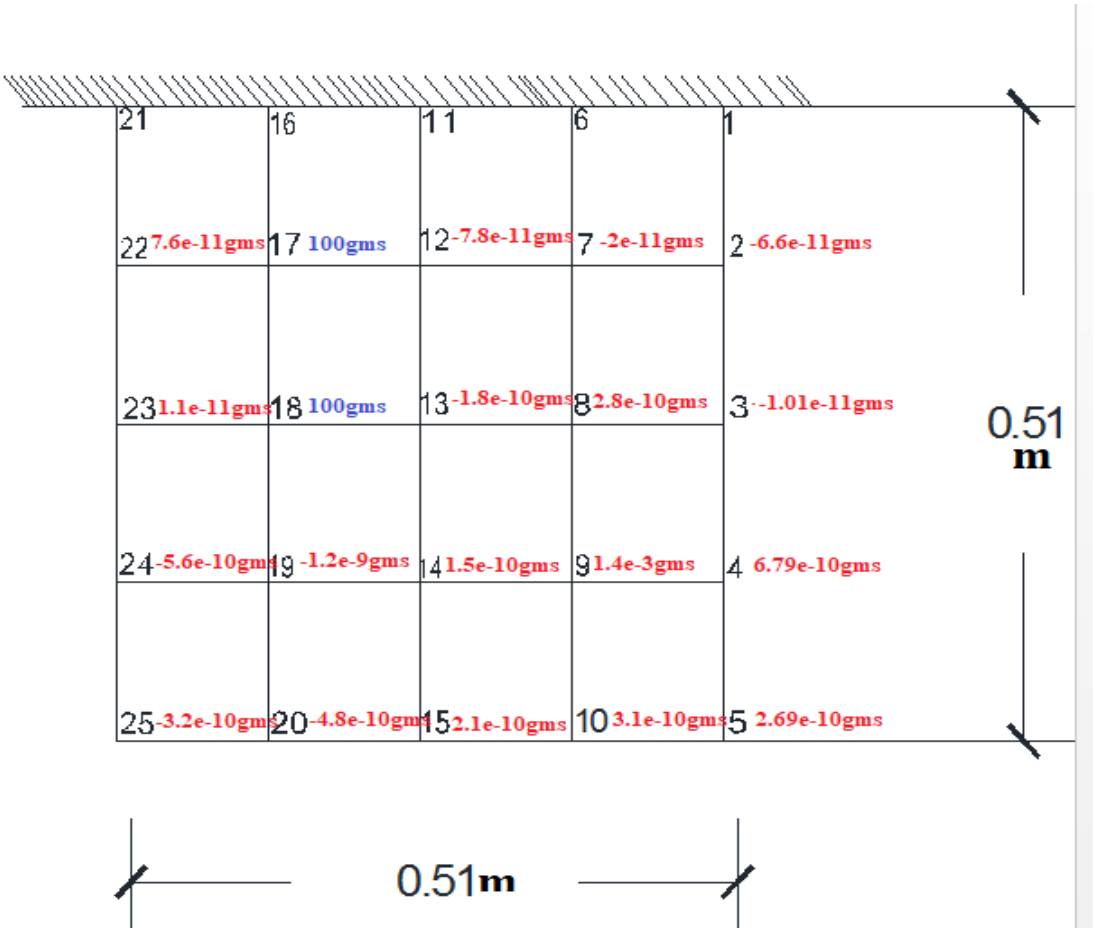

Fig 5.3.1f: Schematic representation nodal mass Change after updation by procedure-I accounting 20 modes

Table 5.3.1j: Percentage recovery of actual mass after updation accounting 20 modes

Node	Numerical mass addition (Gms)	Mass recovered after updation (Gms)	% recovery
At 17	100	100	100
At 18	100	100	100

From the above results, it is observed that only a few number of frequencies of the updated FE model are perfectly similar as that of the frequencies of Model-II when three, five, eight and twelve modes are accounted for model updating. Complete similarity of frequencies between updated model and Model-II is obtained when all the twenty modes are accounted for model updating.

MAC value:

Modal Assurance Criteria (MAC value) represents the correlation between the mode shape values of updated model and the corresponding actual mode shape values of the structure in real condition. Here, MAC value is calculated using equation (1a) (chapter-1) between the obtained mode shapes after updation of baseline finite element model

by procedure I and the mode shape values of Model II for different approaches as discussed earlier. If MAC value for all the modes become 1, it will be a perfect representation of the actual system or structure. So, in the case of exact updation, the matrix representation of the MAC values will be an Identity matrix as the correlation between 2 different modes is zero.

Table 5.3.1k: MAC value of the modes after updation by procedure I for different approaches

Mode	Approach-I	Approach-II	Approach-III	Approach-IV	Approach-V
1st	1	1	1	1	1
2nd	1	1	1	1	1
3rd	1	0.981	1	1	1
4th	0.988	0.976	1	1	1
5th	0.981	0.986	1	1	1
6th	0.997	0.998	1	1	1
7th	0.943	0.946	1	1	1
8th	0.844	0.845	1	1	1
9th	0.915	0.916	0.946	1	1
10th	0.861	0.861	0.945	1	1
11th	0.977	0.977	0.984	1	1
12th	0.900	0.900	0.903	1	1
13th	0.009	0.009	0.009	0.043	1
14th	0.354	0.354	0.358	0.399	1
15th	0.002	0.002	0.002	0.010	1
16th	0.890	0.890	0.890	0.925	1
17th	0.318	0.318	0.319	0.393	1
18th	0.647	0.647	0.647	0.724	1
19th	0.077	0.077	0.077	0.088	1
20th	0.215	0.215	0.215	0.222	1

5.3.2 Procedure-II: Stiffness matrix updation followed by mass matrix updation

As discussed by Baruch [5] in 2nd procedure of model updating using Lagrange multiplier method, the stiffness matrix is first updated using stiffness normalized modal parameters followed by the mass matrix updation. Mode shapes are normalized using the analytical stiffness matrix as stated in chapter 3. In this procedure, same approaches are considered as that of procedure-I to verify the accuracy of this technique. A

convergence study of getting the actual amount and location of mass of these 2 procedures is also carried out. Difference of diagonal elements of mass matrix of updated model and Model I for different approaches (accounting different number of modes) is shown in Table 5.3.2a and frequency of updated model for different approaches is shown in Table 5.3.2b

Table 5.3.2a: Difference of major diagonal elements of mass matrix between updated model & Model-I for different approaches

Node	Approach-I	Approach-II	Approach-III	Approach-IV	Approach-V
1st	Locked	Locked	Locked	Locked	Locked
2nd	-8.92e-02	-3.15e-02	-0.20	-5.68e-02	-2.13e-10
3rd	-0.20	-9.52e-02	-3.76e-02	-0.10	-2.10e-10
4th	-6.77e-02	-6.98e-02	-0.11	-0.18	-8.35e-9
5th	-1.08e-02	-8.08e-03	-0.15	-3.12e-02	4.02e-9
6th	Locked	Locked	Locked	Locked	Locked
7th	-0.20	-3.09e-02	-0.44	-0.99	-3.75e-10
8th	-0.60	-0.11	-0.19	-1.32	-7.48e-9
9th	-1.8e-02	-5.87e-02	-1.27	-1.12	-2.91e-9
10th	-0.17	-1.02e-04	-0.23	-0.16	-5.62e-9
11th	Locked	Locked	Locked	Locked	Locked
12th	-0.24	-0.83	-3.68	-1.87	-1.64e-9
13th	-0.67	-2.63	-3.46	-2.33	-7.22e-11
14th	-4.92e-02	-0.94	-0.85	-0.55	3.05e-8
15th	-0.16	-1.54e-02	-3.12e-02	-4.5e-02	-1.24e-8
16th	Locked	Locked	Locked	Locked	Locked
17th	**8.07**	**14.90**	**46.59**	**86.08**	**100**
18th	**34.37**	**54.03**	**65.29**	**83.00**	**100**
19th	-1.33	-1.37	-2.19	-4.85	2 e-8
20th	-4.23e-02	-0.26	-0.14	-0.50	-1.14e-9
21st	Locked	Locked	Locked	Locked	Locked
22nd	-0.28	-0.84	-1.03	-0.22	5.18e-10
23rd	-1.19	-2.31	-0.63	-7.83e-02	1.76e-9
24th	-1.19	-0.36	-0.34	-1.83e-02	-3.67e-9
25th	-0.14	-0.15	-6.73e-02	-1.28e-02	7.93e-10

Table 5.3.2b: Frequency of Model-II and updated model by procedure-II for different approaches

Mode	Frequency of updated model					Frequency of model II
	Approach-I	Approach-II	Approach-III	Approach-IV	Approach-V	
1st	19.10	19.10	19.10	19.10	19.10	19.10
2nd	46.32	46.32	46.32	46.32	46.32	46.32
3rd	128.41	128.41	128.41	128.41	128.41	128.41
4th	159.54	156.97	156.97	156.97	156.97	156.97
5th	188.87	185.41	185.41	185.41	185.41	185.41
6th	317.96	317.82	316.36	316.36	316.36	316.36
7th	455.37	454.11	436.73	436.73	436.73	436.73
8th	538.09	537.63	521.42	521.42	521.42	521.42
9th	571.63	571.11	570.02	560.24	560.24	560.24
10th	642.67	639.21	627.51	604.05	604.05	604.05
11th	701.64	701.53	700.84	697.89	697.89	697.89
12th	1037.33	1036.43	1030.64	964.42	964.42	964.42
13th	1336.05	1334.33	1327.26	1310.82	1148.09	1148.09
14th	1369.34	1360.26	1350.88	1327.50	1268.93	1268.93
15th	1440.24	1440.14	1424.15	1351.25	1344.60	1344.60
16th	1481.94	1479.49	1477.35	1474.55	1468.34	1468.34
17th	2278.78	2277.62	2267.12	2191.13	2039.87	2039.87
18th	2295.63	2295.11	2292.75	2290.53	2290.02	2290.02
19th	2444.91	2444.79	2443.93	2430.96	2404.75	2404.75
20th	2506.16	2503.58	2489.45	2455.47	2449.93	2449.93

MAC value:

Here, MAC value is calculated using equation 1 between the obtained mode shapes after updation of baseline finite element model by procedure II and the mode shapes of Model II for different approaches. MAC values are tabulated in Table 5.3.2c.

Table 5.3.2c: MAC value of the modes after updation by procedure II for different approaches

Mode	Approach-I	Approach-II	Approach-III	Approach-IV	Approach-V
1st	1	1	1	1	1
2nd	1	1	1	1	1
3rd	1	1	1	1	1
4th	0.993	1	1	1	1
5th	0.984	1	1	1	1
6th	0.998	0.999	1	1	1
7th	0.953	0.969	1	1	1
8th	0.858	0.880	1	1	1
9th	0.928	0.946	0.979	1	1
10th	0.873	0.887	0.980	1	1
11th	0.980	0.981	0.992	1	1
12th	0.900	0.898	0.911	1	1
13th	0.004	4e-04	4e-04	0.652	1
14th	0.305	0.218	0.084	0.163	1
15th	0.007	0.009	0.009	0.916	1
16th	0.920	0.935	0.950	0.987	1
17th	0.362	0.383	0.469	0.851	1
18th	0.729	0.760	0.903	0.995	1
19th	0.091	0.097	0.153	0.860	1
20th	0.230	0.234	0.282	0.833	1

Convergence study:

From above 2 procedures of Finite Element model updating, it is observed that the location of lumped mass can be identified considering lesser number of vibration modes but actual amount of lumped mass can't be estimated without considering all the vibration modes for that model. It is also observed that updating procedure-II gives more promising results than procedure-I when lesser number of modes are considered. In this study, the percentage recovery of actual amount of mass with consideration of different number of modes for both the model updating procedures is shown in Figs 5.3.2a and 5.3.2b.

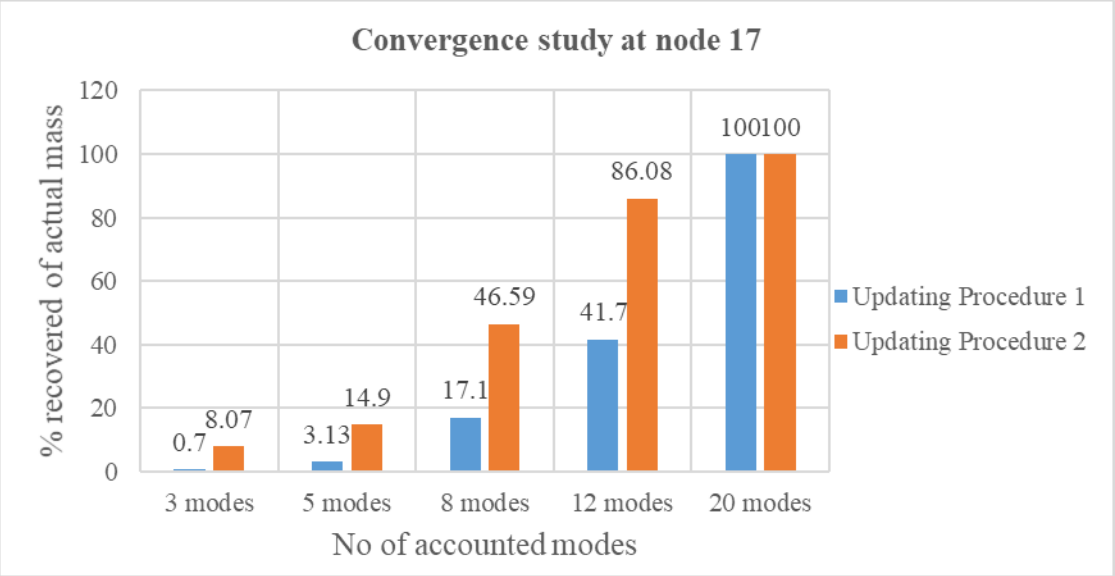

Fig 5.3.2a: Convergence of 2 updating procedures in recovering actual mass at node 17

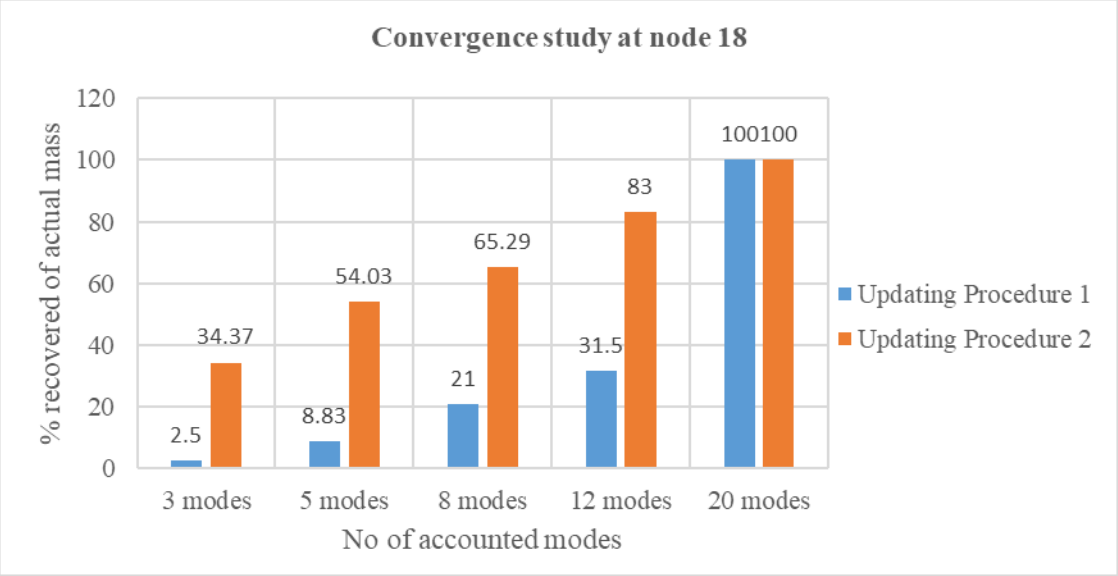

Fig 5.3.2b: Convergence of 2 updating procedures in recovering actual mass at node 18

5.3.3 Discussions on numerical results

Finite Element model updating of a cantilever plate based on numerical has been performed to assess the existing mass and stiffness distribution of the structure using Lagrange multiplier method. Major observations from the obtained results are as follows

I. From FE model updating based on numerical results, it is observed that location of added mass can be traced by accounting lesser number of modes but estimation of actual amount of mass can't be made without considering all the modes for that particular model because the summation of major diagonal elements of mass matrix will be equal to the total generalized modal mass of accounted modes.

II. In Procedure-I of model updating where mass matrix updation is followed by stiffness matrix updation, it is seen that accuracy of lumping mass localization is also very low when only 3 modes are accounted. But, in Procedure-II of model updating where stiffness matrix updation is followed by mass matrix updation, lumping mass can be localized with better accuracy considering 3 modes. Accuracy of localization is increased when higher modes are accounted for both the procedures.

5.4 Experimental results:

5.4.1 Hammer Test results:

Hammer test is performed to estimate the modal parameters (natural frequencies and corresponding mode shapes) and damping value of various modes. The test procedure has been discussed in chapter 4. For measurement of acceleration as response, an accelerometer is mounted at node 7. The impact hammer is roved at all the 25 nodes. From hammer test, natural frequencies, corresponding mode shapes and damping values are estimated for first 3 modes of vibration for 4 numbers of experimental setup.

Setup-I: Cantilever plate without lumped mass

Setup-II: Cantilever plate with 100gms lumped mass near node 17 and 18

Setup-III: Cantilever plate with 200gms lumped mass near node 18

Setup-IV: Cantilever plate with 200gms lumped mass near node 17

5.4.1.1 Setup-I: Cantilever plate without lumped mass

Natural frequencies & damping values are shown in table and non-normalized mode shape values are shown in Table 5.4.1a and measured mode shape values are shown in Table 5.4.1b.

Table 5.4.1a: Measured frequency and Damping value for plate without lumped mass

Mode	Natural frequency (Hz)	Damping value (%)
1st	17.9	3
2nd	43.8	9.39
3rd	107	4.57

Table 5.4.1b: Measured mode shape values for plate without lumped mass

1st mode	2nd mode	3rd mode
2.35	12.1	-166
4.51	25.8	-249
8.49	38.3	-110
11.9	47.5	152
2.74	6.69	-121
5.00	13.2	-159
8.97	20.3	-10.2
13.4	27.4	236
2.90	1.63	-103
6.47	0.978	-127
9.27	1.14	24.8
14.0	2.02	277
2.01	-4.77	-108
4.77	-12.4	-150
8.69	-20.4	-14.0
12.7	-26.5	233
1.5	-10.4	-146
4.67	-25.5	-229
8.37	-40.4	-99.6
12.8	-47.4	130

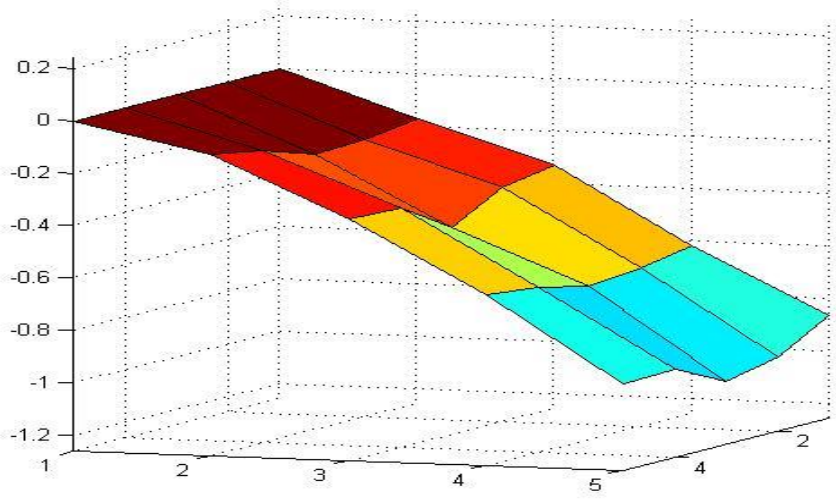

Fig 5.4.1a: Experimental mode shape of plate without added mass (1st mode)

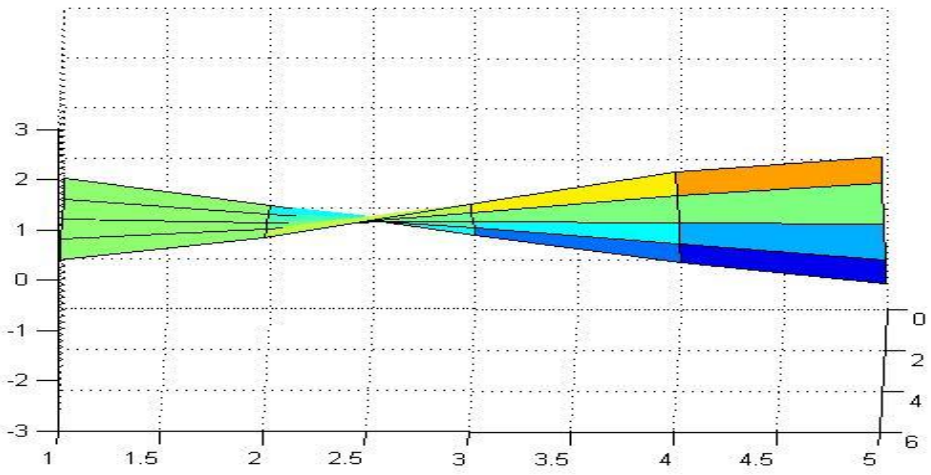

Fig 5.4.1b: Experimental mode shape of plate without added mass (2nd mode)

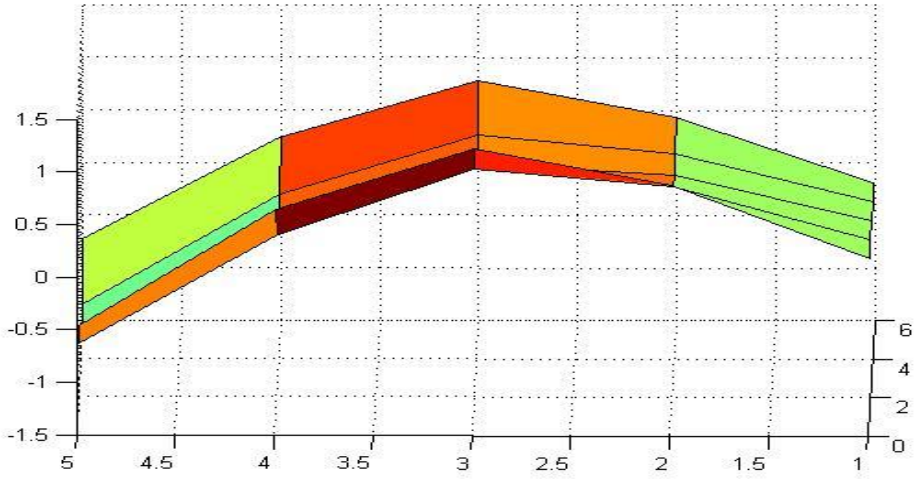

Fig 5.4.1c: Experimental mode shape of plate without added mass (3rd mode)

5.4.1.2 Setup-II: Cantilever plate with 100gms lumped mass near node 17 & 18

Table 5.4.1c: Measured frequency and damping value for plate with 100gms lumped mass near node 17 & 18

Mode	Natural frequency (Hz)	Damping (%)
1st	17.7	3
2nd	43.4	9.49
3rd	104	4.58

Table 5.4.1d: Measured mode shape values for plate with 100gms lumped mass near node 17 &18

1st mode	2nd mode	3rd mode
2.38	11.4	-130
3.72	25.1	-200
7.38	37.3	-90.7
11.2	46.8	108
2.22	6.34	-100
4.25	13.2	-132
8.04	20.8	-13.9
12.5	26.8	202
2.64	1.36	-89.4
4.87	1.08	-113
8.18	1.01	25.5
11.6	2.07	265
1.72	-4.96	-100
4.59	-12.3	-133
7.96	-19.6	8.33
11.5	-25.1	222
1.66	-9.68	-127
4.28	-24.1	-194
7.89	-38.2	-59.9
10.8	-46.5	166

5.4.1.3 Setup-III: Cantilever plate with 200gms lumped mass near node 18

Table 5.4.1e: Measured frequency and damping value for plate with 200gms lumped mass near node 18

Mode	Natural frequency (Hz)	Damping value (%)
1st	17.5	3
2nd	43.3	9.7
3rd	104	4.6

Table 5.4.1f: Measured mode shape values for plate with 200gms lumped mass near node 18

1st mode	2nd mode	3rd mode
2.83	12.1	-135
3.97	25.7	-198
7.04	38.8	-88
9.59	46.5	118
2.59	7.06	-105
4.64	14.2	-137
7.89	20.7	-9.16
10.9	27.5	209
2.01	1.11	-93
4.68	1.08	-113
7.47	1.27	20.3
10.8	2.01	251
2.3	-3.85	-98.7
4.28	-11.7	-135
7.63	-18.5	1.0
10.5	-23.8	228
2.19	-9.49	-123
4.06	-24.5	-191
7.67	-37.0	-65.5
9.75	-44.6	159

5.4.1.4 Setup-IV: Cantilever plate with 200gms lumped mass near node 17

Table 5.4.1g: Measured frequency and damping value for plate with 200gms lumped mass near node 17

Mode	Natural frequency (Hz)	Damping value (%)
1st	17.7	3
2nd	43.5	9.55
3rd	103	4.69

Table 5.4.1h: Measured mode shape values for plate with 200gms lumped mass near node 18

1st mode	2nd mode	3rd mode
1.35	10.2	-125
2.97	22.7	-187
6.84	35.7	-99.3
12.2	46.2	87.5
1.65	5.82	-93.7
4.27	12.6	-121
7.69	19.9	-14.3
12.4	27.2	174
1.96	1.11	-82.4
4.7	1.34	-99.0
8.21	2.01	28.4
11.8	2.51	234
1.96	-4.33	-97.1
4.59	-11.7	-128
7.6	-19.6	-0.64
10.8	-25.5	209
3.2	-9.29	-131
5.38	-24.1	-203
7.34	-39.1	-79.2
9.41	-46.3	123

5.4.2 Shaker Test results:

The main objective of the Shaker test is estimating of the modal mass to convert the mode shape values obtained from Hammer test to mass normalized mode shape values. The theory behind Shaker test is discussed in chapter 4. The plate with existing setup is oscillated with sinusoidal signal at the frequencies obtained using Hammer test to calculate the modal impedance value. But, to check the lowest impedance value of every mode, a tuning process is undertaken considering the frequency values closer to that modal test frequency and it is observed that the impedance value is not minimum at frequency obtained from modal test. The introduction of the stringer connected to the plate results in change in the boundary condition, thereby change in the overall stiffness. This might have resulted in shift in the frequencies at which least impedance values are observed. The altered frequencies with the lowest impedance value is considered for further calculation. From the modal impedance value, generalized stiffness and corresponding generalized modal mass is calculated. In calculation of generalized modal mass, damping values are required which are kept same as obtained from Hammer test. The mass normalized mode shapes are then calculated by dividing the measured un-normalized mode shape values with the square root of generalized modal mass. Before mass normalization, unit normalization is applied to the un-normalized mode shape values. Impedance values, generalized stiffness, generalized modal mass and mass normalized mode shape values for four experimental setup are as follows-

5.4.2.1 Setup-I: Cantilever plate without lumped mass

Table 5.4.2a: Impedance value, generalized stiffness and generalized modal mass for plate without lumped mass

Mode	Hammer test frequency (Hz)	Frequency of lowest impedance value (Hz)	Impedance value (N/m)	Damping value (%)	Generalized stiffness (N/m)	Generalized modal mass (Kg)
1st	17.9	17.7	718	3	11966.67	0.967
2nd	43.8	43.7	3331.52	9.39	17739.72	0.235
3rd	107	106.8	30411.49	4.57	332729.62	0.738

Actual mass of the plate= 3.99Kg

Total generalized modal mass up to 3 modes= 1.94Kg which is 48.62% of actual mass of the plate.

Table 5.4.2b: Mass normalized measured mode shape values for plate without lumped mass

1st mode	2nd mode	3rd mode
0.170	0.525	-0.698
0.328	1.120	-1.046
0.617	1.662	-0.462
0.865	2.062	0.639
0.199	0.290	-0.508
0.363	0.573	-0.668
0.652	0.881	-0.043
0.974	1.189	0.992
0.210	0.070	-0.433
0.470	0.042	-0.534
0.674	0.049	0.104
1.017	0.088	1.164
0.146	-0.207	-0.454
0.347	-0.538	-0.630
0.631	-0.885	-0.059
0.923	-1.150	0.979
0.109	-0.451	-0.613
0.339	-1.107	-0.962
0.608	-1.754	-0.418
0.930	-2.057	0.546

5.4.2.2 Setup-II: Cantilever plate with 100gms lumped mass near node 17 & 18

Table 5.4.2c: Impedance value, generalized stiffness and generalized modal mass for plate with 100gms lumped mass near node 17 & 18

Mode	Hammer test frequency (Hz)	Frequency of lowest impedance value (Hz)	Impedance value (N/m)	Damping value (%)	Generalized stiffness (N/m)	Generalized modal mass (Kg)
1st	17.7	17.5	793.50	3	13225.09	1.094
2nd	43.4	43.3	5655.34	9.49	29796.31	0.402
3rd	104	103.3	34379.01	4.58	375316.70	0.890

Actual mass of the setup= 4.19Kg

Total generalized modal mass up to 3 modes= 2.386Kg which is 56.94% of actual mass of the setup.

Table 5.4.2d: Mass normalized measured mode shape values for plate with 100gms lumped mass near node 17 & 18

1st mode	2nd mode	3rd mode
0.182	0.384	-0.520
0284	0.846	-0.799
0.564	1.257	-0.362
0.856	1.577	0.432
0.170	0.214	-0.400
0.325	0.445	-0.528
0.615	0.701	-0.055
0.956	0.903	0.807
0.202	0.046	-0.357
0.372	0.036	-0.452
0.625	0.034	0.102
0.887	0.070	1.059
0.131	-0.167	-0.400
0.351	-0.414	-0.532
0.609	-0.660	0.033
0.879	-0.846	0.887
0.127	-0.362	-0.508
0.327	-0.812	-0.775
0.603	-1.287	-0.239
0.826	-1.567	0.663

5.4.2.3 Setup-III: Cantilever plate with 200gms lumped mass near node 18

Table 5.4.2e: Impedance value, generalized stiffness and generalized modal mass for plate with 200gms lumped mass near node 18

Mode	Hammer test frequency (Hz)	Frequency of lowest impedance value (Hz)	Impedance value (N/m)	Damping value (%)	Generalized stiffness (N/m)	Generalized modal mass (Kg)
1	17.5	17.3	747.41	3	12456.83	1.054
2	43.3	43.2	5966.51	9.7	30723.53	0.417
3	104	103.2	33061.90	4.6	359358.69	0.855

Actual mass of the setup= 4.19Kg

Total generalized modal mass up to 3 modes= 2.326Kg which is 55.51% of the actual mass of the setup

Table 5.4.2f: Mass normalized measured mode shape values for plate with 200gms lumped mass near node 18

1st mode	2nd mode	3rd mode
0.253	0.403	-0.582
0.355	0.855	-0.854
0.629	1.292	-0.379
0.857	1.548	0.509
0.231	0.235	-0.453
0.415	0.473	-0.590
0.705	0.689	-0.039
0.974	0.915	0.901
0.179	0.037	-0.401
0.418	0.036	-0.487
0.667	0.042	0.087
0.965	0.067	1.082
0.205	-0.128	-0.425
0.382	-0.389	-0.582
0.682	-0.616	0.004
0.938	-0.792	0.983
0.196	-0.316	-0.530
0.363	-0.816	-0.823
0.685	-1.232	-0.282
0.871	-1.485	0.685

5.4.2.4 Setup-IV: Cantilever plate with 200gms lumped mass near node 17

Table 5.4.2g: Impedance value, generalized stiffness and generalized modal mass for plate with 200gms lumped mass near node 17

Mode	Hammer test frequency (Hz)	Frequency of lowest impedance value (Hz)	Impedance value (N/m)	Damping value (%)	Generalized stiffness (N/m)	Generalized modal mass (Kg)
1st	17.7	17.6	806.24	3	13437.33	1.099
2nd	43.5	43.2	5538.02	9.55	28994.87	0.393
3rd	103	103.7	31772.34	4.69	338724.30	0.798

Actual mass of the setup= 4.19Kg

Total generalized modal mass up to 3 modes= 2.29Kg which is 54.65% of the actual mass of the setup

Table 5.4.2h: Mass normalized measured mode shape values for plate with 200gms lumped mass near node 17

1st mode	2nd mode	3rd mode
0.104	0.351	-0.598
0.228	0.782	-0.895
0.526	1.230	-0.475
0.939	1.591	0.419
0.127	0.200	-0.448
0.328	0.434	-0.579
0.592	0.685	-0.068
0.954	0.937	0.832
0.151	0.038	-0.394
0.362	0.046	-0.474
0.632	0.069	0.136
0.908	0.086	1.120
0.151	-0.149	-0.465
0.353	-0.403	-0.612
0.585	-0.675	-0.003
0.831	-0.878	1.000
0.246	-0.320	-0.627
0.414	-0.830	-0.971
0.565	-1.347	-0.379
0.724	-1.595	0.589

5.5 Model updating using Lagrange multiplier method based on experimental modal parameters:

The effectiveness of Lagrange multiplier method in Finite Element model updating to localize the added mass based on numerical modal parameters is discussed in section 5.3. Here, this method is applied to update the baseline FE model of the plate structure as coded in the MATLAB platform using dimensions, material properties and boundary conditions to estimate the actual mass and stiffness distribution of the plate in the existing condition. From mass distribution of the updated model, major change in mass matrix is located which is then validated with the experimental setup. Application of the method is in two different ways as stated in earlier section. As higher modes cannot be estimated properly by experimental setup, first 3 modes and corresponding frequency values are considered for model updating.

5.5.1 Procedure-I: Mass matrix updation followed by stiffness matrix updation

In this procedure, mass matrix is first updated using experimental modal parameters and then stiffness matrix is updated using that updated mass matrix. Mass normalized mode shape values of first 3 modes are used for updating purpose. Application of this procedure for different experimental setup is as follows-

5.5.1.1 Setup-I: Cantilever plate without lumped mass

Table 5.5.1a: Frequency of updated model and experimental frequency

Mode	Frequency of updated model (Hz)	Experimental frequency (Hz)
1st	17.7	17.7
2nd	43.7	43.7
3rd	106.8	106.8

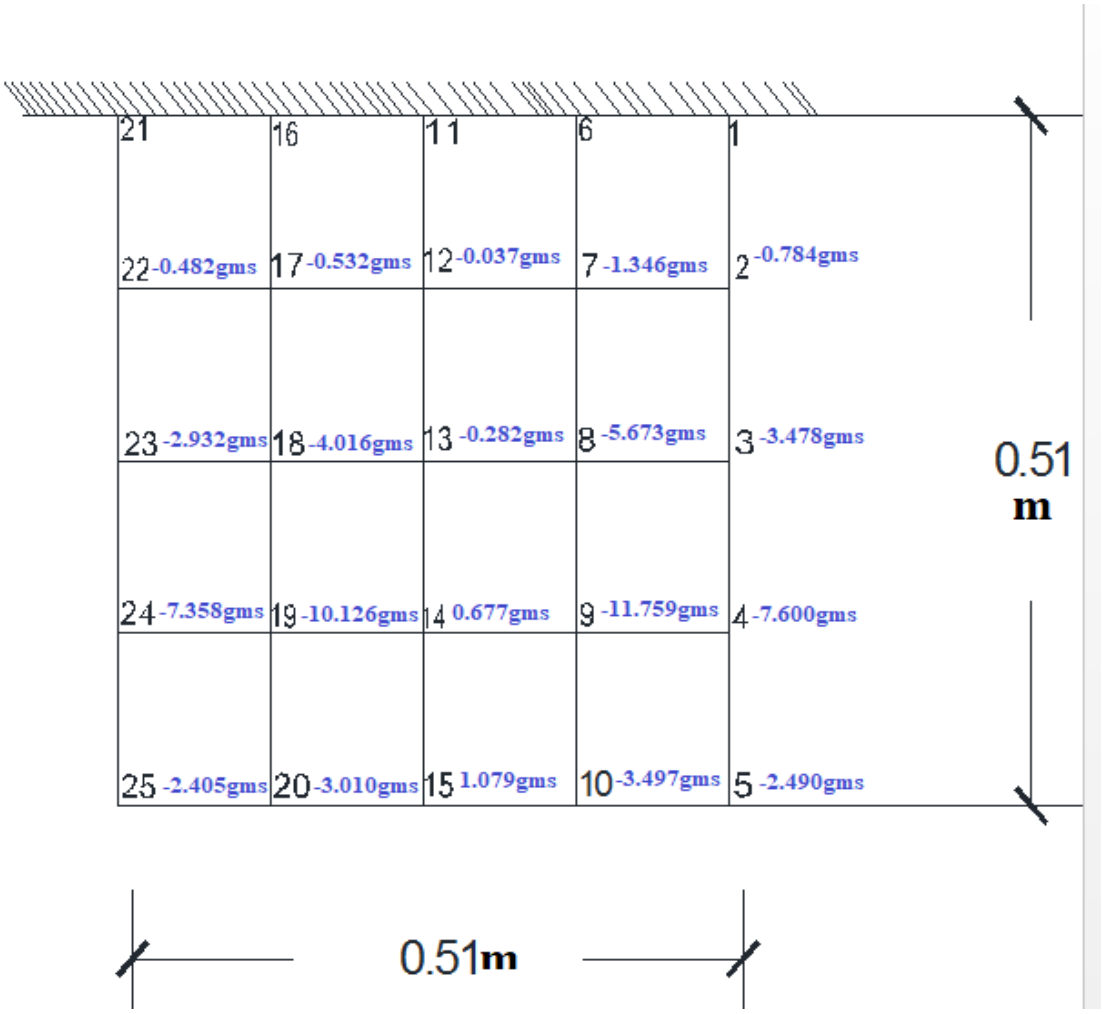

Fig 5.5.1a: Schematic presentation of change of nodal mass after updation by procedure-I using experimental modal parameters of plate without lumped mass

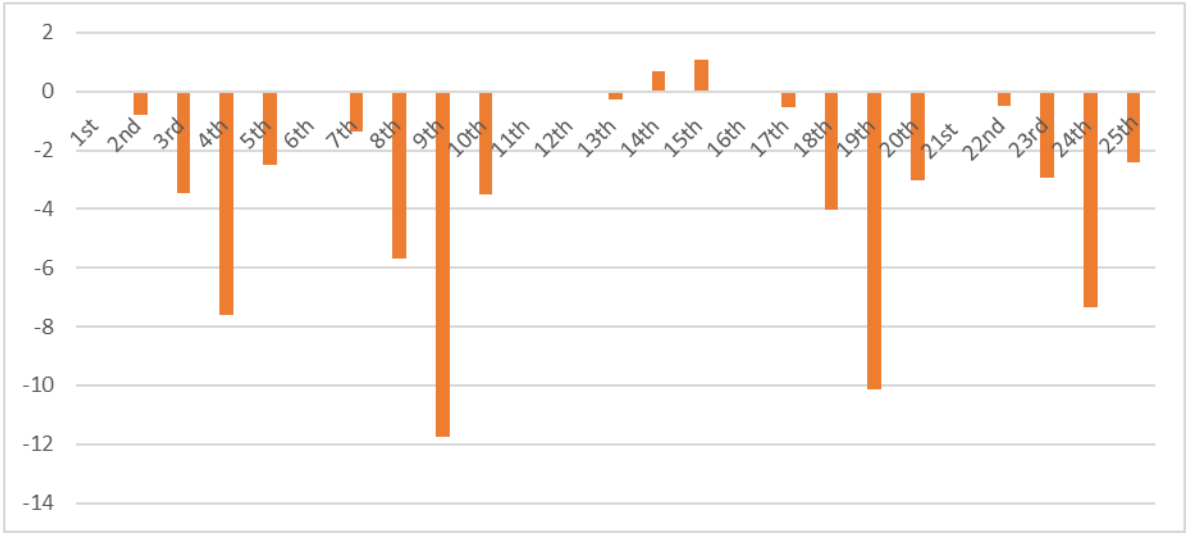

Fig 5.5.1b: Change in major diagonal elements of mass matrix after model updating by procedure-I for plate

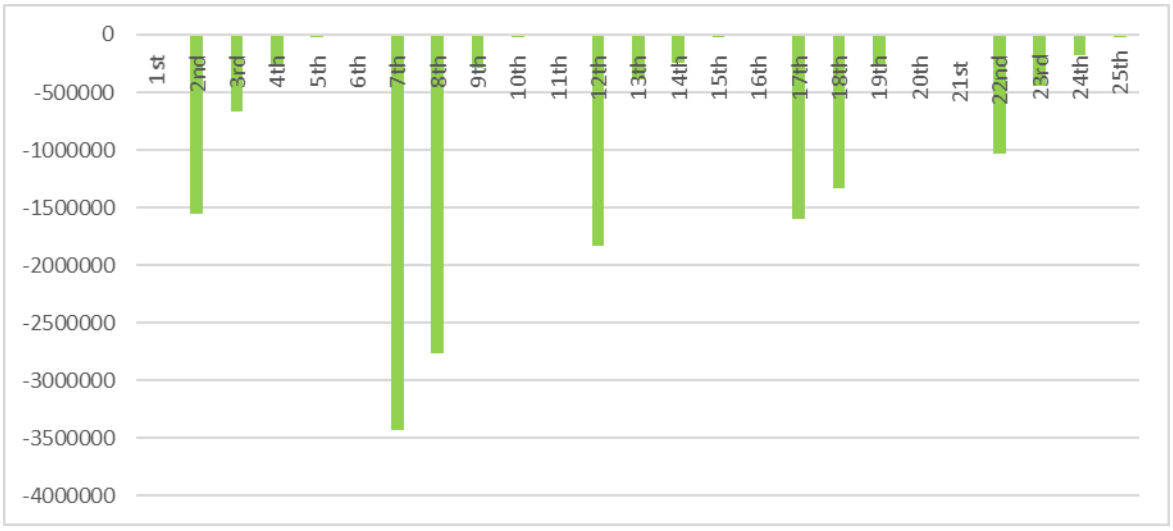

Fig 5.5.1c: Change in major diagonal elements of stiffness matrix after model updating by procedure-I for plate

Table 5.5.1b: Mode shape values of updated model

1st mode	2nd mode	3rd mode
0.170	0.525	-0.698
0.328	1.120	-1.046
0.617	1.662	-0.462
0.865	2.062	0.639
0.199	0.290	-0.508
0.363	0.573	-0.668
0.652	0.881	-0.043
0.974	1.189	0.992
0.210	0.070	-0.433
0.470	0.042	-0.534
0.674	0.049	0.104
1.017	0.088	1.164
0.146	-0.207	-0.454
0.347	-0.538	-0.630
0.631	-0.885	-0.059
0.923	-1.150	0.979
0.109	-0.451	-0.613
0.339	-1.107	-0.962
0.608	-1.754	-0.418
0.930	-2.057	0.546

MAC value:

MAC values are calculated between modes of updated model and experimental modes. The values are given in Table 5.5.1c.

Table 5.5.1c: MAC value of plate without lumped mass before updation

Mode	1st mode	2nd mode	3rd mode
1st mode	0.9894	1.27e-06	0.0769
2nd mode	4.09e-06	0.9931	1.27e-06
3rd mode	0.0769	1.27e-06	0.8384

Table 5.5.1d: MAC value of plate without lumped mass after updation

Mode	1st mode	2nd mode	3rd mode
1st mode	1	0.0001	0.046
2nd mode	0.0001	1	6.1e-07
3rd mode	0.046	6.1e-07	1

As MAC values are 1 for same modes, mode shapes obtained from updated model perfectly represents the experimental mode shapes which is the prime concern in FE model updating.

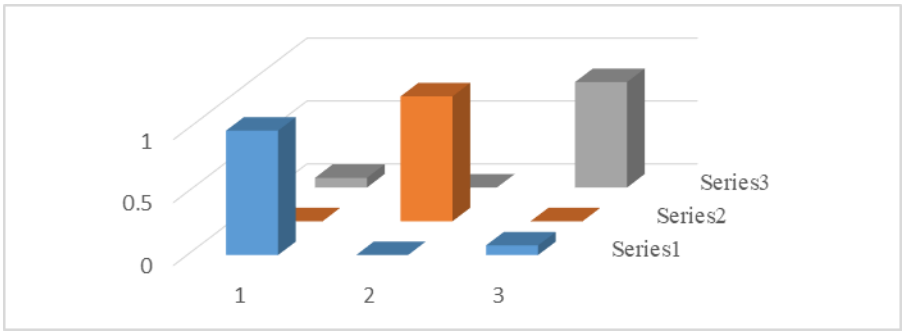

Fig 5.5.1d: MAC value of the plate without lumped mass before updation

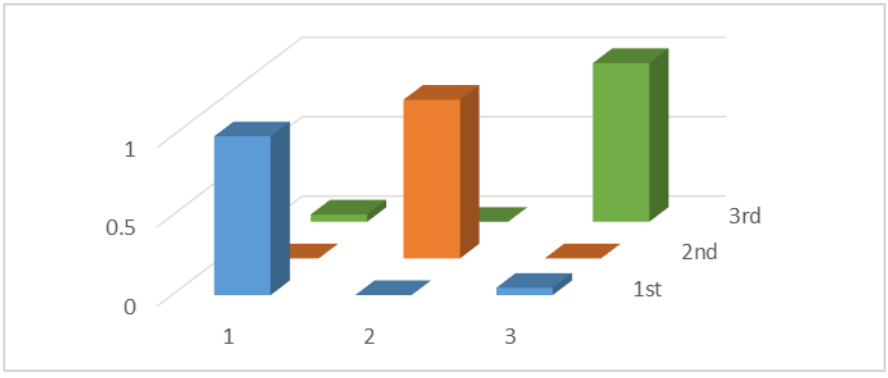

Fig 5.5.1e: MAC value after model updating of plate without lumped mass by procedure-I

5.5.1.2 Setup-II: Cantilever plate with 100gms lumped mass near node 17 & 18

Table 5.5.1e: Frequency of updated model and experimental frequency

Mode	Frequency of updated model (Hz)	Experimental frequency (Hz)
1st	17.5	17.5
2nd	43.3	43.3
3rd	103.3	103.3

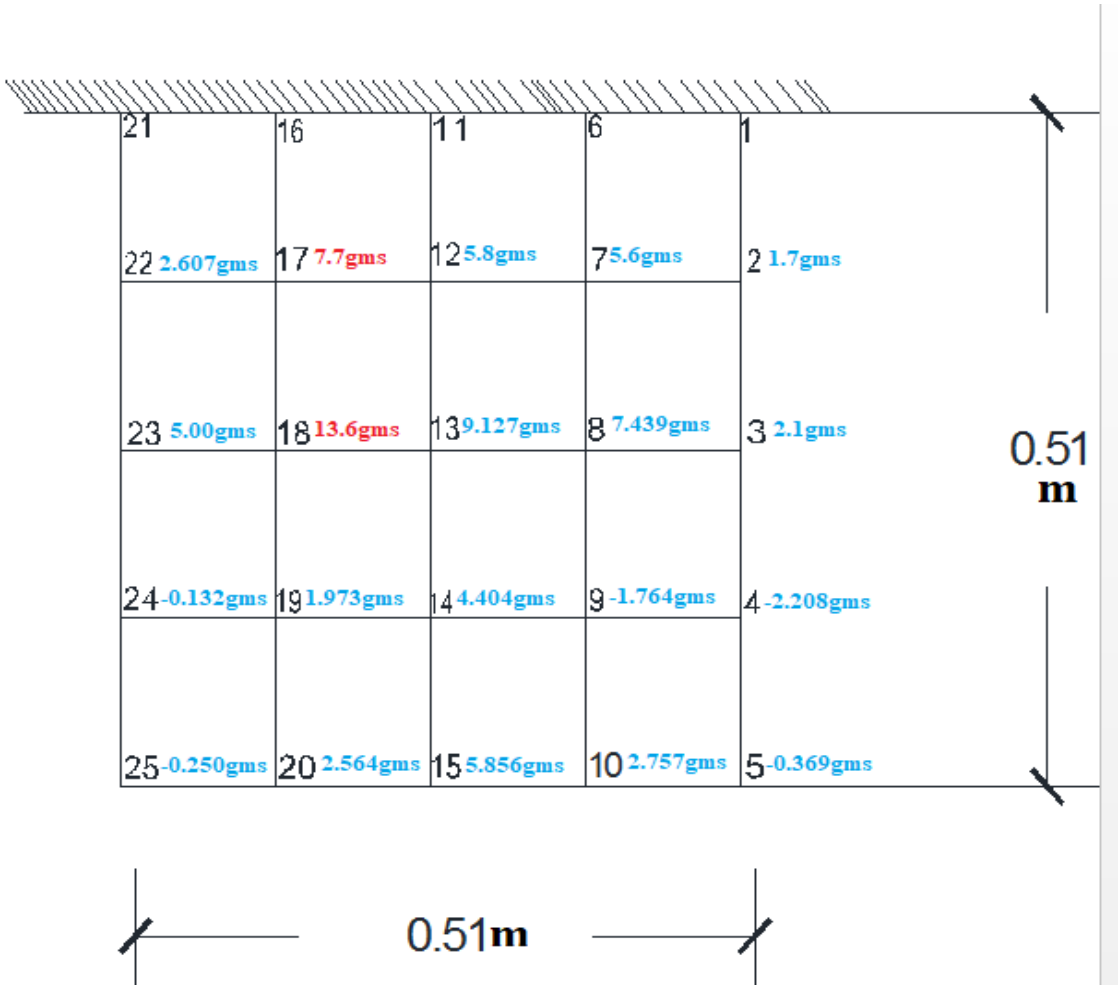

Fig 5.5.1f: Schematic presentation of change of nodal mass after updation by procedure-I using experimental modal parameters of plate with 100gms lumped mass near node 17 & 18

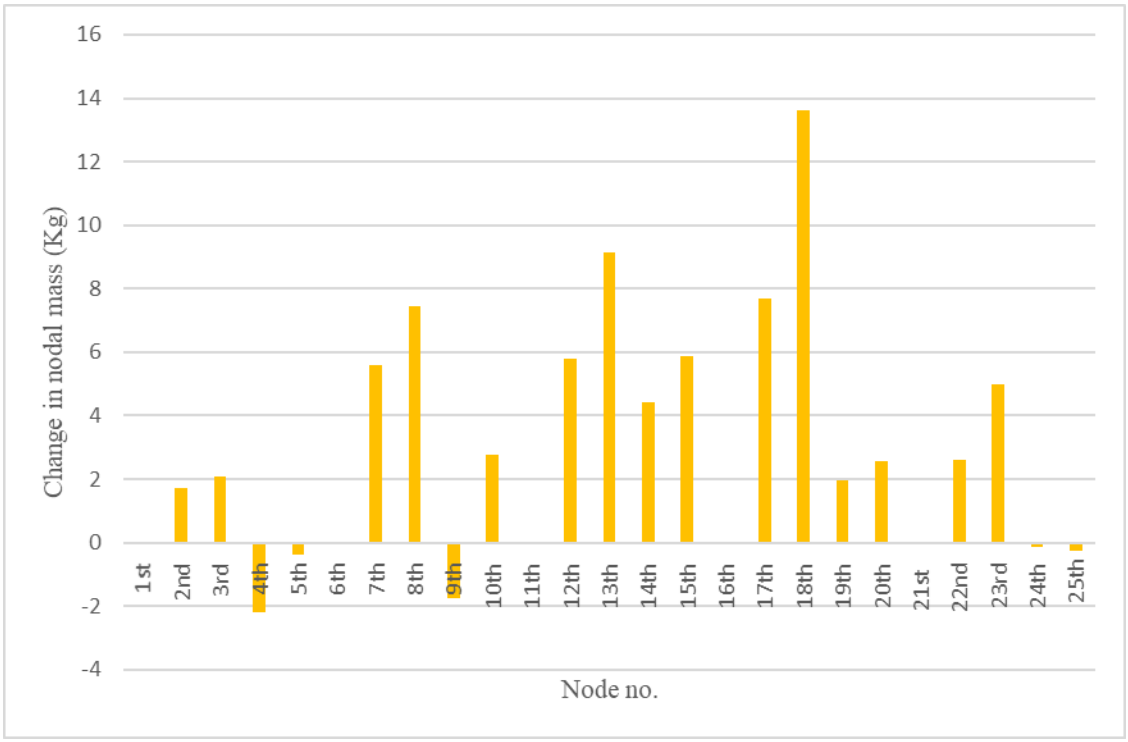

Fig 5.5.1g: Change in major diagonal elements of mass matrix after model updating by procedure-I for plate with 100gms lumped mass near node 17 & 18

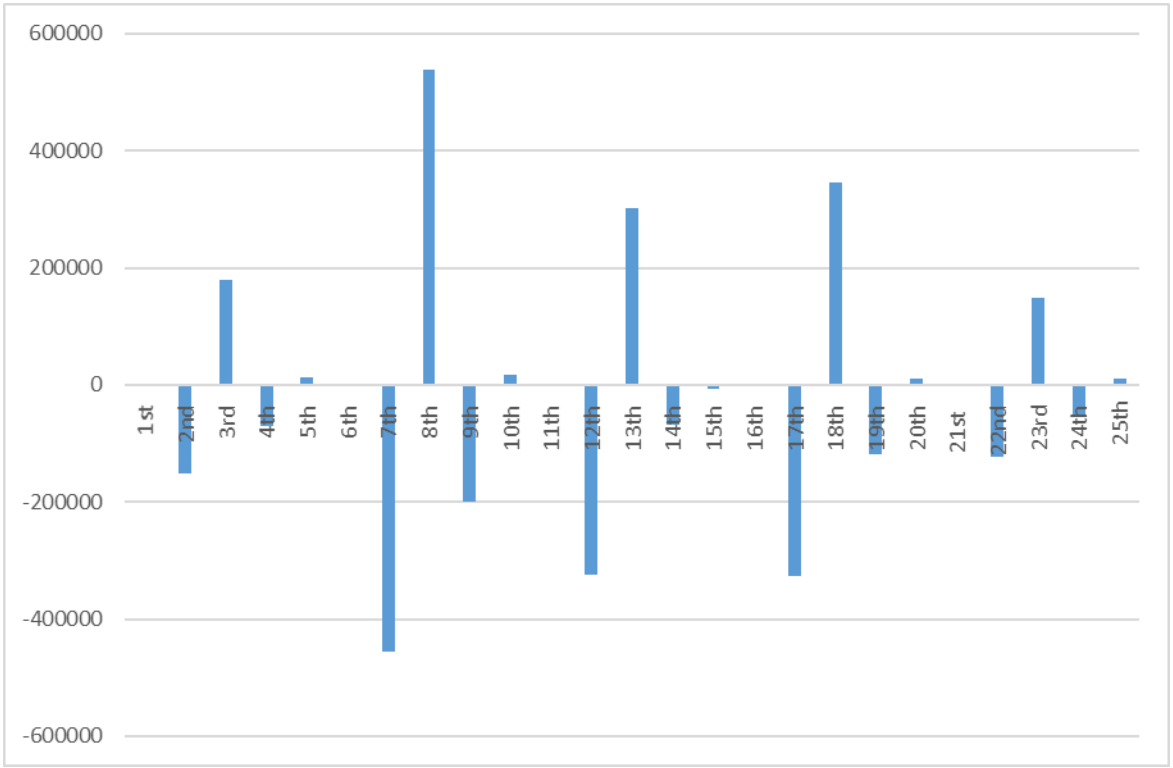

Fig 5.5.1h: Change in major diagonal elements of stiffness matrix after model updating by procedure-I for plate with lumped mass near node 17 & 18

Table 5.5.1f: Mode shape values of updated model

1st mode	2nd mode	3rd mode
0.170	0.525	-0.698
0.328	1.120	-1.046
0.617	1.662	-0.462
0.865	2.062	0.639
0.199	0.290	-0.508
0.363	0.573	-0.668
0.652	0.881	-0.043
0.974	1.189	0.992
0.210	0.070	-0.433
0.470	0.042	-0.534
0.674	0.049	0.104
1.017	0.088	1.164
0.146	-0.207	-0.454
0.347	-0.538	-0.630
0.631	-0.885	-0.059
0.923	-1.150	0.979
0.109	-0.451	-0.613
0.339	-1.107	-0.962
0.608	-1.754	-0.418
0.930	-2.057	0.546

MAC value:

MAC values are calculated between modes of updated model and experimental modes. The values are given in Table 5.5.1g.

Table 5.5.1g: MAC value of updated model

Mode	1st mode	2nd mode	3rd mode
1st mode	1	0.0008	0.0752
2nd mode	0.0008	1	0.005
3rd mode	0.0752	0.005	1

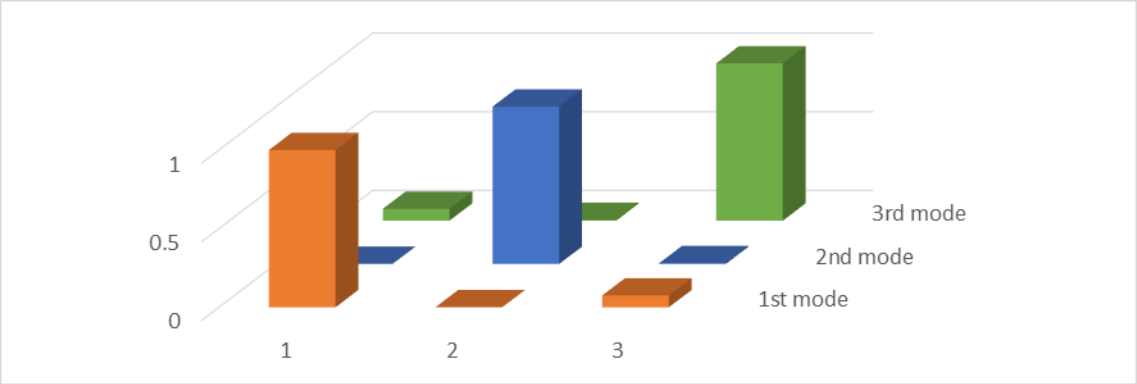

Fig 5.5.1i: MAC value after model updating of plate with 100gms lumped mass near node 17 & 18 by procedure-I

5.5.1.3 Setup-III: Cantilever plate with 200gms lumped mass near node 18

Table 5.5.1h: Frequency of updated model and experimental frequency

Mode	Frequency of updated model (Hz)	Experimental frequency (Hz)
1st	17.3	17.3
2nd	43.2	43.2
3rd	103.2	103.2

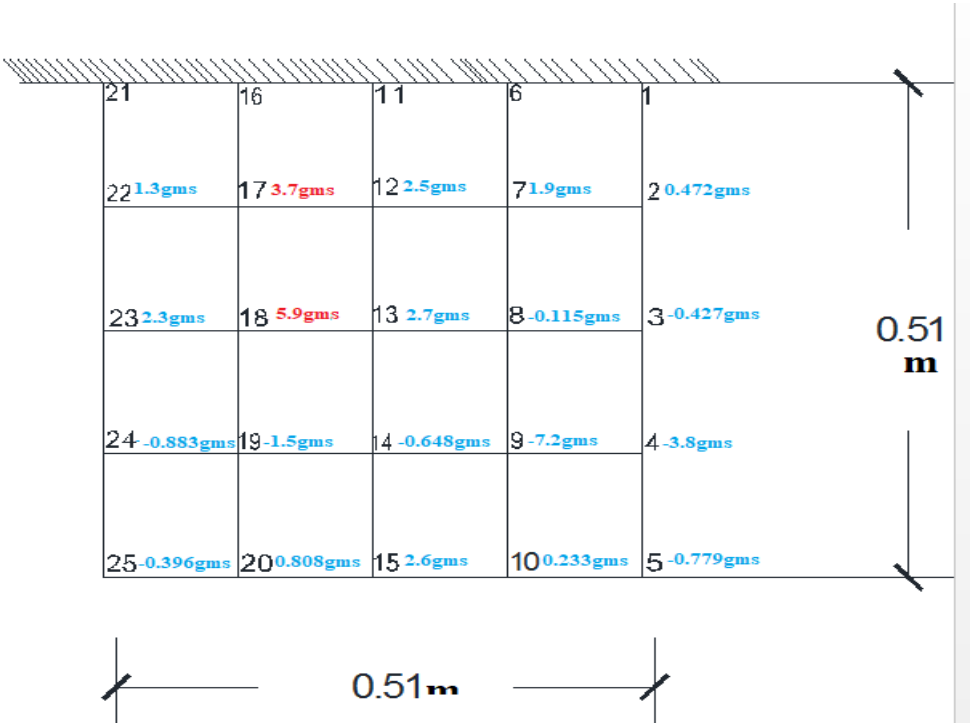

Fig 5.5.1j: Schematic presentation of change of nodal mass after updation by procedure-I using experimental modal parameters of plate with 200gms lumped mass near node 18

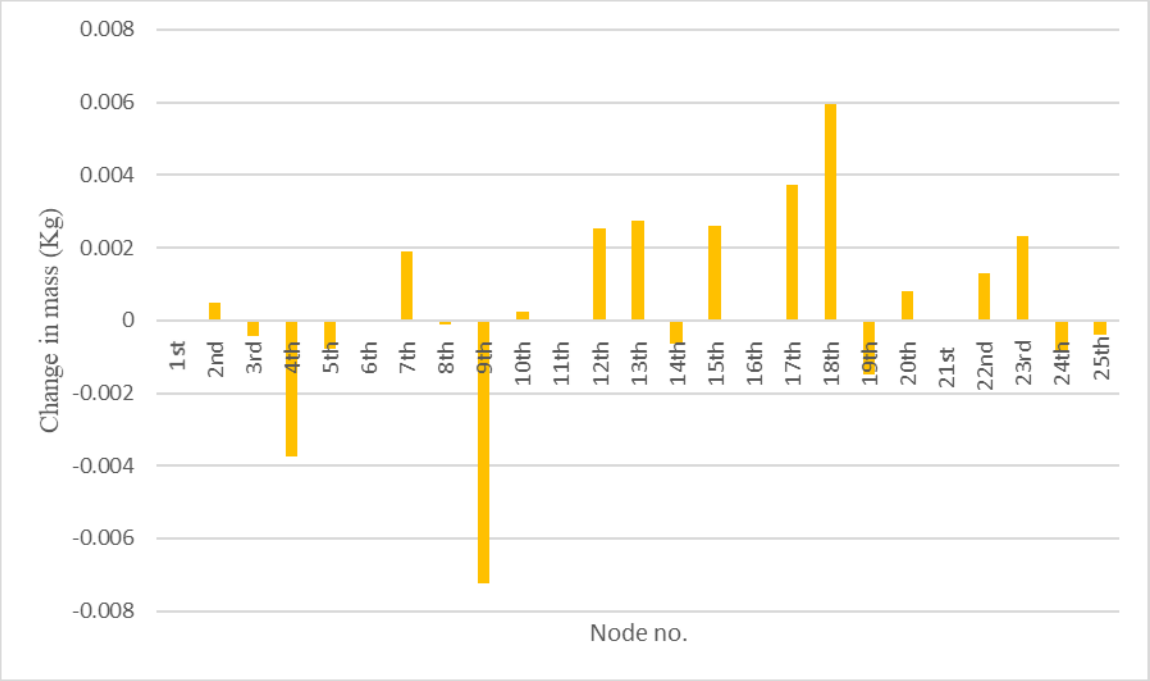

Fig 5.5.1k: Change in major diagonal elements of mass matrix after model updating by procedure-I for plate with 200gms lumped mass near node 18

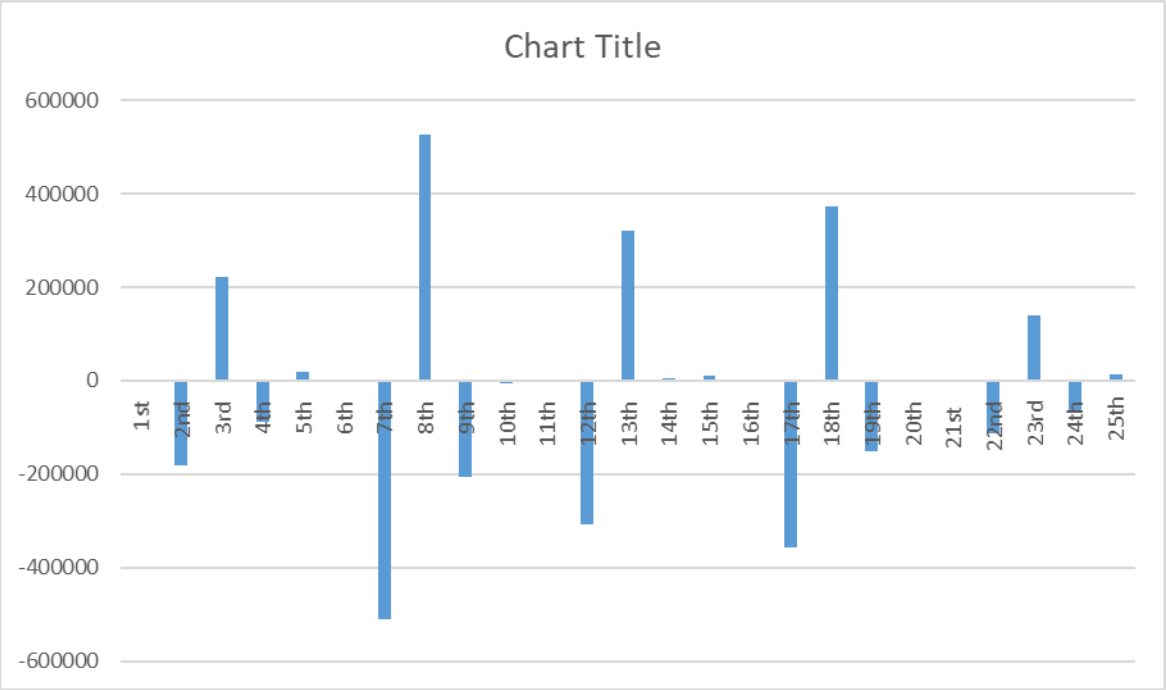

Fig 5.5.1l: Change in major diagonal elements of stiffness matrix after model updating by procedure-I for plate with 200gms lumped mass near node 18

Table 5.5.1i: Mode shape values of updated model

1st mode	2nd mode	3rd mode
0.253	0.403	-0.582
0.355	0.855	-0.854
0.629	1.292	-0.379
0.857	1.548	0.509
0.231	0.235	-0.453
0.415	0.473	-0.590
0.705	0.689	-0.039
0.974	0.915	0.901
0.179	0.037	-0.401
0.418	0.036	-0.487
0.667	0.042	0.087
0.965	0.067	1.082
0.205	-0.128	-0.425
0.382	-0.389	-0.582
0.682	-0.616	0.004
0.938	-0.792	0.983
0.196	-0.316	-0.530
0.363	-0.816	-0.823
0.685	-1.232	-0.282
0.871	-1.485	0.685

MAC value:

MAC values are calculated between modes of updated model and experimental modes. The values are given in Table 5.5.1j.

Table 5.5.1j: MAC value of updated model

Mode	1st mode	2nd mode	3rd mode
1st mode	1	0.0022	0.0514
2nd mode	0.0022	1	0.0032
3rd mode	0.0514	0.0032	1

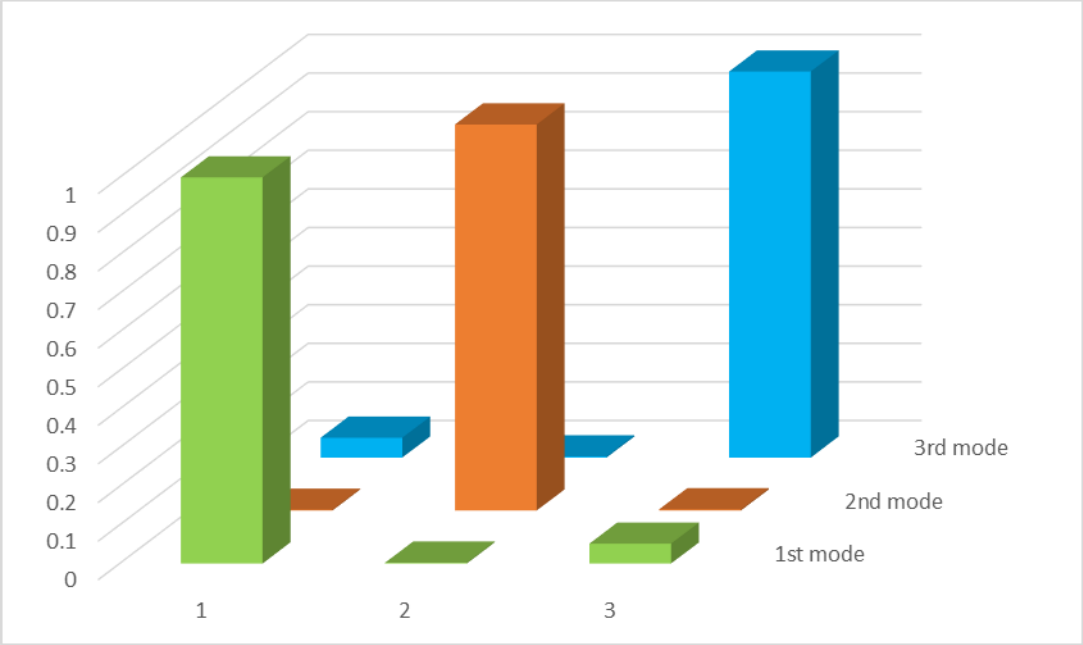

Fig 5.5.1m: MAC value after model updating of plate with 200gms lumped mass near node 18 by procedure-I

5.5.1.4 Setup-IV: Cantilever plate with 200gms lumped mass near node 17

Table 5.5.1k: Frequency of updated model and experimental frequency

Mode	Frequency of updated model (Hz)	Experimental frequency (Hz)
1st	17.6	17.6
2nd	43.2	43.2
3rd	103.7	103.7

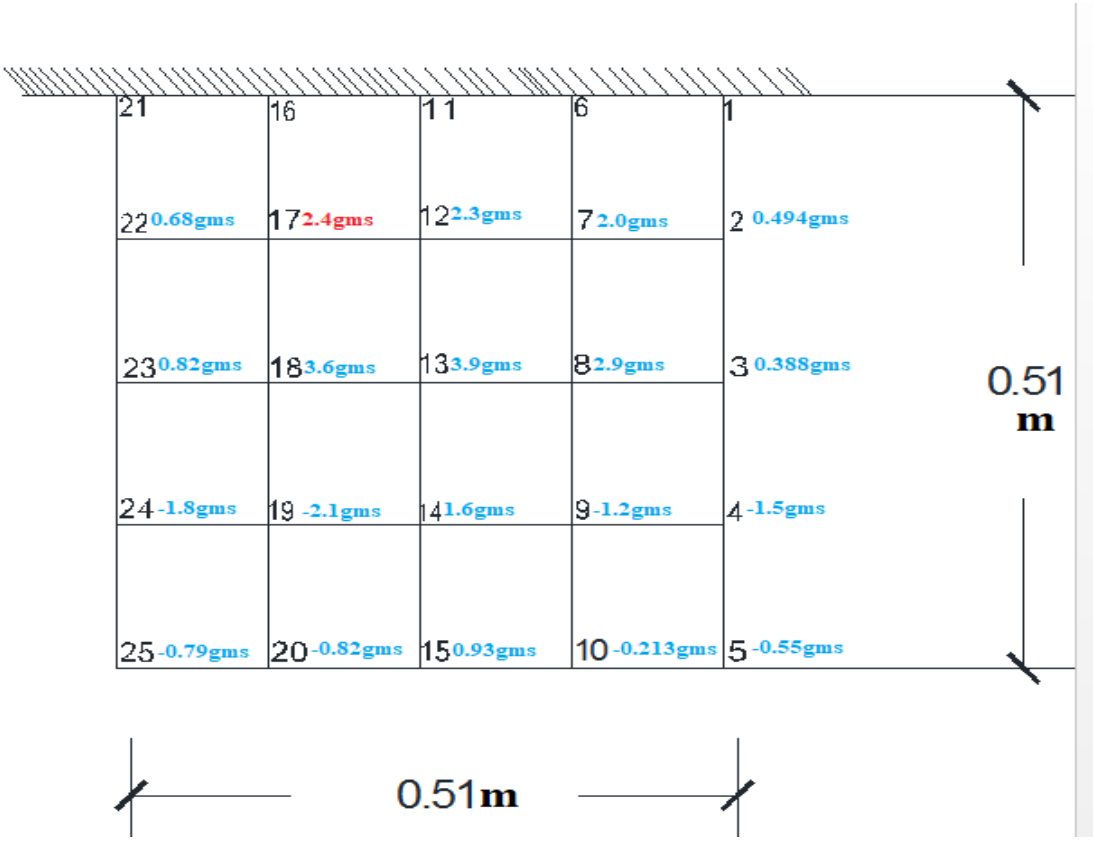

Fig 5.5.1n: Schematic presentation of change of nodal mass after updation by procedure-I using experimental modal parameters of plate with 200gms lumped mass near node 17

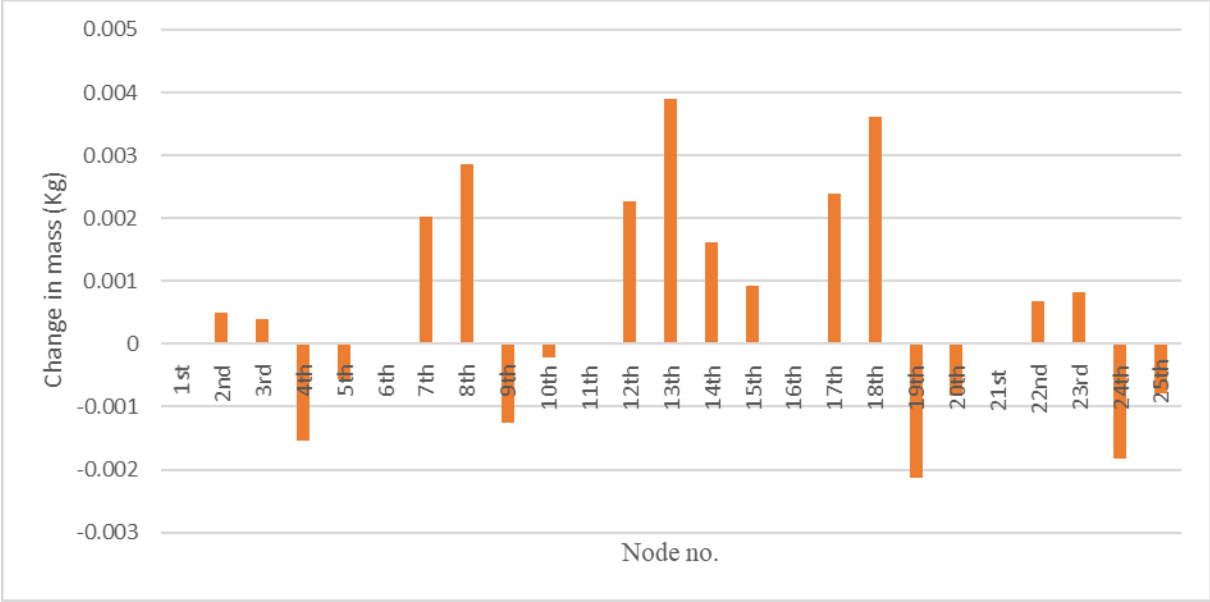

Fig 5.5.1o: Change in major diagonal elements of mass matrix after model updating by procedure-I for plate with 200gms lumped mass near node 17

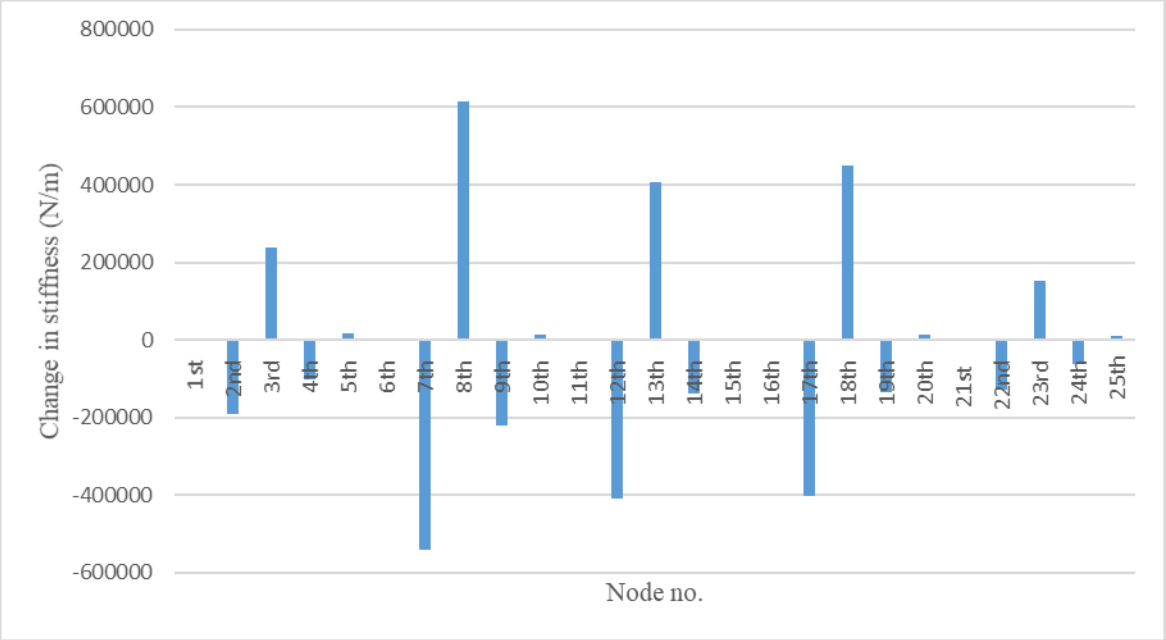

Fig 5.5.1p: Change in major diagonal elements of stiffness matrix after model updating by procedure-II for plate with 200gms lumped mass near node 17

Table 5.5.1l: Mode shape values of updated model

1^{st} mode	2^{nd} mode	3^{rd} mode
0.104	0.351	-0.598
0.228	0.782	-0.895
0.526	1.230	-0.475
0.939	1.591	0.419
0.127	0.200	-0.448
0.328	0.434	-0.579
0.592	0.685	-0.068
0.954	0.937	0.832
0.151	0.038	-0.394
0.362	0.046	-0.474
0.632	0.069	0.136
0.908	0.086	1.120
0.151	-0.149	-0.465
0.353	-0.403	-0.612
0.585	-0.675	-0.003
0.831	-0.878	1.000
0.246	-0.320	-0.627
0.414	-0.830	-0.971
0.565	-1.347	-0.379
0.724	-1.595	0.589

MAC value:

MAC values are calculated between modes of updated model and experimental modes. The values are given in Table 5.5.1m

Table 5.5.1m: MAC value of updated model

Mode	1st mode	2nd mode	3rd mode
1st	1	0.0014	0.0431
2nd	0.0014	1	0.0012
3rd	0.0431	0.0012	1

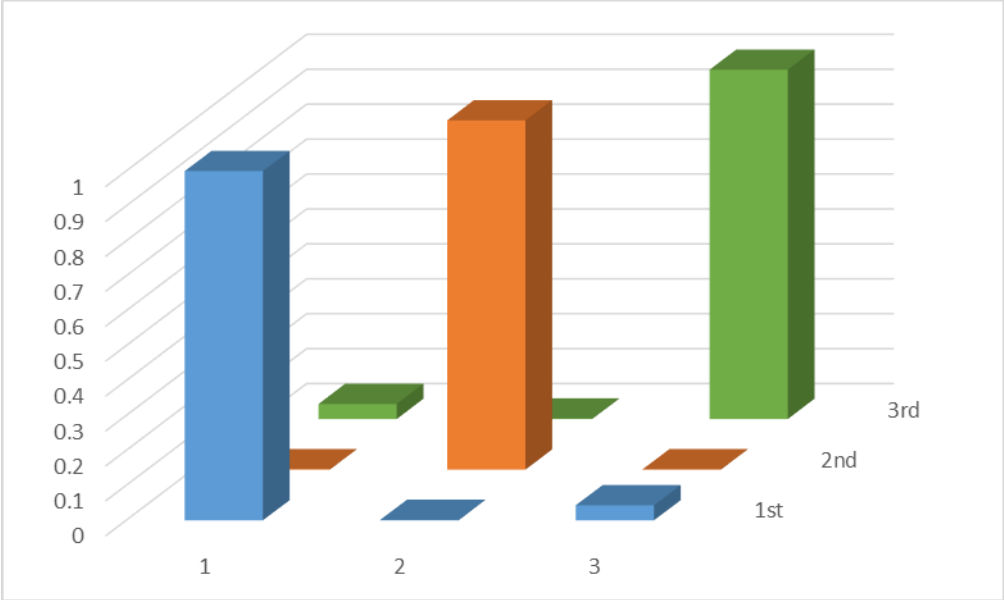

Fig 5.5.1q: MAC value after model updating of plate with 200gms lumped mass near node 18 by procedure-I

5.5.2 Procedure-II: Stiffness matrix updation followed by mass matrix updation

As discussed by Baruch [5] in 2nd procedure of model updating using Lagrange multiplier method, the stiffness matrix is first updated using stiffness normalized experimental modal parameters followed by the mass matrix updation. Mode shape values are normalized using the analytical stiffness matrix as stated in chapter 3. In this study, only one experimental setup (setup II) is considered to estimate the updated mass and stiffness matrix and corresponding modal parameters.

When baseline FE model is updated by this procedure, insignificant mass matrix is obtained. So, the values are not provided here and further study is going on.

5.5.3 Discussions on experimental results

Finite Element model updating of a cantilever plate based on numerical modal parameters as well as experimental has been performed to assess the existing mass and stiffness distribution of the structure using Lagrange multiplier method. Here, it is seen that when two 100gms masses are lumped near node 17 & 18 (setup-II) and the FE model is updated by Procedure-I, maximum change of mass from baseline FE model is at node 18 and a notable change of mass occurs at node 17. But, change of mass at node 13 is higher than node 17. So, accuracy of Procedure-I in lumping mass localization is not satisfactory with only 3 modes of vibration as like numerical updation. For experimental setup-III, where 200gms mass is lumped near node 18, maximum change of mass occurs at node 18 after updation of baseline FE model by Procedure-I. But, the amount of mass change at node 18 is lower than setup-II. As total generalized mass estimated considering 3 modes is only up to 50% of the total mass for different experimental configurations, accurate estimation of the added mass is not possible. But, when total estimated generalized mass from experimental setup is higher, added mass localization is more prominent as it is seen in the case of Setup-II. For experimental setup-IV, where 200gms mass is lumped near node 17, maximum change of mass occurs at node 13 after updation of baseline FE model by procedure-I. It is due to reduction of effect of lumped mass as it is located near the fixed end and consideration of lesser number of vibration modes.

Although the accurate identification of the added mass location could not be achieved fully, the updated stiffness and mass matrix resulted in obtaining system parameters (frequency and mode shape) identical to those obtained from experiment. It is primarily understood that without considering higher modes, accurate prediction might not be possible. However, if one observes the true experimental setup, the mass lumped is little bit away from node 17 & 18 which might have in reality introduced a smeared mass effect causing an increase in mass at node 13 that incidentally a neighbour node of node 18.

CHAPTER-6

CONCLUSIONS AND FUTURE SCOPE OF WORK

6.1 Conclusions:

In the present research work an attempt has been made to implement a finite element model updating technique based on Lagrange Multiplier methodology for both numerical and experimental models. Some of the salient features of the work carried out are listed below -

i) A detailed literature review on FE model updating is carried out and some of the major observations are listed. Thereafter, the objectives of the present work are formulated.

ii) A FE model of the plate structure is coded in MATLAB platform using 4 noded iso-parametric elements and necessary condensations are carried out.

iii) Numerical nodal masses are added to the plate and corresponding modal parameters are calculated.

iv) Experimental modal parameters are estimated in the laboratory using Experimental modal analysis.

v) Lagrange Multiplier method is used to update the baseline FE model.

vi) Lagrange multiplier method is found to be effective in FE model updating. Two procedures of model updation (Procedure-I & Procedure-II) as discussed in previous chapter are very accurate in lumped mass localization when worked with numerical modal parameters and more number of vibration modes.

vii) Model updated by Procedure-I (mass matrix updation followed by stiffness matrix updation) also results in reasonably good results when worked with experimental modal parameters. Accuracy of updation would have been much better if higher modes are accounted.

viii) Model updated by Procedure-II (stiffness matrix updation followed by mass matrix updation) is producing insignificant results when worked with experimental modal parameters which should be studied further.

ix) More accurate updation is possible if the effect of higher modes can be accounted in the lower modes.

x) Experimental modal analysis should be as noise free as possible.

6.2 Scope of future work:

i. Measurement of higher modes by experimental modal analysis if possible.

ii. Application of proper algorithm to account the effect of higher modes into lower modes.

iii. There may be lack of proper fixity at the fixed end. So, proper fixity have to be ensured if required.

iv. Estimation of the stringer stiffness in the original FE model.

v. Application of the aforesaid updation methods in assessment of real-life structures. For that purpose, operational modal analysis have to be performed in place of experimental modal analysis.

References:

[1] Zadeh. L. A, “From Circuit Theory to System Theory”, Proceedings of the IRE, May, 1962.

[2] Ross. R. G, “Synthesis of Stiffness and Mass Matrices”, SAE conference paper 710787, 1971

[3] Gersch. W, Nielsen. N. N, Akaike. H, “Maximum Likelihood Estimation of Structural Parameters from Random Vibration Data”, Journal of Sound and Vibration, 1973, 31(3), 295-308,

[4] Berman. A, “Mass Matrix Correction Using an Incomplete Set of Measured Modes”, AIAA Journal, 1147-1148, 1979

[5] Baruch. M, “Optimal Correction of Mass and Stiffness Matrices Using Measured Modes”, AIAA Journal, 1623-1626, 1982.

[6] Berman. A, Nagy. E, “Improvement of a Large analytical Model Using Test Data”, AIAA Journal, 1168-1173, 1983

[7] Sheena. Z, Unger. A, Zalmanovich. A, “Theoretical stiffness matrix correction by using static test results”, Israel Journal of Technology, January, 1982.

[8] Sanayei. M, Nelson. B. R, “ Identification of Structural Element Stiffnesses from Incomplete Static Test data”, SAE Technical paper861793, 1986.

[9] Cheng. S. lin, “ Location Of Modelling Errors Using Modal Test Data”, AIAA Journal, Vol 28, No 9, pp. 16501654, 1990.

[10] Sanayei. M, Onipede. O, “Damage Assessment of Structures Using Static Test Data”, AIAA journal, VOL. 29, NO. 7, 1991.

[11] Hjelmstad. K. D, Wood. S. L, Clark. S. J, “Mutual Residual Energy Method for Parameter Estimation in Structures” ASCE, J. Struct. Eng. 1992.118:223-242.

[12] Mottershead. J, Friswell. M, “ Model updating in Structural Dynamics: a Survey”, Journal of Sound and Vibration, 167 (1993) 347-375.

[13] Banan. M. R, Hjelmstad. K. D, “Parameter Estimation of Structures from Static Response”, ASCE Journal of structural engineering, 3243-59, November, 1994.

[14] Sanayei. M, Saletnik. M. J, “Parameter Estimation From Static Strain Measurement” Journal of structural Engineering, Vol. 122, May, 1996.

[15] Hjelmstad. K. D, Shin. S, “Damage Detection and Assessment of Structures from Static Response”, ASCE Journal of Engineering Mechanics, 123(6): 568-76, 1997.

[16] Bakhtiari-Nejad. F, Rahai. A, Esfandiari. A, “A Structural Damage Detection Method Using Static Noisy Data”, ELSEVIER, Enginerring Structures, 1784-1793, 2005.

[17] Sanayei. M, McClain. J. A. S, , “Parameter Estimation Incorporating Modal Data and Boundary Conditions”, ASCE Journal of Structural Engineering 1048-1055,1999.

[18] Sanayei. M, Slavsky. E et al, “Damage Localization and Finite Element Model Updating using Multi-response NDT data”, ASCE Journal of Bridge Engineering, Vol 11, November, 2006.

[19] Khoshnoudian. F, Esfandiari. A, Scientia Iranica A (2011) 853-860, “Structural Damage Diagnosis Using Modal Data”.

[20] Idehara. S. J, Junior. M. D, “Modal Analysis of Structure under Non-Stationary excitation”, Engineering Structures, Vol 99, 2015, pages 56-62.

[21] Yu. Minli, Feng. Ningsheng, “Experimental Evaluation of a Modal Parameter based system identification Procedure”, Mechanical Systems and Signal Processing, vol 68-69, February 2016, pages 302-315.

[22] Arora. V, “Comparative Study of Finite element Model Updating Methods”, Journal of Vibration and control, 17 (2011) 2023-2039.

[23] Kabe. A. M, “Stiffness Matrix Adjustment using Mode Data”, AIAA Journal, 23 (1985) 1431-1436.

[24] Caesar. B, Peter. J, “ Direct Update of Dynamic Mathematical Models from Modal Test Data”, AIAA Journal, 25 (1987) 1494-1499

[25] Wei. F. S, “Analytical Dynamic Model Improvement using Vibration Test Data”, AIAA Journal, 28 (1990) 175-177.

[26] Yang. Y. B, Chen. Y. J, “A New Direct Method for Updating Structural Models based on Measured Modal Data”, Engineering Structures, 31 (2009) 32-42

[27] Lee. E. T, Eun. H. C, “Correction of Stiffness and Mass Matrices Utilizing Simulated Measured Modal Data”, Applied Mathematical Modelling, 33 (2009) 2723-2729

[28] Carvalho. J, Datta. B. N, Gupta. A, Lagadapati. M, “A Direct Method for Model Updating with Incomplete Measured Data and Without Spurious Mode”, Mechanical Systems and Signal Processing, 21 (2007) 2715-2731.

[29] Mukhopadhyay. S, Lus. H, Betti. R, “Modal Parameter based Structural Identification using Input-Output Data: Minimal Intrumentation and Global Identi-Fiability Issues”, Mechanical systems and Signal processing, 45 (2014) 283-301.

[30] Chen. H. P, Maung. T. S, “Regularised Finite Element Model Updating using Measured Incomplete Modal Data”, Journal of Sound and Vibration, 333 (2014) 5566-5582.

[31] Fu. Y, Lu. Z, Liu. J, “Damage Identification in plate using Finite Element Model Updating in Time Domain”, Journal of Sound and Vibration, 332 (2013) 7018-7032.

[32] Zhou. L, Wang. L, Chen. L, Ou. J, “Structural Finite Element Model Updating by Using Response Surfaces and Radial Basis Functions”, Advances in Structural engineering, 2016, Vol 19(9) 1446-1462.

[33] Atalla. M. J, “Model Updating using Neural Networks”, Dissertation submitted to the faculty of the Virginia Polytechnic Institute and State University.

[34] Miller. B, “Application of Neural Networks for Structure Updating”, Department of Structural Mechanics, Rzeszow University of Technology W. pola 2, 35-959 Rzeszow, Poland

[35] Santamaria. F, Arras. M, Coppotelli. G, “Application of Neural Networks for FE model updating of Structures in Operational Conditions”, 6th International Operational Modal Analysis Conference, 2015, Gijon, Spain.

[36] Marwala. T, Mdlaziand. L, Sibisi. S, “Finite Element Model Updating using Bayesian Approach”, School of Electrical and Information Engineering, University of Witwatersrand.